

PROCESSING AND CHARACTERISATION OF NANO-ENHANCED COMPOSITES

by

Armstrong FREDERICK



Institute of Biomedical Technologies

Auckland University of Technology

Auckland, New Zealand.

**This thesis is submitted in fulfilment of the degree of Master of Engineering by
research. This thesis contains confidential material and shall not be used,
copied, given or conveyed to anyone is not involved in the examination of this
work.**

February 2008

***To my fellow researchers at
The Institute of Biomedical Technologies***

ACKNOWLEDGMENTS

I express my sincere gratitude to my guru Prof. Ahmed Al-Jumaily, Director, Institute of Biomedical Technologies (IBTec), Auckland University of Technology, who has mentored me through the postgraduate study and to my supervisor and guide, Dr. Maximiano Ramos, Research Fellow, Institute of Biomedical Technologies (IBTec), Auckland University of Technology, for his generous sharing of knowledge, time and friendship combined with seemingly unlimited patience throughout my work to enable me attain my goal. Also, I extend my thanks to Mr. David White, Research Manager, Auckland University of Technology for all his support and encouragement.

My heartfelt thanks to Mark A. Hildesley of Materials OPTIMIZATION Ltd, not only for supporting my research project but also for sharing his precious time and materials.

Also, I express my gratitude to Technology New Zealand - Technology Industry Fellowships (TIF) for funding my research project vide contract number: MTRL0601.

Finally, I thank God for all his mercy and guidance through my studies and my Dad for his prayers and encouragements, my wife and my daughter Rofi Lyza for their help and sacrifices.

ABSTRACT

Since the discovery of nanomaterials in early ninety's, a remarkable progress in the synthesis of nanocomposites has been reported looking for a new better material with improved physical and chemical properties for a variety of applications in almost all fields. The science and technology of nanocomposites has created great excitement and expectations in the last decade too. In addition to that, researches in this area have been focusing on the nanoscale second phase embedded in the polymeric matrix that gives physical and chemical properties that cannot be achieved by ordinary material synthesis methods. Researchers have also discovered that incorporating the right amount of nanoparticles into a polymer matrix pose a remarkable strength and flexibility and that industries should be able to integrate the outcome of their researches widely in high performance applications in the field of biomedical engineering, aerospace, marine, high speed parts in engines, packaging and sports gadgets. With the new methods of synthesis and tools for characterisation, nanocomposite science and technology is now experiencing explosive growth. Taking advantage of the need and the properties of the nanomaterials, through this research a new nano-enhanced composite is developed through addition of nanofiller into epoxy matrix to cater for varied applications.

The physical and mechanical properties of the identified nanomaterial reinforced polymer composite were characterised by experimentation in order to ascertain the improvement in tensile, compressive and flexural properties as well as the adhesion of the matrix to the substrate. Also, while addressing potential enhancements like improved mechanical strength, better dimensional stability, higher thermal stability, better abrasion resistance, hard and wear resistance, better chemical properties like better flame retardance, anticorrosive and antioxidation, adequate importance was given to easy and bulk processability and most importantly the commercial viability as well.

This nano-enhanced nanocomposite was then optimised. Based on these results, it has been established that epoxy reinforced with 1% percent of nanoclay can significantly improve the mechanical properties without compromising the weight or processability of the composite. Thus, a futuristic and much promising nano-enhanced epoxy composite has been successfully made ready for commercialisation.

TABLE OF CONTENTS

Title Page	i
Acknowledgement	ii
Abstract	iii
Table of Contents	iv
List of Figures	v
List of Tables	vi
Statement of Originality	vii
Chapter 1 Introduction and Literature review	1
1.1 Introduction	1
1.2 Background	1
1.3 Study of possible nanofillers for their properties	3
1.3.1 Carbon nanotubes	4
1.3.2 Nanoclay	7
1.3.3 Nanocarbon	10
1.3.4 Aluminium oxide nanopowder	12
1.4 Study of possible resins for their properties	15
1.4.1 Thermoset resins	16
1.4.1.1 Epoxy	16
1.4.2 Thermoplastic resins	19
1.4.2.1 Polymethyl methacrylate (PMMA)	19
1.4.2.2 Polyvinylidene fluoride (PVDF)	21
1.4.2.3 Polyurethane	23
1.5 Analysis of the market demand and applications	24
1.6 Objectives	28
Chapter 2 Experimental Investigation	30
2.1 Study of different synthesis processes and characterisation	30
2.1.1 Mixing techniques	31
2.1.1.1 Ultrasonic dispersion	31
2.1.1.2 Mechanical mixing	35
2.1.2 Moulding techniques	36

2.1.2.1 Sintering	37
2.1.2.2 Moulding	38
2.1.2.3 Infusion	40
Chapter 3 Synthesis and Testing	42
3.1 Introduction	42
3.2 Synthesis	43
3.2.1 Synthesis using thermoplastic resins	43
3.2.2 Synthesis using epoxy resin	46
3.2.3 Lay-up preparation of laminates	49
3.3 Testing	52
3.3.1 Tensile test as per ASTM Standards D638	52
3.3.2 Three point bending test as per ASTM Standards D790M	57
3.3.3 Phase contrast microscopy	60
3.3.4 High speed photography	64
3.3.5 Surface tension measurement using the Drop shape method	66
3.3.5.1 Principle	67
3.3.5.2 Procedure	67
Chapter 4 Modelling and Validation	70
4.1 Introduction	70
4.2 Modelling	70
4.3 Validation and analysis on the influence of surface tension in bonding ...	79
Chapter 5 Results and Discussions	83
5.1 Introduction	83
5.2 Results	84
5.3 Analysis	92
5.3.1 Analysis based on various nanofillers used	93
5.3.2 Analysis based on various ratios or concentrations of nanofillers used	95
5.3.3 Analysis based on various duration of mixing	98
5.3.4 Analysis based on nature of mixing	100
5.4 Discussions	102

5.4.1 Bonding theories to support crack analysis	103
Chapter 6 Conclusions and Recommendations	110
6.1 Conclusions	110
6.2 Recommendations	111
6.2.1 Material selection	111
6.2.2 Process selection	112
6.2.3 Lay-up techniques	112
References	114
Appendix	124
Appendix A	124

LIST OF FIGURES

Figure 1.1: Layout of a Single Walled carbon nanotube	5
Figure 1.2: Structure of a Single Walled carbon nanotube	5
Figure 1.3: Molecular structure of nanocarbon	11
Figure 1.4: Typical structure epoxy molecule	16
Figure 1.5: IC Forecasts	25
Figure 1.6: Predicted demand of various nanofillers in the composite industry	25
Figure 1.7: Expected share of nanotechnology in the market by 2011	26
Figure 2.1: Frequency ranges of sound	31
Figure 2.2: Ultrasonic probe	32
Figure 2.3: Schematic representation of cavitation progression	33
Figure 3.1: Ball mill mixer	44
Figure 3.2: Flow chart for mixing thermoplastic resins	44
Figure 3.3: Ultrasonic liquid processor	47
Figure 3.4: Flow chart for mixing thermoset resins	47
Figure 3.5: Flow chart for making lay-up	50
Figure 3.6: Schematic drawing of carbon fibre lay-up	50
Figure 3.7: Schematic picture of lay-up	50
Figure 3.8: Mould design	53
Figure 3.9: Layout of matrix sample for tensile testing	53
Figure 3.10: Sample of 1% nanoclay/epoxy matrix for tensile testing	54
Figure 3.11: Tensile testing by Hounsfield machine	54
Figure 3.12: UTP Vs Elongation of various samples of nanoclay/epoxy composite matrix	55
Figure 3.13: Stress-strain graphs	55
Figure 3.14: Stress-strain comparison for various materials	56
Figure 3.15: Stress analysis summary	58
Figure 3.16: Mounted samples used during phase contrast microscopy	61
Figure 3.17: Phase contrast microscopy at 200X and 1000X of 3% nanoclay/epoxy matrix	62
Figure 3.18: Phase contrast microscopic samples of 1% nanoclay/epoxy lay-ups at different magnifications	63
Figure 3.19: Samples used during High speed camera photography	64

Figure 3.20: Samples of 1 % nanoclay/epoxy composite lay-up at 0 degrees (1 hr mixing)	65
Figure 3.21: Samples of 1 % nanoclay/epoxy composite lay-up at 45 degrees (1 hr mixing)	65
Figure 3.22: Samples of 1 % nanoclay/epoxy composite lay-up at 90 degrees (1 hr mixing)	65
Figure 3.23: Profile of the droplet under experiment	68
Figure 4.1: Schematic representation of a drop on a glass substrate	72
Figure 4.2: Liquid drop on solid surface	72
Figure 4.3: Effect of wetting on contact angle	73
Figure 4.4: Profile of the droplet under experiment	73
Figure 4.5: Graphical reproduction of the water droplet	73
Figure 4.6: Analysis on a water droplet	74
Figure 5.1: Comparison based on the angle of lay-up with various matrices	86
Figure 5.2: Stress comparison on different lay-ups	86
Figure 5.3: Stress comparison on various matrices	86
Figure 5.4: Summary of stress analysis	87
Figure 5.5: Summary of effect analysis on nanoclay lay-ups based on UTP	89
Figure 5.6: Summary of effect analysis on nanoclay lay-ups based on Stress	92
Figure 5.7: Stress analysis between 1% nanoclay and 1% nanocarbon	94
Figure 5.8 Stress analysis between 1% nanoclay and 1% nanocarbon at different lay-up angles	94
Figure 5.9: Stress analysis on different ratios of nanoclay/epoxy composites	96
Figure 5.10: Stress analysis for different ratios of nanofillers at different angle of lay-up	96
Figure 5.11: Effect of interfacial strength between the composite matrix and the fibre	97
Figure 5.12: Stress analysis for different mixing durations of nanofillers at different angle of lay-ups	99
Figure 5.13: Schematic representation of acoustic cavitation	100
Figure 5.14: Typical tensile testing graph showing a lay-up yielding	103
Figure 5.15: Crack analysis on 3% nanoclay/epoxy composite lay-up at 0° (1 hr mixing)	105

LIST OF TABLES

Table 1.1: Properties of carbon nanotubes	5
Table 1.2: Properties of nanocarbon	12
Table 1.3: Physical and Chemical properties of Aluminium oxide	13
Table 1.4: Mechanical, Thermal and Electrical properties of Aluminium oxide	14
Table 1.5: Properties of Epoxy	17
Table 1.6: Properties of Polymethyl methacrylate (PMMA)	20
Table 1.7: Properties of Polyvinylidene fluoride (PVDF)	22
Table 1.8: Applications of polyurethane during 2006	24
Table 1.9: Predicted growth of nanocomposite industry by 2011	26
Table 3.1: Composition while using Ball mill mixing	45
Table 3.2: Composition while using ultrasonic mixing	45
Table 3.3: Composition of epoxy synthesis	48
Table 3.4: Tensile test samples to ASTM D638	57
Table 4.1: Analysis results on the surface tension of water and epoxy using Drop shape approach	80
Table 4.2: Effect of surface tension on adhesion	81
Table 5.1: Summary of the analysis on tensile test at 0° degree	84
Table 5.2: Summary of the analysis on tensile test at 45° degree	85
Table 5.3: Summary of the analysis on tensile test at 90° degree	85
Table 5.4: Effect analysis on nanoclay lay-ups using factorial design method	87
Table 5.5: Effect analysis on nanoclay lay-ups based on UTP	87
Table 5.6: Effect analysis on nanoclay lay-ups based on Stress	90
Table 5.7: Comparison of tensile properties based on various nanofillers	93
Table 5.8: Comparison of tensile properties at various ratios of nanoclay	95
Table 5.9: Comparison of tensile properties at various mixing durations	98
Table 5.10: Comparison on mixing processes with 1% nanoclay/epoxy matrix	101

STATEMENT OF ORIGINALITY

‘I hereby declare that this submission is my own work and that, to the best of my knowledge and beliefs, it contains no material previously published or written by another person nor material which to a substantial extent has been accepted for the qualification of any other degree or diploma of a university or other institution of higher learning, except where due acknowledgement is made in the acknowledgements’.

.....(Signed)

.....(Date)

Chapter 1

Introduction and Literature review

1.1 Introduction

Since the discovery of nanomaterials in early nineteen's, tremendous progress in the synthesis of nanocomposites has been reported looking for better physical and chemical properties towards various applications. An increasing amount of research has resulted in many nanocomposite polymers being applied in a larger extent to industrial, biomedical and electronic consumer products.

While taking advantage of the advanced processing techniques available from synthesis through characterisation to commercialisation, this research project is aimed at identifying, establishing, developing and characterising a nano-enhanced composite to suit a variety of applications. Also, through this research, a detailed understanding about the properties of potential nanofillers, matrices, possible processing techniques and compositing methods were established through in-depth study adopted with utmost care at every stage to identify an optimal solution. In the latter part, the results were discussed in correlation with different bonding theories to substantiate the conclusions made.

1.2 Background

Composites are becoming common in the polymer science. The term composite often refers to a specific category of advanced material prepared by combining or compositing different materials of required properties to suit particular niche applications. Thus, these composites have emerged primarily as a result of the need where enhanced strengths and performances were required. For example, many

conventional materials that we use in our day-to-day life like plywood and reinforced concrete are composites since they consist of combination of materials. Whereas, the newly developed nano-enhanced composites meet not only the above said demand but are also capable of resisting fatigue, corrosion and vibration besides offering improved physical, mechanical and electrical properties [1]. These nano-enhancements are normally done using reinforcement of nanofillers like nanocarbon, nanoclay, carbon nanotubes, nanometals and metal oxides etc into the polymer matrix. These composites can also be moulded into any shapes to suit varied applications where less weight, good strength and high flexibility are basic needs. These nanocomposites take advantage of the unique properties of the added nanofillers that are developed to optimise the mechanical and electrical properties, besides cutting down the cost of the end product as well. Some of the specific applications using these nanocomposites include structural materials, high performance coatings, catalysts, electronic and photonic components, magnetic materials, biomedical materials, grinding wheels, underground electrical cables, super conducting ribbons and sports materials [2].

As mentioned earlier, nanoparticle reinforced composites consist of nanoparticles dispersed in a matrix of a polymer material. The prefix of the word 'nano' indicates a scale factor of 10^{-9} . A particle of nano size has at least one linear dimension in the range of nanometers. Since it requires about 3 atoms to 10 atoms, depending upon the element, to span one nanometer, a few hundred atoms are about the limit of the dimension of a nanoparticle. But being of a nano size is not what attracts such great interest in nanomaterials, it is their properties. These nanoparticles may have any shape and size but are mostly spherical, ellipsoidal or polyhedral in shape. In this research, spherical nanocarbon and nanoclay were used to reinforce the epoxy resin matrix. These nanofillers weigh less, mould more easily, process dramatically faster and produce better properties. Also, it is important to note that the properties of these nanofillers are different from those of the same material at the macro scale. While these nanofillers possess excellent mechanical properties to play the role as reinforcement by imparting strength and toughness, nanofiller reinforced composites could ultimately provide the foundation for a new class of strong and lightweight materials with mechanical and electrical properties which were not available in the conventional composites. While nanocomposites have been widely reported to

enhance polymers, both mechanically and physically, at this time, there are only a few structural applications, despite a large number of reports claiming improved mechanical properties. However, limited studies in the synthesis and lack of processing technique to uniformly distribute these nanoparticles in a resin base hinder the development of new composites.

Nanotechnology is anticipated to lead a wide range of technical innovations in the near future. Nano-science seeks to gain knowledge and understanding of nano scale phenomena, while nanotechnology employs this knowledge in the development of new products. These products can be materials like nanocomposites with enhanced strength, wear resistance, corrosion resistance or high temperature endurance as discussed earlier. But in general, they are the materials with enhanced performance. On the whole, nanocomposite materials are going to provide novel opportunities in a wide range of technical fields.

In this research, we have included earlier research results reported so far in the literature and work from then on towards synthesising and characterising a nano-enhanced epoxy composite. Therefore the entire preliminary research process is carried out in three steps. They are as follows.

- Study of possible nanofillers for their properties
- Study of possible resins for their properties
- Analysis of the market demand and applications

1.3 Study of possible nanofillers for their properties

A good deal of research work has been carried out on few of the chosen nanoparticles and their contribution in the field of plastics. While we look at the applications, they demonstrate that just a small portion of these tiny particles can cut weight compared to higher loadings of conventional fillers. And at the same time, they do not compromise the benefits such as improved mechanical properties, scratch resistance, barrier properties, fire resistance and dimensional stability. Researchers have found that, carbon nanotubes possess such a remarkable flexibility and strength

which industries should be able to incorporate them into high performance sports and aerospace materials [3]. Carbon fibre composites using graphite are already been used in manufacturing tennis rackets and other products because of their strength and lightness.

While selecting and studying nanofillers for their properties towards the proposed research, besides considering the application and the availability, more weight has been given to the market demand and the commercial aspect of the end product in order to ensure that the outcome of the research would certainly become a value added product. This also ensures the easy processability and marketability of the final nano-enhance composite. Some of the below stated nanofillers considered for this research are substantiated on the grounds of their properties and the end applications. They are:

- Carbon nanotubes
- Nanoclay
- Nanocarbon
- Aluminium oxide nanopowder

1.3.1 Carbon nanotubes

In 1991, long and thin cylinders of carbon nanotubes (CNT) were discovered by S. Iijima [3]. After the discovery, there has been a phenomenal growth in the synthesis of various composites using these carbon nanotubes. Most syntheses were aimed at enhancement of the matrix properties in order to meet special needs and applications. A carbon nanotube is what result if a single graphite sheet is rolled into a long thin tube. It is basically a large molecule of unique size and shape and entirely made-up of carbon atoms, with interesting and remarkable properties. However, the carbon nanotubes vary in size and are not always perfectly cylindrical. They are similar to the structure of graphite.

There are two types of carbon nanotubes defined according to the structure. They are single-walled nanotubes (SWNT) and multi-walled nanotubes (MWNT). SWNTs have only one wall, so they are like a single sheet rolled up into a tube. MWNTs are

a bundle of SWNTs arranged in a concentric fashion to look like an expandable telescope. The former one has a typical outside diameter of 1 nm to 2 nm as shown below while the latter one has an outer diameter of 8 nm to 12 nm [3]. They can range in length from the typical 10 microns to as much as 100 microns and have at least a 1000:1 aspect ratio [3].

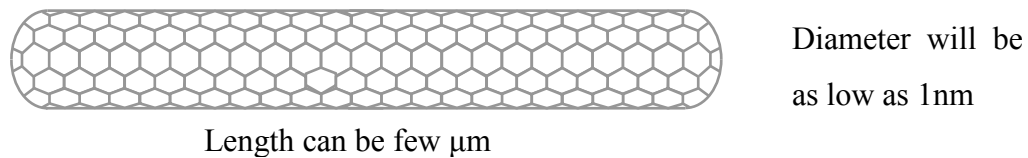


Figure 1.1: Layout of a Single Walled Carbon nanotube [3]

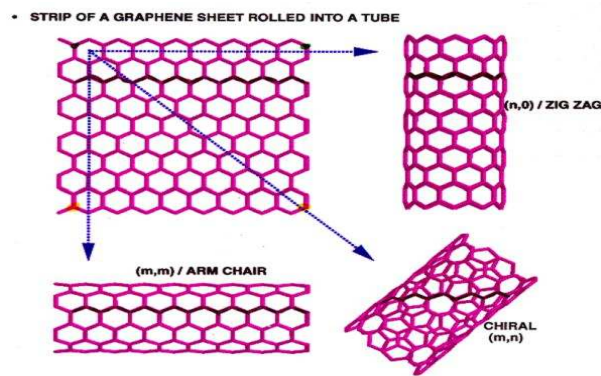


Figure 1.2: Structure of a Single Walled Carbon nanotube [3]

Table 1.1: Properties of carbon nanotubes [4]

Properties of carbon nanotubes	
Young's Modulus	1250 GPa
Tensile breaking strength	11- 63 GPa
Elongation to failure	20% - 30%
Density	1.33 g/cm ³ - 1.40 g/cm ³
Size	5 nm - 50 nm Diameter

A nanotube thread is extremely light in weight and extremely strong because each nanotube has a very strong molecular structure. Recent studies have suggested that single-wall carbon nanotubes have a tensile strength upto 50 GPa to 100 GPa and a modulus of 1 TPa to 2 TPa [5]. Carbon nanotubes have 50 times the tensile strength of stainless steel and 5 times the thermal conductivity of copper [5]. When

incorporated into a polymer matrix, they have the potential to boost the electrical and thermal conductivity over those with traditional fillers like carbon black or metal powders [6].

The addition of low volume i.e. less than 5% by weight of carbon nanotubes to plastic will make it electrically conductive. This interesting property of carbon nanotubes has resulted in the development of electrostatic paints. These types of anti-static coatings are used in the shipping and storing of electronic goods to prevent damages to any of its sensitive electronic components. Also, static dissipative compounds containing carbon nanotubes protect disc read or write heads [6]. Similarly, low loading of carbon nanotubes would increase the speed of thermal dissipation from the coating of resin, resulting in a much faster curing time. This would clearly be of interest in automated processes where the speed of curing limits the rate of production, to save cost on production. Also, carbon nanotubes possess excellent mechanical properties such as reinforcement, for imparting strength and toughness. These carbon nanotubes can be dispersed to develop nano-enhanced composites using two methods. They are by physical mixing or ultrasonic dispersion techniques [6].

However, the physical properties are still being fully discovered and disputed, and the market for these carbon nanotubes has already started growing in finding niche applications. There are still some major barriers to overcome in processing nanotubes for nano-enriched composites. Currently, investigations are carried out to find creative ways to catalyse the production of nanotubes from carbon, besides compositing them. It has been confirmed that identifying the optimum operating parameters and right processing techniques can only produce high-yielding nanotube composites. While optimising the operating parameters, what makes it so difficult is that the property of nanotubes exhibiting a very broad range of electronic, thermal and structural properties for every little change in its diameter, length and twist [7]. And the lack of processing techniques to uniformly distribute these carbon nanotubes has restricted further studies. Also limited knowledge about the toxicity of carbon nanotubes also kept researchers in dispute for long [7]. All these factors at large contribute to the cost of the carbon nanotubes.

1.3.2 Nanoclay

Nanoclay is usually a layered material with a thickness in the order of 10 \AA and with a width extending up to 1000 nm. One gram of powdered material can have billions of nanoparticles with a surface area of many square meters [8]. The particle size is one of the most important aspects of nanoclay and the knowledge of knowing not only the average size but also understanding how the sizes are distributed would be of great importance in nano-compositing. Nanoclay increases stiffness, strength and heat resistance but decreases moisture absorption, flammability and permeability to gas and water. This in turn can result in significant weight reduction, which is of obvious importance in various military, boat building and aerospace applications. Here in this research, some of the vital properties of nanoclay with relevance to their applications in the advancement of nano-science are discussed in detail.

Currently, polymer barrier technology is one of the areas getting a boost from nanoclays. Mitsubishi and Honeywell are both using Nanocor's nanoclays in nylons as barrier layers, in multi-layer PolyEthylene Terephthalate (PET) bottles and films for food packaging. Honeywell has launched its Aegis nylon-6 nanocomposites initially with PET bottles for beer. The U.S. military and National Aeronautics and Space Administration (NASA) in conjunction with Triton Systems Inc., are looking into nanoclay as a barrier enhancer in long shelf-life packaging up to 3 years to 5 years without refrigeration, besides taking advantage of its good clarity, processability and recyclability [9].

Extensive research at National Institute of Standards and Technology (NIST) has established the effectiveness of nanoclay as flame-retardant synergists. According to their research report, loading of nanoclay level up to 2% and 5% in nylon6 reduces the rate of heat release by 32% and 63% respectively [10]. Specialty compounder Foster Corporation is the first company to introduce flame retardant nylon-12/nanoclay compounds for tubing and film making in 2001. Germany's Sud-Chemie also has offered a modified nanoclay called Nanofil as flame-retardants. It has been found that, in general, loading of 1% to 5% nanoclay into a polymer matrix improves flame-retardency [11]. Also, the ability of nanoclay incorporation to reduce the flammability of polymeric materials was the major theme of the paper presented by

Gilman of the National Institute of Standards and Technology in the US. In his work, Gilman demonstrated the extent to which flammability behaviour could be restricted in polymers such as polypropylene with as little as 2% nanoclay loading [12]. Also, by increasing to 8% nanoclay, it reduces the heat distortion temperature (HDT) to nearly 30% per degree Centigrade. This led to potential utilisation as housings on vehicles, door handles, engine covers and timing belt covers.

Among its many other virtues, nanoclay can work as a nucleating agent to control foam cell structure and enhance properties of polymeric foams for applications in insulation and packaging. According to a study in chemically foamed Low Density Polyethylene (LDPE)/wood-fibre compounds by The University of Toronto's Department of Mechanical and Industrial Engineering, addition of 5% nanoclay to the mix would decrease the cell size but increase the cell density to facilitate foam expansion. During one of their experiments, when they burned the foam, it showed good char formation [13]. Similar results were obtained in LDPE/nano-clay foam blown with CO₂ gas. Researchers at Ohio State University's Department of Chemical Engineering have found that when Polymethyl methacrylate (PMMA) is surface coated with small amount of nanoclay, reduces cell size and increase cell density in microcellular Polystyrene foamed with CO₂ [14]. Another study showed that smaller cell size and higher density could be achieved with 5% nanoclay in polyurethane foams blown with pentane or water.

While clays are distinguished from other small particles present in soils by their size or layered shape, their affinity towards water and the tendency toward plasticity are high. Clay is plastic when it is wet which means it can easily be shaped and when it dries, it becomes firm. Also, when it is subjected to high temperatures such as firing, permanent physical and chemical reactions occur which cause the clay to be converted into a ceramic material. In addition to that, water-laden atmospheres have always been considered as one of the most damaging and difficult environments to the growth of polymeric nanocomposites in such applications. In this situation, the ability to minimise the water absorption could be of great advantage. Data provided by Beall from Missouri Baptist College indicate that a significant volume of incorporation of nanoclay into a polymer matrix can reduce the extent of water absorption. Thus, applications in which contact with water or moist environments

involved is likely to be benefited by incorporating nanoclay as fillers in hygroscopic polymers [15].

Nanoclay particles are one of the most widely used nanofillers in many structural applications because they are abundant in nature and thus are inexpensive and moreover they have high in-plane strength and stiffness. Nanoclay composites are usually used to provide various rheological characteristics to solvent based or oil based formulations. Also, in-comparison with conventionally filled polymers, incorporation of nanoclay into a polymer matrix has shown a significantly improved transparency besides reducing haze. Apart from the above-discussed applications of nanoclay in composites, these are some of the more general applications currently being considered as impellers and blades for vacuum cleaners; power tool housings; mower hoods and covers for portable electronic equipment such as mobile phones, pagers, laptops etc.

One of the few disadvantages associated with nanoparticle incorporation is concern about toughness and impact performance. Louisiana State University's Mechanical Engineering Dept. reports that 4% to 5% nanoclay increases the flexural strength and elongation of epoxy syntactic foams, when used as core material for composites in structural applications [16]. At the same time, the most discussed benefit of nanoclay is its impact modulus balance. Data provided by Hartmut Fischer of Netherlands Organization for Applied Scientific Research (TNO) relating to polyamide montmorillonite nanocomposites indicate tensile strength improvements of approximately 40% and 20% at temperatures of 23°C and 120°C respectively and modulus improvements of 70% and remarkable 220% at the same temperatures [17]. Similar mechanical property improvement like increase in stiffness was also noticed with Polymethylmethacrylate/nanoclay composites while reducing the warp to control shrinkage. During this research, the importance of complete exfoliation of nanoclay in epoxy matrix was stressed as the key performance requirement to achieving nano-enhanced properties because complete exfoliation will enhance the physical property modulus. The physical property modulus is the indication of reinforcing effect with the aspect ratios.

While there are a handful of fully compounded, nanocomposite materials in the market, there are also highly loaded nanoclay master batch materials available which can provide the processor the ability to truly tailor an existing material to the requirements needed for various applications.

1.3.3 Nanocarbon

Carbon is widely distributed in nature as an element of prehistoric discovery, which can exist as black graphite, colourless gem diamond or as fullerenes. Carbon is found in abundance in the sun, stars, comets and atmospheres of most planets. It is found in hydrocarbons like methane gas, oil and coal and also as carbonates like limestone and dolomite. Carbon is unique among other elements by the variety of compounds it can form. Mostly with the combination of hydrogen, oxygen and nitrogen it forms very large numbers of compounds because of its unique ability to form chains are thought to be the most important reason for the dependence of life on this element. It is also an indispensable source for various everyday products.

Carbon is more essential to life, because only carbon forms strong single bonds to itself that are stable enough to resist chemical attack under ambient conditions [18]. This gives carbon the ability to form long chains and rings of atoms as shown in figure 1.3. These long chains and rings of atoms become the structural basis for many compounds that comprise the living cell, of which the most important is the DNA [18]. There are several million known carbon compounds, many of which are vital to organic and life processes as above.

Carbon oxides exist in several allotropic forms such as amorphous, graphite and diamond. While graphite is used in lubricants, diamond is one of the hardest known materials. This difference is purely because of the arrangement of atoms in each of the two forms. In graphite, hexagonal rings are joined together to form sheets, and the sheets lie one on top of the other. In diamond, the atoms are arranged tetrahedral in a tetrahedrally continuous array [19].

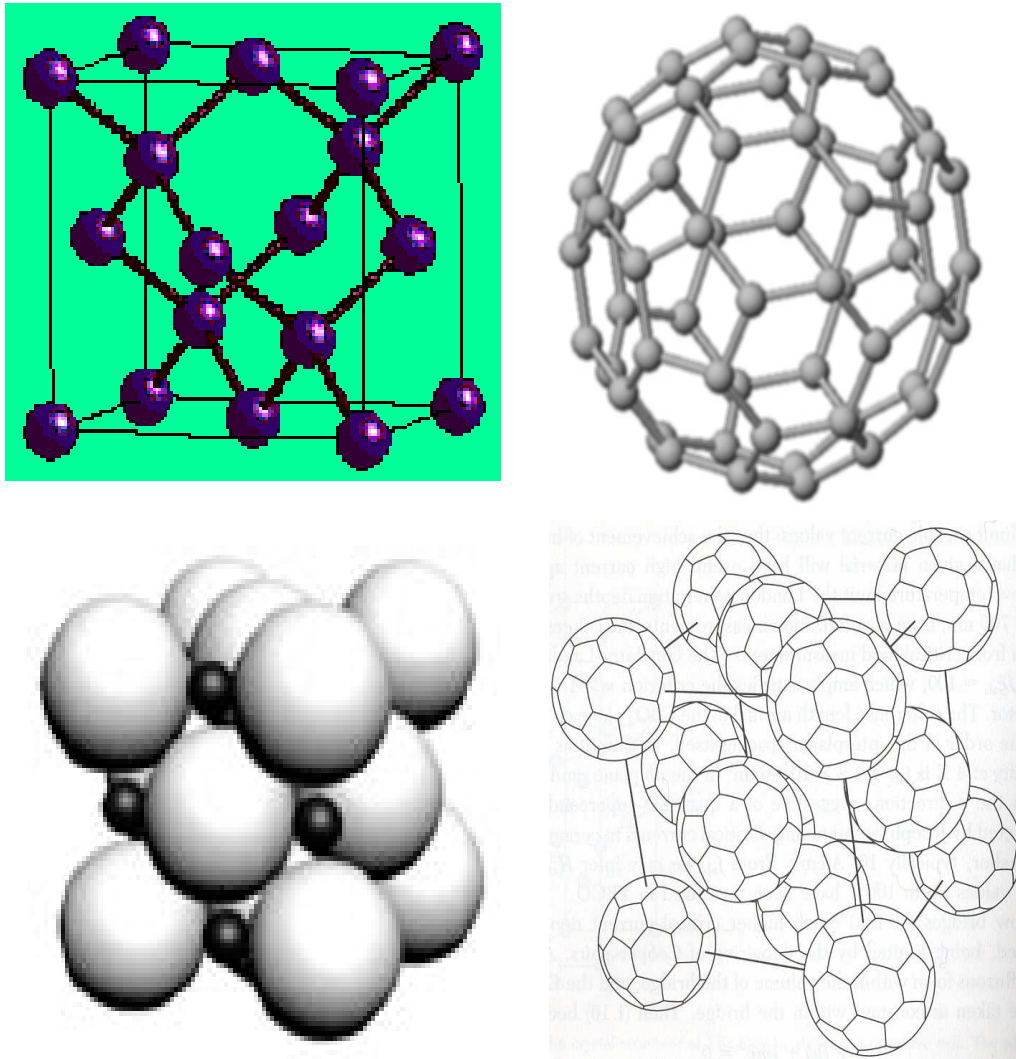


Figure 1.3: Molecular structure of nanocarbon [18]

But carbon nanoparticles occur in five different basic forms. They are diamond, graphite, fullerenes, nanotubes and nanocones. Most of the research activities in nanocarbon are focussed on the last two, which are of the most interest for new technological applications because of their enormous tensile and compressive strength.

Table 1.2: Properties of nanocarbon [20]

Properties of nanocarbon	
Atomic Number	6
Melting Point	3652°C
Boiling Point	4827°C
Density	2.2 g/cm ³ at 20°C
Size	10 ⁻⁹ m (1 nm)
Atomic radius	0.077 nm
Heat of fusion	100 kJ·mol ⁻¹
Crystal structure	Hexagonal
Thermal conductivity	300 K for graphite
Mohs hardness	1-2 for graphite

Nanocarbon is known for its self-lubricating and dry lubricating properties. It is unique in its chemical properties because it forms a number of components greater than the total of all the other elements in combination with each other. Nanocarbons are sold to the tune of 1 million tonnes annually worldwide because they are far less expensive than carbon nanotubes. This adds the advantage of being used as the most widely adopted nanofiller for many advanced industrial applications.

1.3.4 Aluminium oxide nanopowder

Aluminium oxide, commonly referred as alumina with the chemical formula Al₂O₃. As indicated, it is a chemical compound of aluminium and oxygen with strong ionic interatomic bonding, giving rise to its desirable material characteristics. This can exist in several crystalline phases, which can be reverted to the most stable hexagonal alpha phase at elevated temperatures. Alpha phase alumina is the strongest and the stiffest of the oxide ceramics. Its high hardness, excellent dielectric properties and good thermal properties make it the material of choice for a wide range of applications [20]. It is also known for its excellent size and shape capabilities with high strength and stiffness too. Annual world production of aluminium oxide is approximately 65 million tonnes, over 90% of which goes to the manufacture of aluminium metal.

Aluminium oxide nanopowder with an average particle size of 40 nm to 50 nm holds a specific surface area of $35 \text{ m}^2/\text{g}$ to $45 \text{ m}^2/\text{g}$ [21]. It has twice as many particles per kg but approximately 50% less dense than the metallic media. Aluminium oxide is also known for its resistance to weathering and its resistance to strong acids and alkalis, even at elevated temperatures [22].

Table 1.3: Physical and Chemical properties of Aluminium oxide [20]

Physical and Chemical properties of Aluminium oxide	
Odour	Odourless
Solubility	Insoluble in water
Boiling Point	2980°C
Melting Point	2000°C
Stability	Stable under ordinary conditions
Hazardous Polymerisation	Will not occur
Incompatibilities	Chlorine trifluoride, Ethylene oxide
Conditions to Avoid	Incompatibles
Water Absorption	Nil
Crystal structure	Cubic
Average Particle Size	10 nm - 50 nm
Specific Surface Area	$35 \text{ m}^2/\text{g}$ - $45 \text{ m}^2/\text{g}$
Colour	Ivory

It has been found that the thermo-mechanical characteristics of nanocomposite using nanoaluminium oxide can also be improved by controlling the nanostructure. Melting points and sintering temperatures can be reduced up to 30%, if the material is made of nanoaluminium oxide powders [23]. Such materials are investigated as alternatives for titanium in components of liquid propelled rocket engines, since they are lighter and less susceptible to the embrittlement by hydrogen.

Table 1.4: Mechanical, Thermal and Electrical properties of Aluminium oxide [24]

Mechanical	Units of Measure	SI/Metric
Density	g/cm ³	3.89
Porosity	%	0
Flexural Strength	MPa	379
Elastic Modulus	GPa	375
Shear Modulus	GPa	152
Bulk Modulus	GPa	228
Poisson's Ratio	—	0.22
Compressive Strength	MPa	2600
Hardness	Kg/mm ²	1440
Fracture Toughness KIC	MPa•m ^{1/2}	4
Maximum Use Temperature	°C	1750
Thermal		
Thermal Conductivity	W/m°K	35
Coefficient of Thermal Expansion	10 ⁻⁶ /°C	8.4
Specific Heat	J/Kg•°K	880
Electrical		
Dielectric Strength	kv/mm	16.9
Dielectric Constant	@ 1 MHz	9.8
Dissipation Factor	@ 1 kHz	0.0002
Volume Resistivity	ohm•cm	>10 ¹⁴

Aluminium oxide grit powder has a wide variety of applications ranging from cleaning engine heads, valves, pistons and turbine blades in the aircraft industry to lettering-in monument and marker inscriptions. It is also commonly used for matt finishing as well as cleaning and preparing parts for metallising, plating and welding.

As an angular durable blasting abrasive, aluminium oxide can be recycled many times. It is the most widely used abrasive in blast finishing and surface preparation because of its cost, durability and hardness. It is harder than other commonly used blasting materials and can penetrate and cut even the hardest metals and sintered carbide. Therefore, it is very widely used as an abrasive as a significantly less expensive replacement for industrial diamonds. Many types of sandpaper use aluminium oxide crystals. The major uses of speciality aluminium oxides are in refractories, ceramics, polishing and abrasive applications. Aluminium oxide is used in certain CD and DVD cleaning kits. This can polish the media surface, leaving it clean and relatively scratch free. Aluminium oxide is the best choice for preparing a surface for painting.

Nanoaluminium oxide is one of the most cost effective and widely used materials in composite industry too. With an excellent combination of properties at an attractive price, it is no surprise that this research has included nanoaluminium oxide towards very wide range of applications in biomedical engineering as well.

1.4 Study of possible resin matrix for their properties

Considering the processability and the market potential, the following resins were considered for the synthesis process. While doing so, maximum emphasis was given to accommodate the above-discussed nanofillers towards the enhancement aimed at.

- Thermoset resins
 - Epoxy
- Thermoplastic resins
 - Polymethyl methacrylate (PMMA)
 - Polyvinylidene difluoride (PVDF)
 - Polyurethane

1.4.1 Thermoset resins

Looking at the versatile nature of epoxy, it has been considered to have a greater advantage with regard to the future prospects of this research in extending the

outcome of this research, in developing functional applications and in biomedical engineering. In fact, epoxy can be developed to meet a wide range of applications because of its superior matrix properties.

1.4.1.1 Epoxy

Epoxy resins, both monomers and oligomers, can be powders or they can be thick and clear or yellow liquids with strong and unpleasant odours. They are known for their excellent adhesion, chemical and heat resistance, excellent mechanical and good electrical insulating properties. Moulding a fibre reinforced epoxy composite is much easier compared to other thermoset resins [25]. The typical applications of epoxy are in adhesives, electrical parts, coating and lamination process, moulds/dies/tools and in military, biomedical and automotive fields.

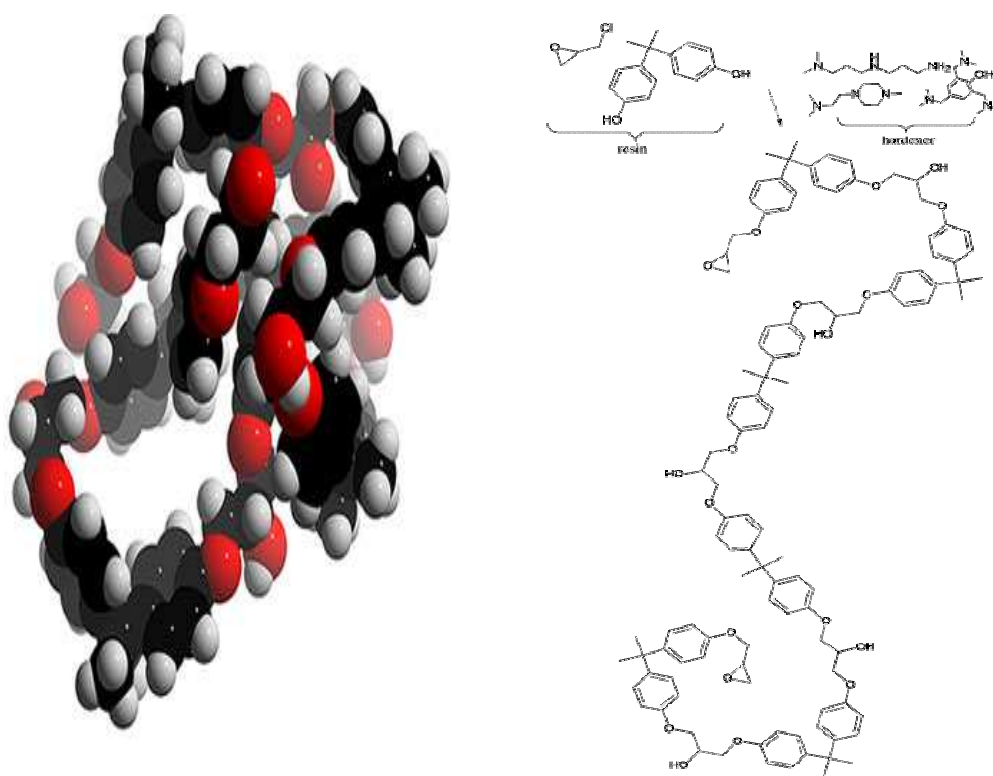


Figure 1.4: Typical structure of epoxy molecule (Courtesy: 3D Chem) [26]

Epoxy being a thermoset polymer, during the process of curing, when mixed with a curing agent or a hardener, polymerises and cross-links. In other words, this curing agent reacts with epoxy resin monomers to form an epoxy product. The curing agent selection will determine to a large extent the performance of the final epoxy

composite. Polyester thermosets typically use a ratio of at least 10:1 of resin to hardener, whereas epoxy composites use as low as from 5:1 to 1:1 [26]. Epoxy composites tend to harden somewhat more gradually while polyester materials tend to harden quickly.

Table 1.5: Properties of Epoxy [25]

Properties of Epoxy	
Density	1.54 g/cm ³
Tensile Modulus, E	3.5 GPa
Poisson's ratio, ν	0.33
Shear Modulus, G	1.25 GPa
Longitudinal Tensile Strength, σ	60 MPa
Longitudinal Thermal Expansion, α	$57.5 \times 10^{-6} \text{ K}^{-1}$

Fillers add bulk and body to epoxy products and thus epoxies can be modified. These fillers are usually powders such as silica, clay, alumina and calcium carbonate and fibres like fibreglass and asbestos. Normally, during industrial applications, machinability of the epoxy-based end product can be improved by adding powdered aluminium, copper, calcium carbonate or calcium silicate to the epoxy resin base. Similarly abrasion resistance can be improved by adding aluminium oxide, flint powder, carborundum, silica or molybdenum disulfide. Impact strength can be improved by adding chopped glass or other fibrous materials. Electrical properties can be improved by adding mica, silica or powdered or flaked glass. Thermal conductivity can be improved by adding metallic fillers or coarse sand or alumina. Finally, anti-settling or flow properties can be improved by adding colloidal silica or clay. Thus, epoxy resin exhibits its versatile nature in accommodating various fillers to develop a variety of end products to suit various applications. Epoxy composites can be developed to meet almost any application. Also, during an epoxy composition, the addition of fillers, flexibilisers, viscosity reducers, colorants, thickeners, accelerators and adhesion promoters can lower the costs, reduce exotherm, extend pot life, improve processing convenience and achieve greater improvement what this research is actually looking for [27].

In addition, epoxy resins are the major part of the class of adhesives called 'structural' adhesives. These high performance adhesives are normally used in the construction of aircraft, automobiles, bicycles, golf clubs, skis, snowboards and other applications where high strength bonds are required. Also, they are exceptional adhesives for wood, metal, glass, stone and some plastics. Epoxy resins can be made flexible or rigid, transparent, opaque or coloured and fast setting or extremely slow setting. Further, epoxy adhesives are almost unmatched in heat and chemical resistance among common adhesives. Usually epoxy requires heat curing for maximum performance [28]. Therefore epoxy adhesives cured with heat will be more heat and chemical resistant than those cured at room temperature. Also, the peak adhesion strengths achievable for epoxy/metal interfaces depends greatly on the types and sequences of wet chemicals used to treat the surface. For all these reasons, they are used in high performance and decorative flooring applications too. Whereas, in the aerospace industry, epoxy reinforced with fibre is used as a structural matrix material.

Epoxy coatings are also widely used as primers to improve the adhesion of automotive and marine paints especially on metal surfaces where corrosion resistance is important. However, they are not used in the outer layer of a boat as they can deteriorate when exposed to ultra violet light. But they are often used during boat repair and assembly and also over-coated with conventional paints or marine varnishes which can provide ultra violet protection [29]. Also, metal cans and containers are often coated with epoxy to prevent rusting especially for foods like tomatoes, which are acidic in nature.

Epoxy resin is an excellent electrical insulator too. It helps to protect electrical components from short-circuiting due to dust and moisture. Hence, epoxy resins are important in the electronic industry, finding application in motors, generators, transformers, switchgears, bushings and insulators. Also, in the electronic industry, epoxy resins are the primary resin used in moulding integrated circuits, transistors and hybrid circuits. The cured epoxy is an insulator and a much better conductor of heat than air. Using epoxy in transformers and inductors, greatly reduces hot spots which in turn give the component a stable and longer life than unpotted products

[30]. Normally, wet chemical surface synthesis reactions are employed on thin epoxy layers for usage as a build-up layer in microelectronics.

Another interesting property of epoxy is that it does not stick to mould release compounds like paraffin wax, polyethylene sheeting, sandwich bags and the non glued side of packaging tape which is of great use during lay-ups and also during the manufacturing of precision parts.

Though they are more expensive than polyester resins, in brief, the purpose of selecting epoxy as the base resin for this research is because of its unmatched high chemical and thermal resistance, good adhesion to various materials, compatibility with various substrates and other additives, low shrinkage, availability of solvent free formulations, light in colour, easy to control viscosity and low vapour pressure besides holding good to excellent mechanical properties and very good electrical insulating properties.

1.4.2 Thermoplastic resins

Thermoplastic resins for their reversible property besides being easy to process find wider applications in nano-science too. With these advantages in the background, during this research an attempt has been made to develop nano-enriched polymer composites. Some of the thermoplastic resins considered for this research are discussed below for their properties.

1.4.2.1 Polymethyl methacrylate (PMMA)

Polymethyl methacrylate (PMMA) was developed in 1928 in various laboratories but was then first brought to the market during 1933 by a German company called Rohm and Haas (GmbH & Co. KG). PMMA is a clear and rigid plastic and often used as an alternative to glass. It is a low dense plastic and its density can range between 1150 kg/m³ to 1190 kg/m³, which is less than half the density of glass. PMMA has higher impact strength than glass. So it does not shatter but instead breaks into large pieces during high impacts. On the other hand, PMMA is softer and can be more easily scratched than glass. But this can be overcome by using a scratch-resistant coating. PMMA is typically processed at a lower temperature than glass, i.e. around 240°C to

250°C which is one of the good reasons for its wider market than glass. PMMA does not filter ultraviolet (UV) light. PMMA transmits UV light down to 300 nm. PMMA allows infrared light up to 2800 nm wavelength to pass but aids as a resistance in the electron beam lithography process [31].

Table 1.6: Properties of Polymethyl methacrylate (PMMA) [31]

Properties of Polymethyl methacrylate (PMMA)	
Density	1.19 g/cm ³
Refractive index	1.492 ($\lambda=589.3$ nm)
Specific gravity	1.18
Melting point	130°C - 140°C
Boiling point	200°C
Tensile strength	70 MPa
Flexural modulus	2.9 GPa
Maximum operating temperature	55°C

Since PMMA is basically a clear material it can take a very good glossy finish. PMMA windows can be made as thicker as 33 cm, and still they remain transparent. This makes it a right material for making large aquariums, whose windows must be thick in order to contain the high pressure due to a large volume of water. PMMA glasses are used in viewing ports and even in the complete hulls of submersibles. Polycast stretched acrylic sheet is the most widely used material in aircraft windows [32]. PMMA are also employed in domed skylights, swimming pool enclosures, aircraft canopies, instrument panels, spectator protection in ice hockey stadia and luminous ceilings. PMMA is also occasionally used as a glass substitute in picture framing for cost saving reasons besides being light in weight and its shatter-resistance. Also it can be ordered in larger sizes than standard picture framing glass [32].

PMMA can also be easily polished to restore cut edges to full transparency and hence it finds greater applications in lighting and glazing. PMMA is used in the lenses of exterior lights of automobiles. Motorcycle helmet visors and glasses in police vehicles used for riot control often have the acrylic glass to protect the

occupants from thrown objects. Many other products like electric guitars and drums are sometimes made with acrylic glass to get a transparent look.

In the field of medicine, PMMA has a high degree of compatibility with human tissue, so it can be used for replacement of intraocular lenses in the eye, when the original lenses are removed during the treatment of cataracts [33]. In orthopaedics, PMMA bone cement is used to affix implants and to remodel lost bones. Dentures are often made of PMMA and can be colour matched to the patient's teeth and gum tissue. In cosmetic surgery, tiny PMMA microspheres suspended in some biological fluid are injected under the skin to reduce wrinkles or scars permanently [33].

Apart from the above-discussed applications of PMMA with regard to its properties, here are some of the varied ranges of other applications. Acrylic paints essentially contain PMMA suspended in water. PMMA can be joined using cyanoacrylate cement, which is commercially called Superglue to dissolve the plastic at the joint, which then fuses and sets to form almost an invisible weld.

1.4.2.2 Polyvinylidene fluoride (PVDF)

Polyvinylidene fluoride (PVDF) is a highly non-reactive and thermoplastic fluoropolymer. It was developed primarily for applications demanding excellent chemical resistance, high levels of purity and superior mechanical properties. PVDF is often used as a lining or protective barrier in chemical industry applications. Compared to other fluoropolymers, it has relatively low melting point which in-fact enables easier melt processing [34]. It can also be injection moulded and welded and hence it is commonly used in the chemical, semiconductor, medical and defence industries. Also it has a relatively low density and it is of low cost too.

Table 1.7: Properties of Polyvinylidene fluoride (PVDF) [34]

Properties of Polyvinylidene fluoride (PVDF)	
Density	1.76 g/cm ³
Coefficient of expansion, α	$0.18 \times 10^{-6} \text{ K}^{-1}$
Appearance	Whitish or translucent solid
Solubility in water	Not soluble in water
Melting point	134 °C - 169 °C
Thermal conductivity	$0.18 \text{ W m}^{-1} \text{ K}^{-1}$
Specific gravity	1.77
Percentage of elongation	300 to 450
Tensile strength	4500psi - 6200psi
Flexural strength	8600psi - 9500psi
Compressive strength	11,600psi
Tensile elastic modulus (Young's modulus)	160,000psi
Flexural modulus	90,000psi ~ 168,000psi

PVDF is a ferroelectric polymer too and hence it can exhibit efficient piezoelectric and pyroelectric properties. These particular characteristics of PVDF make it useful in sensor and battery applications. Thin films of PVDF are used in some newer thermal camera sensors [35].

PVDF is also used as a principal ingredient in many high-end paints for metals. These PVDF paints have extremely high gloss look and good colour retention too.

The main purpose of including PVDF in this research is because it is known for its excellent resistance to creep and fatigue, excellent thermal stability, excellent radiation resistance, superior tensile properties and impact strengths, excellent resistance to reduce high dielectric strength over a wide temperature ranges.

1.4.2.3 Polyurethane

Polyurethane is a polymer consisting of a chain of organic units joined by urethane links. The German chemist, Friedrich Bayer in the year 1937, initiated research in the chemistry of polyurethane materials. Polyurethanes are light in weight and have a high degree of stretchability, which makes them good for applications in sports

apparels. Though the properties of the polyurethane are determined mainly by the choice of polyol and to some extent by the di-isocyanate, the curing rate is influenced by the functional group. And the molecular shape influences the mechanical properties. But the existence of di-isocyanate affects the stability of polyurethane when exposed to light [36].

As polyurethane products have many uses, some of the relevant ones are discussed here. Over three quarters of the global consumption of polyurethane products is in the form of flexible and rigid foams, roughly equal in market size. Rigid foams are usually inside the metal and plastic walls of most refrigerators and freezers or behind other surface materials in the case of thermal insulation panels in the construction sector. The precursors of expanding polyurethane foam are available in many forms for the use in insulation, sound deadening, flotation, packing material and even in upholstery padding. Since they adhere to most surfaces and automatically fill voids, they have become quite popular in these applications [37]. As an adhesive, polyurethane is also used to glue windshields into automobiles. Polyurethane is used as an adhesive, especially as woodworking glue for its main advantage of being water resistant over more traditional wood glues.

In addition, polyurethane has many characteristics that make them useful in a much wider variety of applications. Polyurethane is also used in making solid tyres. Microcellular foam variants are widely used in tyres of wheelchairs and bicycles. It is widely used in high performance adhesives and sealants, gaskets, condoms, carpet underlay and hard plastic parts. These foam types are also widely used in car steering wheels and other interior and exterior automotive parts including bumpers and fenders due to its unique property of good stretchability and also in places where tight grips are needed [37]. Polyurethane ensures grip and wraps neatly. Polyurethane has been used to make tennis overgrips. It is used on the bottom of some mouse pads too.

With additives like nanofillers, polyurethane can improve its fire resistance and stability difficult chemical environments besides, as well as other physical and mechanical properties to suit the need of the desired end product [38]. The following Table 1.8 show where polyurethanes are used.

Table 1.8: Applications of polyurethane during 2006 (US Chemical data Inc., 2006)

Application	Amount of polyurethane used (Millions of pounds)	Percentage of total
Building and Construction	1,298	23.8
Transportation	1,298	23.8
Furniture and Bedding	1,127	20.7
Appliances	278	5.1
Packaging	251	4.6
Textiles, Fibres and Apparel	181	3.3
Machinery and Foundry	178	3.3
Electronics	75	1.4
Footwear	39	0.7
Other uses	558	10.2
Total	5,444	100

Polyurethanes are considered for this research for their excellent electrical properties, excellent adhesion, impact strength and low temperature flexibility, besides being cheap and easily available in the market, making a commercial project viable in the latter stage.

1.5 Analysis of the market demand and applications

The purpose of carrying out a detailed market survey is to understand the overall market demand and growth rate in the field of nanocomposites, in order to ascertain the target segment towards capitalising the outcome of this research. Apart from that, this market survey provided adequate information to develop a product, which will be viable in terms of commercial aspect. In short, the market survey gave an overall picture of the global trend in the nanocomposite industry, which is vital at this juncture.

Nanoparticle reinforced polymers have already entered the market in automotive, packaging and structural applications in a low profile manner and slower than had been anticipated. But that pace is expected to speed up considerably as indicated by the enthusiasm of researchers and marketers. Though the nano-researches are still in the early stage, if the forecasts are right, nanocomposites would become the biggest little thing to hit plastics in decades. Polymers reinforced with as little as 2% to 5% of these particles exhibit dramatic improvements in thermo-mechanical properties and electrical properties, which are really promising.

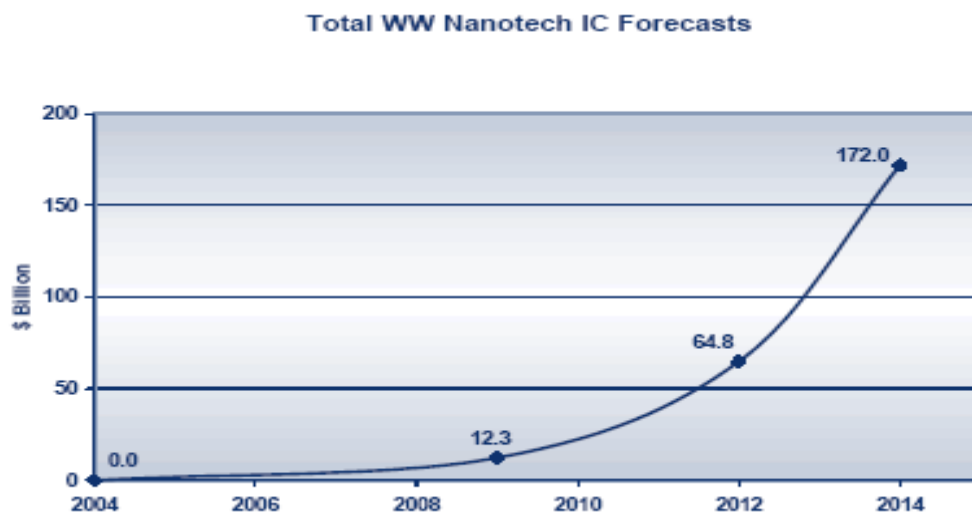


Figure 1.5: IC Forecasts (Courtesy: Nanotech) [39]

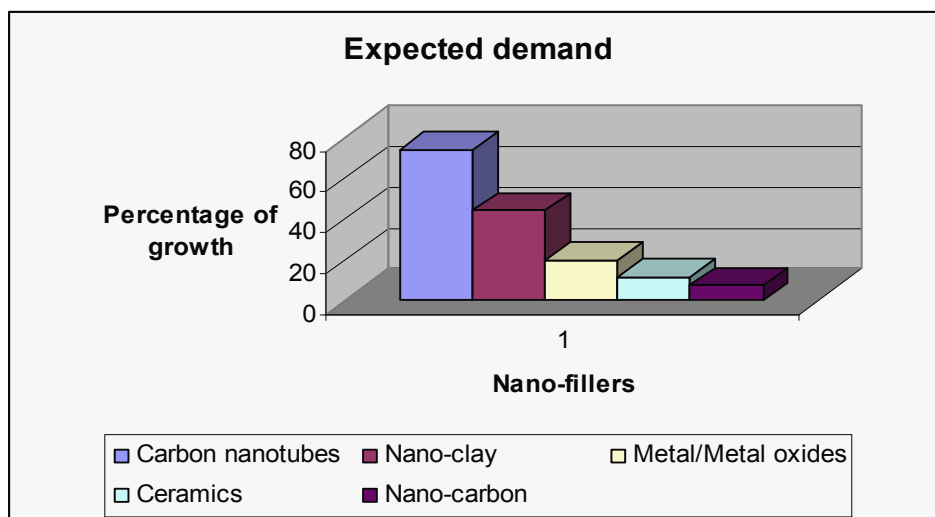


Figure 1.6: Predicted demand of nanofillers in the composite industry [40, 43, 45]

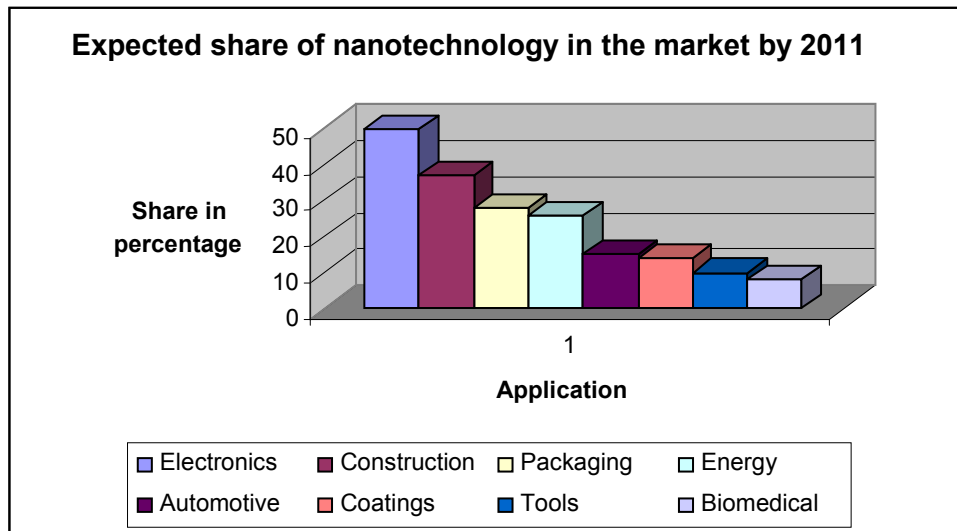


Figure 1.7: Expected share of nanotechnology in the market by 2011. [41, 42, 44]

Reports from a market research firm Business Communications Co. Inc. (BCC), Norwalk, say that the total worldwide market for nanocomposites were around 26 million kgs during the recent years which is valued at US\$ 90.8 million. The firm projects the market to grow at an average annual rate of 18.4% to reach USD 211.1 million by 2011. Even if these nano-developments hit some technical hitches, BCC also says that some of the applications like construction, packaging and automotives will grow more than 20% each year [40, 41].

Table 1.9: Predicted growth of nanocomposite industry by 2011 [40,41,42,43,44,45]

Nanofillers wise	Expected growth by 2011 (In Percentage)	Applications wise	Expected share by 2011 (In Percentage)
Carbon nanotubes	73.8	Electronics	50
Nanoclay	44	Construction	37
Metal/Metal oxide	20	Packaging	28
Ceramics	11.5	Energy	26
Nanocarbon	7.5	Automotive	15
		Coatings	14
		Tools	10
		Biomedical	8

Nanoclay composites accounted for nearly one quarter (24%) of total nanocomposite consumption by value in 2005 followed by metal and metal oxide nanocomposites (19%) and carbon nanotube composites (15%). According to BCC, the consumption of nanoclay composites is projected to increase their market share to 44% by the year 2011 [41]. Apart from that, other market share gainers include metal/metal oxide nanocomposites and ceramic nanocomposites, which are projected to attain market shares of 20% and 11.5% respectively between 2009 and 2011, whereas nanocarbon composites are expected to lose market share down to 7.5% [41].

On the other hand, according to Andrew McWilliams, a business consultant specialising in the plastics industry, nanocomposites incorporating nanoclay and nanocarbon reinforcements expect to become a major growth segment by 2011[42]. Automotive, electrical/electronics and packaging were the main nanocomposite applications in 2005, with 29%, 28%, and 19% market shares respectively [42]. Other major applications in 2005 were coatings (14%) and tooling (8%). But by the year 2011, packaging is expected to become the leading nanocomposite application with over 28% of the market. Energy applications will remain in second place in 2011 with more than 26% of the market. Again, automotive applications will be the third largest application in 2011 with over 15% of the market, followed by coatings with 14% [43].

General Motors has already taken the lead in putting nanocomposites on the road. They have launched their first commercial use of a nanocomposite in the auto exterior in the 2002 models of GMC Safari and Chevrolet Astro van. Also, in their 2003 and 2004 year models, they have included more parts made out of nanocomposites. More recently, a PP/nanoclay composite appeared on the body side moulding of General Motors' highest volume car, the Chevrolet Impala. General Motors reports that it currently uses about 73,000 kgs of nanocomposite materials per year [44].

On all these above-mentioned market researches, the leading nanofillers that have been most widely discussed are the ones to first break into the commercial market. They are nanoclays, nanocarbon and carbon nanotubes. Besides these, other candidates being actively considered for our future research are synthetic clays and

natural fibres like flax and hemp. All these nanofillers have demonstrated improvements in structural, thermal, barrier and flame-retardant properties. So far, nanoclays have shown the broadest commercial viability due to their lower cost of US\$ 5 per kg to US\$ 7 per kg [45].

While nanoclay adds strength to plastics, carbon nanotubes impart electrical and thermal conductivity. The commercial potential of carbon nanotubes in general has is being limited by the complications involved in their bulk processing and high price tags, reportedly in the range of US\$ 100 per gram. Still, nearly every car produced in the US since the late 1990s contains some carbon nanotubes, typically blended into nylon to protect against static electricity in the fuel system [45].

1.6 Objectives

This research is aimed at studying the potential enhancement of the material properties of polymer resin base through the addition of nanofillers.

Although there is a significant amount of research done in studying the property changes occurring with the use of nanofillers, not much involve improving the process used in preparing these composites. The difficulties of handling and processing of nanomaterials have prevented the widespread commercial application of nanofilled composites. Developing a feasible process of preparing nano-enhanced composites is the main part of this research. This includes the following aspects:

- Identifying the right nanofiller.
- Identifying the optimal volume of nanofiller and resin matrix.
- Finding a suitable process to ensure even dispersion of nanoparticles in the resin matrix.
- Testing and characterising the samples of the nano-enhanced matrix and the lay-up.
- Analysis, modelling and validation to ascertain the enhancement.

However, previous work has indicated that addition of nanofillers in composites resulted in increase in strength and other beneficial property enhancements such as

thermal, electrical etc. When compared to the composites using ordinary fillers, during this research, the newly developed nanocomposite matrix and the lay-up will be tested and characterised to attain optimal values with regard to enhancement.

In the next chapter, in order to identify and to determine the need for specialised process to suit the application, preliminary experimental research processes are discussed in detail, towards sample preparation and characterisation of the newly developed nano-enhanced composites.

Chapter 2

Experimental Investigation

2.1 Study of different synthesis processes and characterisation

When materials are reduced to small sizes, typically less than 50 nanometers, novel physical, chemical and electrical properties arise that provide opportunities for new applications. These surface properties can be optimised for a particular application through molecular modifications also [46]. Working with nano-scale systems requires special tools for manipulating, measuring and controlling the size and properties.

With an aim to ensure even dispersion of nanoparticles along the resin matrix the following synthesis processes are carefully studied with due importance to their revolutionary commercial applications in biomedical engineering. This should defeat the problems encountered during synthesis faced by the earlier researches which in-turn should bring an end to the persisting problem hurdling the growth of research in developing an enhanced nanocomposite material. While doing so, this research also considered the fact that the mechanical properties of nanocomposites are strongly influenced by slight change in the processing route. With this in the background, through this research, an optimal way of synthesising a nanocomposite has been developed and demonstrated in two stages as follows.

- Mixing techniques
 - Ultrasonic mixing
 - Mechanical mixing
- Moulding techniques
 - Sintering
 - Moulding
 - Infusion

2.1.1 Mixing techniques

In any compositing operation, mixing is one of the most important processes. Mixing is a process by which the ingredients are thoroughly blended to for uniform distribution of composite. In the field of nano-compositing, mixing is the basic process through which perfect impregnation or dispersion of the nanoparticles in the base matrix can be achieved. Some of the commonly used mixing techniques are shear mixing, extrusion, ultrasonic mixing, mechanical mixing and mixing through vapour evaporation. In this research, ultrasonic mixing and mechanical mixing are considered, due to their most favourable mixing results, operational ease and their viability on mass production.

2.1.1.1 Ultrasonic mixing

Sound is not always audible. Ultrasound, often referred to as ultrasonics, literally means beyond sound, or above the human audible spectrum. The human ear is most sensitive to the frequency range of 1 kHz to 5 kHz, which is in-between the lower and upper limits of 0.3 kHz to 19 kHz whereas ultrasonics refers to sound above 19 kHz. Langevin, a pioneer in the field of ultrasonics, designed, built and experimented with high-power, magnetostrictive ultrasonic equipment [47].

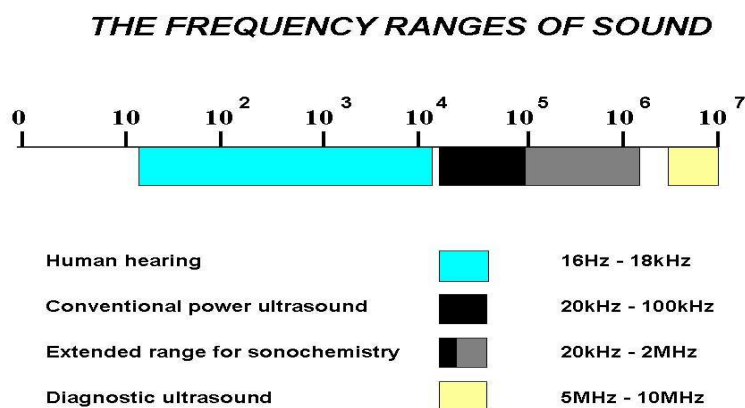


Figure 2.1: Frequency ranges of sound

The growing list of markets utilising short range ultrasonics includes, biotechnology, analytical chemistry, environmental testing, industrial processing and pharmaceuticals besides underwater range finding (SONAR) and in the non-

destructive testing of metals for flaws too. During any chemical process, to increase the chemical reactivity, external elements like heat, pressure, light and even catalysts are used during conventional methods. But off late it has been found that ultrasonics has potential to enhance the chemical reaction during such processes. Sound waves are transmitted through a medium as pressure waves and the mere act of transmission causes excitation in the medium, in the form of enhanced molecular motion [47]. However, in order to produce the fullest effect, the sound energy must be generated within the liquid itself, because the transfer of sound energy from the air into a liquid will not be efficient. With this principle in the background, ultrasonics is used in analytical chemistry for many common procedures, which include breaking of chemical bonds, forming free radicals, polymerising and depolymerising long chain molecules, besides sample preparation and analysis. Thus ultrasound has been found to be beneficial for the initiation or enhancement of catalytic reactions in both homogeneous and heterogeneous cases [47].

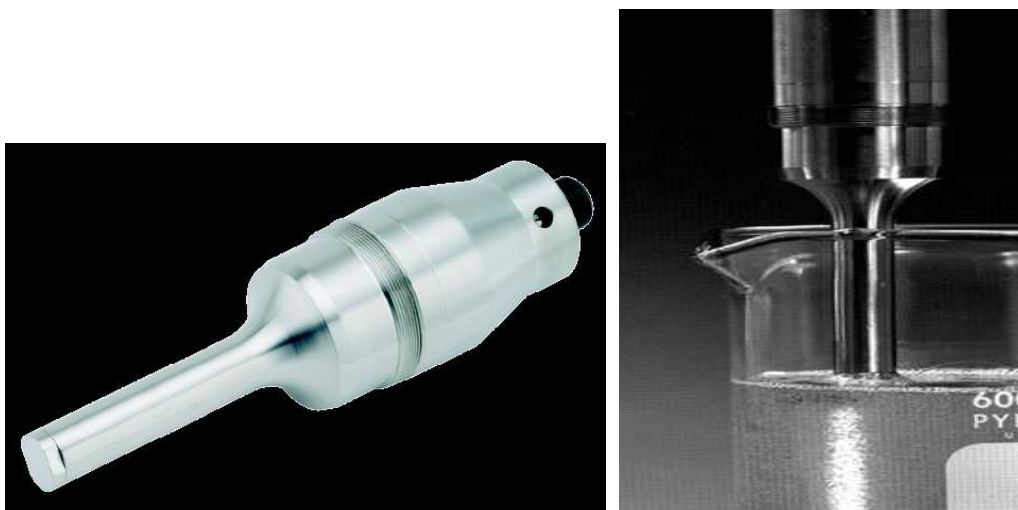


Figure 2.2: Ultrasonic probe (Courtesy: Sonics & Materials Inc.)

These ultrasonic devices rely on transducers or energy converters, which are composed of piezoelectric materials. Such materials respond to the application of an electrical potential across opposite faces with a small change in dimension. This is the inverse of the piezoelectric effect. The converter changes the high frequency electrical energy from the power supply into mechanical vibrations. That is, when the potential is alternated at high frequencies, the piezoelectric material or the crystal

converts the electrical energy to mechanical vibration, which is the sound energy. At sufficiently high alternating potential, high frequency ultrasound is generated.

In the above shown probe, a converter containing Lead Zirconate Titanate discs is employed. Here again, when an alternating voltage is applied to the opposing faces of the discs, they expand and contract with the change in polarity and vibrate at a frequency to acoustically generate cavitation. Cavitation is the development of air bubbles. This is similar to that observed when water is heated towards boiling point, where the bubbles develop and collapse with a noise. In ultrasound processing, these bubbles grow over the period of a few cycles to an equilibrium size at the particular frequency applied, and then they collapse in succeeding compression cycles, generating the energy which is induced throughout the liquid, yielding a chemical and mechanical effect [48]. Thus during ultrasound processing, chemical and physical changes are induced in a liquid medium through the generation and subsequent destruction of these cavitation bubbles. A schematic diagram in figure 2.3 shows this.

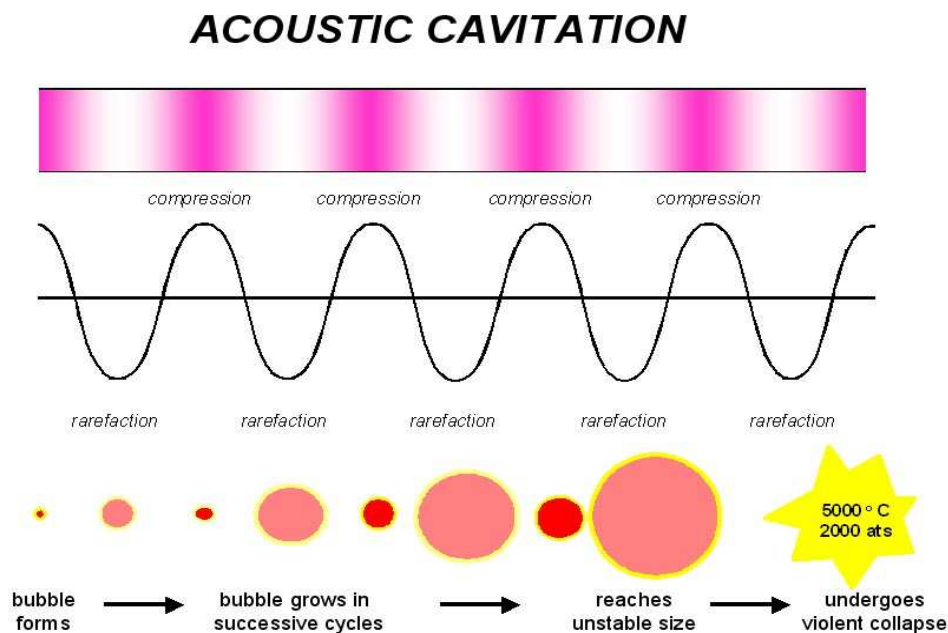


Figure 2.3: Schematic representation of cavitation progression

The power supply transforms 50 Hz to 60 Hz electrical power into high-frequency electrical power at 20,000 Hz. This alternating voltage applied to the disc shaped

ceramic piezoelectric crystals within the converter, causes them to expand and contract with each change of polarity. These longitudinal vibrations are then amplified by the probe and transmitted to the liquid as ultrasonic waves consisting of alternate expansions and compressions, as shown in the previous page. It should be noted that using a power supply with a higher Wattage rating does not mean that more power will automatically be transmitted to the liquid. Rather, it is the resistance to the movement of the probe or the horn that determines how much power will be delivered into the liquid. The load is determined by three factors. They are volume of the liquid, viscosity of the liquid and the probe size and geometry [49].

Probes are normally of one-half wavelength long sections to act as mechanical transformers to increase the amplitude of vibration generated by the converter. It is noted that, greater the mass ratio between the upper section and the lower section of the tip, the greater will be the amplification factor [49]. Probes with smaller tip diameters produce greater intensity of cavitation. Conversely, probes with larger tip diameters produce lesser intensity, but the energy is released over a greater area. Therefore probes with larger tip diameter and at lower intensity help processing larger volume of liquid [49]. Also, as the viscosity of the liquid increases, the fluid's ability to transmit vibrations decreases. Typically the maximum viscosity at which a material can be processed effectively is 4000 cps. Solid probes can safely be used for both aqueous solutions and low surface tension liquids like solvents. Industrial applications requiring high volumes of liquids to be emulsified, dispersed or homogenised can be accomplished by passing this high intensity ultrasonic vibrations through these probes, where the practical upper limit on temperature without air-cooling is approximately 100°C [50]. Usually the beaker or the vessel containing the chemicals will be partially immersed in a tub of ice water in order to dissipate the excess heat generated during the mixing process.

While both ultrasonic baths and ultrasonic processors use piezoelectric technology, ultrasonic baths work well for most cleaning and dispersion applications. However, they can deliver a low, fixed and uneven intensity and be ultrasonic location dependent and inconsistent, due to the fluctuation in the level of the liquid and its temperature. Ultrasonic processors are more versatile, significantly faster and highly

consistent. The energy at the probe tip is high, which will be at least 50 times more than the energy produced in a bath and can be focused and adjusted [50].

In order to get a perfect focus, the amplitude control allows the ultrasonic vibrations at the probe tip to be set to any desired level. Although the degree of cavitation required to process the sample could readily be determined by visual observation, the amount of power required cannot be predetermined. It has been found during this research that whenever a greater amount resistance to the movement of the waves due to higher viscosity is noticed, the amount of power to be delivered into the system can be increased by immersing the probe deeper into the liquid and also by employing a probe of larger diameter [49].

Compared to the mechanical mixing, ultrasonic processing is fast and highly consistent. Probes are practically self-cleaning and by virtue of their design and finish account for negligible sample losses. With ultrasonic processing, commercial mixing is possible with increased Wattage and larger probes as discussed. For a commercial application, probe selection has to be carefully reviewed in order to ensure the implied processing capabilities of the unit under valid consideration. For example, a 100 Watts unit should be able to drive a 13 mm probe, which can effectively process up to 100 ml of liquid in 1 hour. In order to form a colloid, the chemicals are gradually mixed under ultrasonic vibrations [50].

2.1.1.2 Mechanical mixing

Two types of mechanical mixing were tried during this research. One is used a ball mill and the other used a mechanical stirrer. While the first one is suitable for mixing nanopowders with the thermoplastic resins in the powder form, the latter one is used in combination with the ultrasonic method to disperse the nanopowders during the solvent evaporation technique as well. The mechanical stirring works well while dispersing nanopowders into a thermoset resin matrix too.

In a ball mill set-up, a ceramic pot will be rotated at a speed of around 360 rpm with ceramic balls of various diameters inside, along with the thermo plastic resin powder and nanofillers. This process produces structural decomposition of coarser grained

materials resulting in a fine blend of nanocomposite by plastic deformation. During this research, composites with nanoaluminium oxide, nanocarbon and nanoclay were prepared using this high-energy ball mill. The ball milling and rod milling techniques are powerful tools for the fabrication of several advanced composite materials, because in this process, the mixing can be carried out at room temperature. The process can also be performed using high-energy mill or centrifugal type mill or vibratory type mill or energy tumbling mill. While using this high-energy ball mill, rotating the ceramic pot at high-speed developed centrifugal force that in-turn made the ceramic balls inside the pot to agitate the powders. This is one of the most common mixing techniques used in synthesising thermoplastic nanocomposites.

Mechanical stirring, or stir mixing, is also a widely used technique for dispersing nanoparticles into liquid polymer matrix. Use of this technique for synthesis of nanocomposites is highly desired because it can both save the cost of establishing new infrastructure and performed at room temperature. The parameters affecting the mixing process would be temperature, mixing speed, and the impeller design. The processing temperature would affect viscosity and play an important role in achieving exfoliation. The vortices formed by the impeller generate shear forces that can break *Van der Waals* forces between nanoparticle platelets and lead to exfoliation. Hence, the impeller design is also an important parameter in this process [51].

2.1.2 Moulding techniques

In nano-chemistry, moulding is the most important process at the end of mixing. During moulding, the actual reinforcement of the particle with the matrix occurs, which in turn would yield distinct change in the result.

2.1.2.1 Sintering

Sintering is a method for making objects from powders by heating the material to slightly below its melting point under an inert atmosphere and moulding the same at a pressure usually between 100 MPa to 200 MPa until its particles adhere to each other. This melt processing is commercially used for manufacturing ceramic and other metal objects. It has been realised that adding pulverised materials to clay not only improves its workability but also improves the drying process, besides reducing shrinkage of the end product [52].

Normally, in this process, elevating temperatures and external pressure accelerates adhesion. The most widely used inert gas is argon and it is employed during the process in order to prevent the material from oxidation. There is an optimum particle size or a smallest and largest acceptable size for most constituents involved. Surface area and porosity as a function of particle size are the other physical characteristics that play an important role in this technology. The mechanism employed to achieve minimum energy is through the mutual attraction of particles. Here, this non-specific attractive force is commonly referred as *Van der Waals* force. At high temperatures, surface energy is likely to be reduced by electron sharing and valence bonding with gas atoms creating, the phenomenon known as chemical adsorption [53]. Mass movement of particles that occur during this melt processing reduces total porosity by repacking, followed by material transport due to evaporation and condensation from diffusion [53].

Some of the different sintering processes investigated in the thesis are Microwave sintering, Plasma sintering and Laser sintering. There are also two other types of sintering. One uses high pressure and is known as hot pressing. It is used during the manufacture of hard metals, ceramics and diamond tools. The other one is without pressure. Pressure-less sintering is possible with graded metal/ceramic composites, with nanoparticle sintering aid and bulk moulding technology [54]. In microwave sintering, microwave radiation results in a volumetric and uniform heating of the materials. Microwave heating and sintering is fundamentally different from the conventional sintering, which involves radiant or resistance heating followed by transfer of thermal energy via conduction to the inside of the body being processed.

Microwave heating offers a volumetric heating involving conversion of electromagnetic energy into thermal energy, which is instantaneous, rapid and highly efficient. The microwave part of the electromagnetic spectrum corresponds to frequencies between 300 MHz and 300 GHz. However, most research and industrial activities involve microwaves only at 2.45 GHz and 915 MHz frequencies [55]. Based on their microwave interaction, most materials can be classified into one of the three categories as opaque, transparent or absorbers. Laser sintering is an additive rapid manufacturing technique that uses a high power laser beam to fuse small particles of plastic, metal or ceramic powders.

Nanoparticles have been an area of active research in recent years as they have novel and unique properties, which distinguish them from the bulk phase as discussed earlier. The processing techniques also differ from the commonly used moulding techniques on their bulk phase during compositing. Given the difficulties associated with experimental analysis at the nano-scale, the above-discussed systems are good candidates for a study using molecular moulding techniques. However, during the manufacturing of materials containing metal oxide nanoparticles, a phase transformation may also occur during the nanoparticle sintering, which could possibly be traced using molecular dynamics. The driving force for sintering of nanoparticles is the reduction in potential energy due to the decrease in surface area [56].

2.1.2.2 Moulding

Moulding is parts of melt compounding process in polymer science. In this process, the premixed composite is forced to cure under pressure at a certain temperature. Through earlier researches, it is understood that by doing so, a definite proportion of improvement is noticed during impregnation of nanoparticles along the matrix. This process uses a rigid one-sided mould that forms only one surface of the panel. Reinforcement materials can be placed manually. This process is generally done at ambient pressure and then moulding is done by Hand lay-up and Spray-up.

In vacuum bag moulding, the process uses a two-sided mould. One side is a rigid mould and the other is a flexible polymer film. Here again the reinforcement

materials can be placed manually. They include continuous fibre or a chopped fibre during lay-up. The matrix is generally a resin and in this research the resin used will be epoxy. The fibre can also be pre-impregnated with resin in the form of fabrics or unidirectional tapes. This process is also generally performed at vacuum but it can be performed at elevated temperature. Vacuum is applied into the mould cavity. The first step in creating a successful vacuum bagging system is to select a suitable vacuum pump. For best results it is advisable to match the bag size, desired vacuum rate and ultimate pressure that the pump can deliver. If a pump cannot achieve full vacuum in less than five to eight minutes, it is probably too small. Determining the correct pump for an application is based on the area of the mould, which it must surround. By squeezing as much air out of the bag as soon as possible before sealing the bag and applying the vacuum, the work of the pump can be greatly reduced. The bag can completely surround both the mould and the laminate simply by using a tube type polyethylene bag with the vacuum coupling fitted and the two ends sealed with a sealant tape [57].

In case of Autoclave moulding, vacuum is applied into the mould cavity after the assembly is placed inside the autoclave pressure vessel. This process is generally performed at both elevated pressure and temperature. Other types of moulding include pressure moulding, transfer moulding, resin transfer moulding, vacuum infusion moulding, pultrusion moulding, and continuous casting.

In general, during these moulding processes the structure will contain a lightweight core material and a fibre-reinforced polymer composite will mould around the core material. Epoxy being the most commonly used resin; it is often modified using other additives to improve one or more properties of the final product such as toughness or tensile strength. Epoxy resins and their additives contribute to the viscosity of the system and to the shrinking characteristics. The amount of the fillers and diluents will impact both the physical and handling properties of the resin system [57, 58].

2.1.2.3 Infusion

Resin infusion is an advanced laminating technique that greatly improves the quality and strength of the fibre region when compared with a conventional hand lay-up. Applying laminate engineering and resin infusion technology simultaneously allows optimisation of parts in terms of strength and weight. The use of resin infusion has become a standard in yacht construction and has been in use since the 1960s.

During infusion, after applying the usual mould release wax, the gel coat and skin coat of thin fibreglass reinforcement are applied in the conventional manner and allowed to cure. In the infusion process, the parts of the fibre reinforcement fabrics are carefully fitted into the mould over the top of a skin coat. These are put in dry and held in place with a spray contact adhesive. In the case of a cored part, the structural core materials are cut and fitted and adhered in the place. Then the inner skin of reinforcement fabrics is carefully fitted over the core to form a sandwich. After that, the resin distribution hoses and vacuum lines are laid out on top of the fibreglass and the entire inside of the mould is covered with a large sheet of loosely fitting plastic and sealed. With the help of a vacuum pump, all the air in this vacuum bag is evacuated, which compresses the dry stack of reinforcement fabrics. Through the series of feed hoses sealed into the bag, catalysed resin matrix is then sucked by vacuum from a large mixing container. The resin will run through the mould filling the entire stack of laminate. The vacuum is kept on until the resin is cured. The vacuum bag and the feed hoses are then removed, when the parts lamination are over [59].

The advantageous thing about this process is that the infused part is stronger, lighter and superior to the one done by conventional hand lay-up. With resin infusion the benefits and significant strength gains are numerous and intrinsic due to the method used to consolidate the materials within a vacuum chamber all at once. In order to fuse the materials together and to replace the air voids by the resin, a clamping pressure equal to 1 tonne per square feet of vacuum is employed. This process ensures reliability of high quality results, with the elimination of potential errors by the skill of the person who does the lamination. Along with that, vacuum compressing of the fibreglass reduces the amount of resin absorption resulting in

weight saving of 30% compared with the traditional cored fibre laminate, while improving its strength [59, 60]. Other benefits include better fibre-to-resin ratio, very consistent resin usage, unlimited set-up time and a cleaner process. However, it is important to keep the following in mind before deciding to go for a vacuum infusion. They are complicated in set-up and could easily damage the parts. This process can be made perfect only by trial and error. Though the set-up is limitation free with respect to time, it is somewhat more complicated than other processes.

Fibreglass is the most frequently used reinforcement in vacuum infusion. Most fibreglass fabrics offer high permeability in allowing the resin to flow through easily. In general, looser weaves tend to infuse better, as there is less crimping of strands. Carbon fibre and epoxy reinforcements can also be used in vacuum infusion though they tend to infuse more slowly.

Chapter 3

Synthesis and Testing

3.1 Introduction

In the past ten years, scientists have been developing new composite materials wherever there is a need to compensate for the weakness of one material with the strength of the other [61]. Also, these composites tend to develop only when single homogeneous material cannot be found with all of the desired characteristics for a given application.

During this research process, the thrust is given on characterising a new nano-enhanced composite towards identifying varied potential applications including biomedical engineering. It is also strongly believed that the advances at the nano-scale will be meaningless if they cannot be interfaced with the technology at large to produce usable end products. This means, while developing an enhanced nanocomposite, one of the primary objectives of this research is to integrate nanoparticles and nano-scale phenomena into a larger hierarchical system. During this research, the understanding from earlier research literatures on various methods of synthesising nanoparticles into a resin base was well incorporated. This was made possible through the preliminary research. Also the chemistry behind the various syntheses were also analysed and characterised in-depth through trial and error method. This has helped to identify an optimal method of even dispersion of the nanoparticles into the system. Therefore the experimentation process is carried out in two steps as given below

- Synthesis
- Testing

3.2 Synthesis

Since it has been tried through this research to develop a new nano-enhanced composite, an extensive experimentation process was carried out during each synthesis. This was achieved by varying the combinations of different nanofillers of between 10 nm to 30 nm in diameter at various ratios with several solid thermoplastic resin bases. This loading of nanoparticles ranged from 1% to 3% by weight of the resin during each experiment. Experiments were repeated, in order to identify an optimal mixing process that will ensure even dispersion of nanoparticles into the matrix besides identifying the right nanofiller and the optimum volume of it. Therefore the synthesis process was carried out in the following ways

- Synthesis using thermoplastic resins
- Synthesis using epoxy resin
- Lay-up preparation of laminates

3.2.1 Synthesis using thermoplastic resins

First the nanofillers were mixed thoroughly with the polymer powder in Ethanol suspension using a ball mill mixer shown in figure 3.1 for 8 hours and dried for 24 hours at room temperature. Secondly, the composites were mixed with an ultrasonic mixer for 5 minutes in Toluene suspension in order to ensure even dispersion of fillers into the resin matrix. This was again dried for 24 hours at room temperature. Dried nanocomposites were then hot moulded at 200°C for 1 hour and dried again under pressure at room temperature for 24 hours. Samples of these nanocomposites were then tested for various mechanical properties. This synthesis was conducted at Auckland University of Technology's composite lab facility.

During the second stage, ultrasonic mixing was adopted to ensure even mixing through generation of an alternating acoustic pressure above the cavitation threshold in order to create numerous cavities into the liquid polymer matrix. Some of these cavities oscillated at a frequency of 20 kHz to 50 kHz while the gas content inside these cavities remained constant. However, some other cavities grew intensely under tensile stresses while yet another portion of these cavities, which were not

completely filled with gas also started to collapse under the compression stresses of the sound wave. In the latter case, the collapsing cavity generated tiny particles of debris and the energy of the collapse was transformed into pressure pulses. It is noteworthy that the formation of the debris further facilitated the development of cavitation, towards complete exfoliation of nanoclay in the matrix [62].

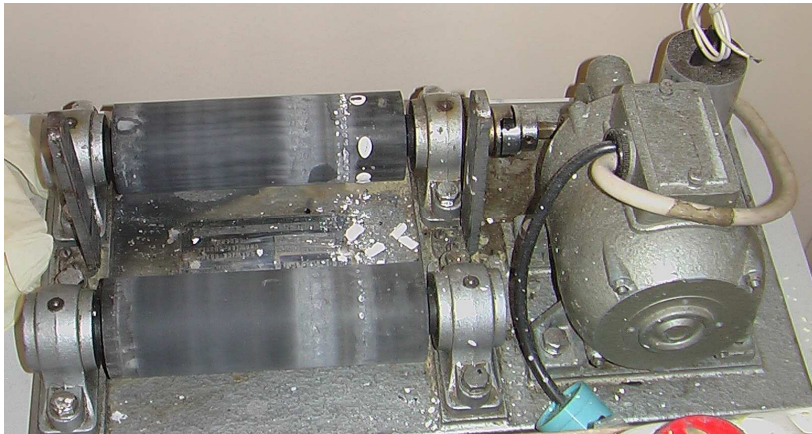


Figure 3.1: Ball mill mixer

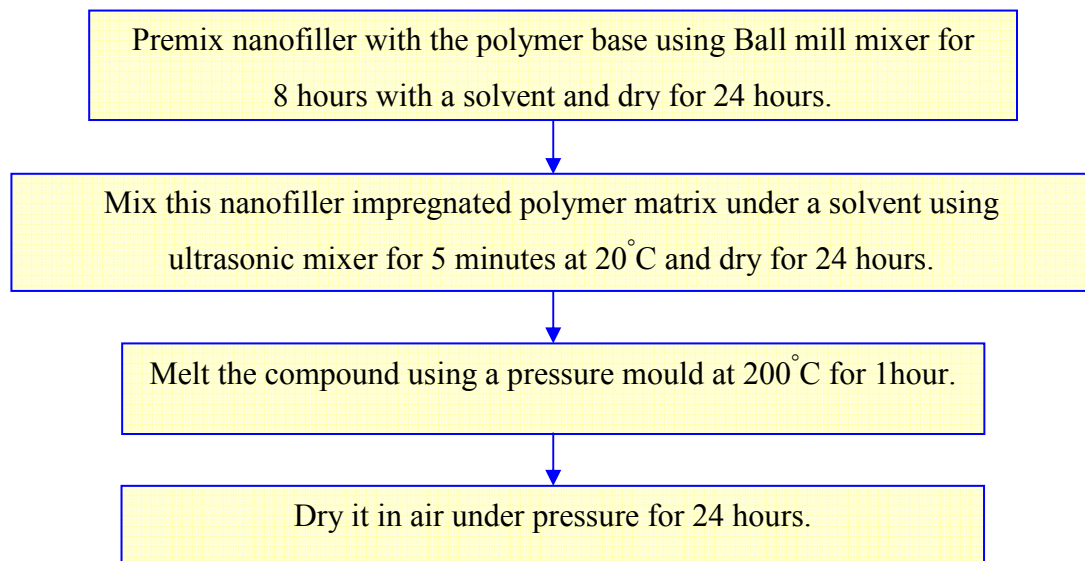


Figure 3.2: Flow chart for mixing thermoplastic resins

It is assumed that acoustic cavitations in this liquid polymer matrix develop and propagate like a chain reaction. Therefore, individual cavities on real nuclei develop so rapidly that within a few microseconds an active cavitation region is created close to the source of the ultrasound probe. It has been noticed that acceleration of polymer reaction take place under ultrasound in both catalysed and uncatalysed reactions.

Acoustic cavitation accelerates heat and mass transfer processes such as diffusion, wetting, dissolution, dispersion and emulsification [63]. The exfoliation process can be explained as a treatment to increase clay gallery distance wherein the primary clay is converted into hydrophobic from hydrophilic [64]. During this process, swelling of the clay created inside the epoxy matrix provides an environment for the curing agents to migrate into the clay interlayer region to form a nanocomposite. Thus the development of cavitation processes by ultrasonics creates favourable conditions for the intensification of various physiochemical processes.

Table 3.1: Composition while using Ball mill mixing

Batch number	Composition					
	Resin Matrix		Nanofillers			Solvent ml
	PMMA grams	PVDF grams	Nanocarbon grams	Garamite grams	Nanoclay grams	
1A	6.82		0.63			30
2A	9.9		0.1			30
3A		9.9		0.1		30
4A		9.9			0.1	30
5A		9.9	0.1			30
6A	9.9			0.1		30
7A	9.9				0.1	30

Table 3.2: Composition while using ultrasonic mixing

Batch number from Table 3.1	Volume of the Composite, grams	Volume of Toluene, grams	Duration of Ultrasonic mixing, mins
2A	3.47	17.35	5
3A	6.38	31.90	5
4A	7.57	37.85	5
5A	4.85	24.25	5
6A	3.43	17.15	5

Besides the techniques like melt mixing, solvent exchange and solvent evaporation methods, shear mixing and mechanical stirring, as stated above, ultrasonic cavitation is one of the more efficient way to disperse nanoparticles evenly into the polymer matrix [65]. In this research, ultrasonic mixing is employed successfully to infuse carbon and clay nanoparticles into PMMA and PVDF matrices.

The moulded samples are tested on a three point bending as per the ASTM standards D790M [66] and the results are discussed in detail in the coming chapters. With regard to these thermoplastic resin matrices like PVDF and PMMA, successful dispersion of these fillers is achieved through this process and it confirms even dispersion, which is potentially promising towards developing a wide range of commodity and applications in biomedical engineering too.

3.2.2 Synthesis using epoxy resin

Normally, composite materials consist of two or more distinct materials with a recognisable interface between them. The term nanocomposite is usually reserved for materials in which the distinct phases are separated on a scale larger than an atom and in which the nanocomposite's mechanical properties have been significantly altered from those of the constituent materials [67]. In this case, the mechanical property of the epoxy resin matrix is modified with the addition of the nanofillers like nanoclay and nanocarbon.

As a part of this research, fabrication of nanofiller/epoxy composites was also carried out but in four steps. In the first step, nanoparticles of between 10 nm and 30 nm in diameter were ultrasonically mixed with neat epoxy resin at various ratios ranged from 1% to 3.0% by weight of resin during each experiment as described earlier. The mixing was carried out using an ultrasonic liquid processor VC505 as shown in the figure 3.3 supplied by Sonics and Materials Inc., which uses a 13 mm solid Titanium alloy probe at 20 kHz at 40% of the amplitude for 1 hour. In order to avoid the rise in temperature during sonication the bath is maintained at 20°C with a pulse rate of 9 seconds ON and 9 seconds OFF. Employing an external cooling set-up, which is by immersing the mixing beaker in a water bath containing ice cubes, also controlled the temperature. During the sonication, the dispersion of nanoparticles seemed uniform, by visual observation. Figure 3.4 shows the schematic diagram of mixing thermoset resins.



Figure 3.3: Ultrasonic liquid processor, VC 505 by Sonics and Materials Inc.

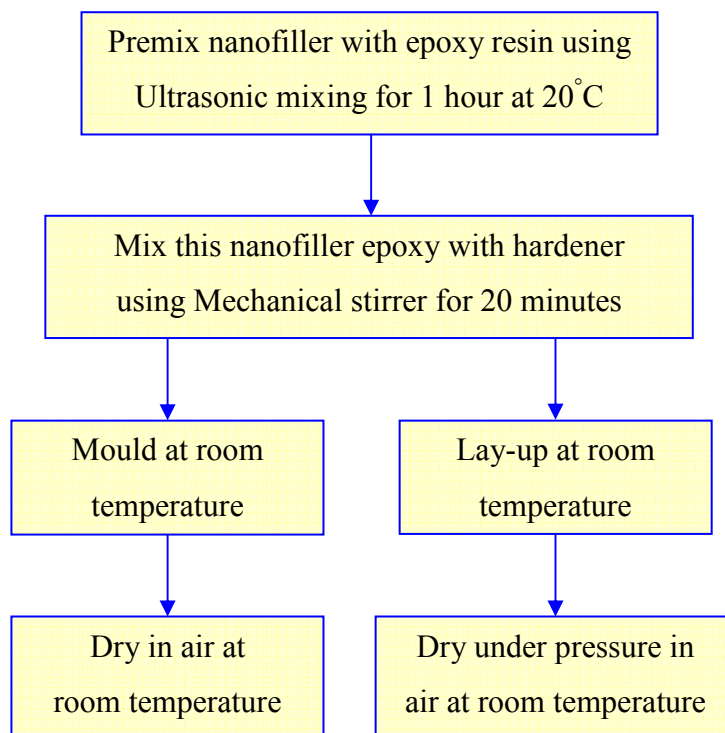


Figure 3.4: Flow chart for mixing thermoset resins

In the second step, a hardener was added into the mixture at a ratio of 1:4 at a slow rate while it was being mechanically stirred. The mixing was carried out mechanically for 20 mins using a high-speed mechanical stirrer, which ran at 650 rpm. In the third step, a portion of the mixture was moulded to make a sample for the tensile test as per the ASTM standards (ASTM D638) in order to test the mechanical yielding properties of the composite matrix, while the balance was used to mould lay-ups [68]. Lay-ups use satin woven carbon fibre to fabricate nanofiller/epoxy

nanocomposite laminates. Finally, the moulds were cured at room temperature whereas the lay-ups were cured under pressure at room temperature.

Table 3.3: Composition of epoxy synthesis

Batch number	Composition			
	Neat Epoxy resin grams	Nanoclay grams (%)	Nanocarbon grams (%)	Hardener grams
1B	10	0.1 (1)		2.5
2B	10		0.1 (1)	2.5
3B	10		0.2 (2)	2.5
4B	10	0.2 (2)		2.5
5B	20	0.5 (2.5)		5
6B	20		0.5 (2.5)	5
7B	20		0.6 (3)	5
8B	20	0.6 (3)		5
9B	20	0.8 (4)		5
10B	20	0.3 (1.5)		5
11B	20	0.6 (3)		5
12B	20		0.3 (1.5)	5
13B	20		0.6 (3)	5
14B	20			5
15B	20			5
16B	20	0.2 (1)		5
17B	20	0.3 (1.5)		5
18B	20		0.2 (1)	5
19B	20		0.3 (1.5)	5

This entire exercise was repeated for several ratios of nanoclay and nanocarbon and also at various sonic durations as well. The synthesis was also tried independently using ultrasonic mixing and mechanical mixing as well, in order to characterise the effects of these two different mixing processes. During each synthesis, equal number of samples was made with and without lay-up.

Since nanoparticle infusion, using ultrasonic mixing, seems to be more promising in ensuring even dispersion of nanoparticles into the matrix than other infusion processes, it was chosen in the first place. However, the two mixing processes used were compared for exfoliation and dispersion of nanoparticles and analysed in order to understand the processing behaviour. The plain matrix samples and the laminated composite samples were tested for their mechanical properties and characterised. The analysis of the test results is discussed in detail in the coming chapters.

The main concern in developing such nanocomposite laminations lay in ensuring adequate bonding between the matrix and the fibre. In order to achieve this, during the lamination process, the matrix was spread using a spatula and evenly rolled using a Teflon roller with a constant set pressure. Penetration and even spreading of the matrix were observed and ensured. The whole process was maintained throughout all the experiments.

3.2.3 Lay-up preparation of laminates

Nanocomposite laminates often exhibit a better performance and enhanced properties than the conventional structural laminates. These composite lay-ups can be divided into two main categories; short fibre reinforced laminate and continuous fibre reinforced laminate, depending upon the nature of the lay-up fibre used. Continuous reinforced laminates often constitute a continuous layer or laminated structure running within a resin matrix. To understand this better, it is important to know that there are two types of materials that constitute a lay-up or lamination. They are the matrix and the reinforcement fibre. The matrix material surrounds and supports the reinforcement materials, by maintaining their relative positions, to provide a means of distributing and transmitting load along the fibre uniformly. The reinforcement fibre, besides being a basic structure to the lamination, imparts special physical properties such as mechanical and electrical properties to the matrix [69]. The fibres normally exhibit linear elastic behaviour. The fibre and the resin matrix complementarily enhance the laminate properties that are not available in virgin or naturally occurring materials. Due to the availability of a wide range of matrix and reinforcement materials, the design options have become versatile and flexible, resulting in huge range of applications.

Matrices include epoxy resins, polyester, vinyl ester, phenolic, polyamide, polyamide resins and thermoplastic resins. The reinforcement materials are often fibres. Fibre materials often have felt, fabric, knitted or stitched construction. Most commonly used fibres are glass fibres, carbon fibres, aromatic polyamide fibres, boron fibres, silicon-carbide fibres and aluminium oxide fibres.

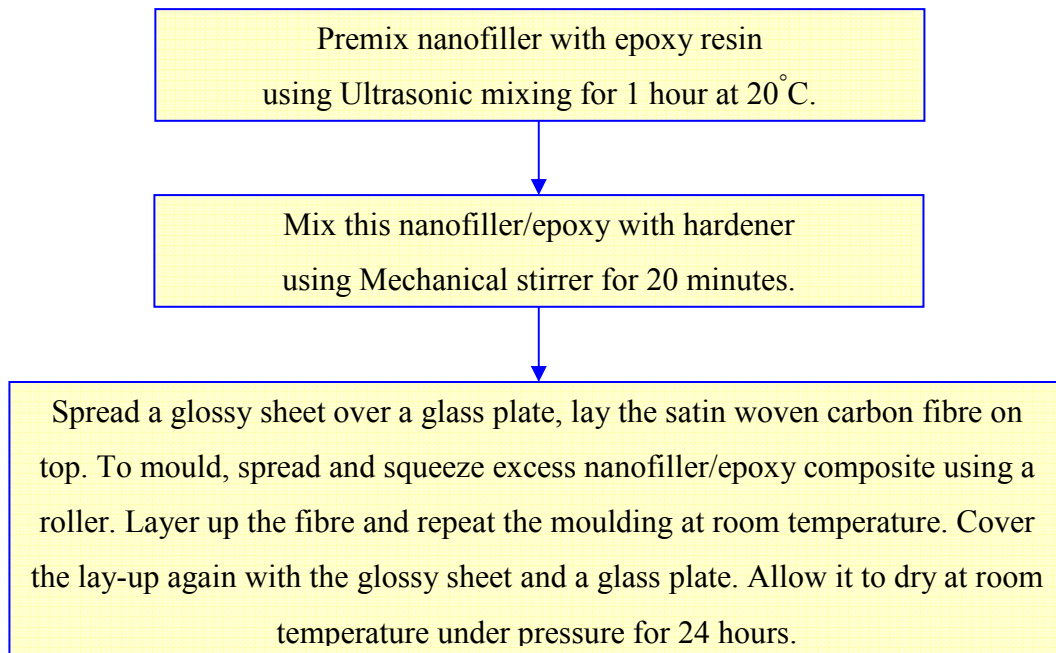


Figure 3.5: Flow chart for making lay-up

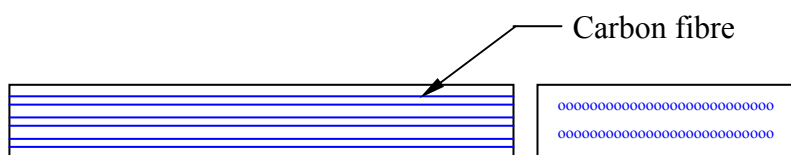


Figure 3.6: Schematic drawing of a carbon fibre lay-up



Figure 3.7: Schematic picture of lay-up

In order to make a lay-up or a laminate, three sheets of the nylon woven carbon fibre were cut into 200 mm by 100 mm. One of them was placed on top of a polyethylene sheet spread over a glass plate. The matrix, containing nanofiller infused in epoxy, was then poured over the carbon fibre and spread evenly using a spatula and pressed using a Teflon roller to ensure penetration and uniform distribution. Similarly, the other two carbon fibre sheets were laid on top of one another and the process was repeated each time. The lay-up was then covered once again with the polyethylene sheet and sealed with a glass plate. A weight of 30 kilograms was mounted on top of the lay-up and allowed to cure for 24 hours. The polyethylene sheets were used to prevent sticking of epoxy on the glass plate and to ease the process of retrieving the lay-up, while the glass plate ensures flatness. In this research, since long and continuous carbon fibres were arranged unidirectionally, the fibre was strongly bonded with the nano-epoxy matrix and they were strong and stiff. Therefore it was considered as a homogeneous body.

This laminate was then cut into a size of 15 mm by 80 mm in order to conduct a three point bending test on each sample. While doing that, the laminates were cut in three different angles. One of which was at 0° angle i.e. along the orientation of the fibre and the other one at 45° angle and the last one at 90° angle i.e. perpendicular to the direction of orientation. This was to understand the mechanical behaviour of the laminate while loading and to understand the formation of crack and its propagation.

Nanocomposite laminates can be formed into any shape. This involves strategic placing of the reinforcement fibre, while enhancing the matrix properties through the addition of nanofillers, to achieve a good welding process. A variety of methods are used according to the end product design and property requirements. These fabrication methods are commonly called moulding, which was discussed in the previous chapter. The principle factors impacting the methodology are the nature of the matrix and the reinforcement fibre chosen, depending upon the application. Another important factor is the method adopted and the volume of the end product to be produced. Large quantities can be used to justify high capital expenditures for rapid and automated manufacturing technology. Small production quantities can be accommodated with lower capital expenditures but at higher labour costs and at a correspondingly slower rate.

The adhesive properties of epoxy are especially useful and important in the construction of honeycomb-cored laminates, where the small bonding surface area means maximum adhesion requirement. Here again this property of epoxy is exploited further by the addition of nanofillers. These nanofillers enhance the advantage of increasing the surface area of the matrix resulting in better adhesion to the carbon fibre during lay-up. Although the strength of the bond between nanofilled epoxy resin matrix and the carbon fibre is not solely dependent on the adhesive properties of the resin system it is also affected by the surface tension and viscosity of the matrix which are discussed in detail in the coming topics.

3.3 Testing

Following were the tests conducted on the samples obtained from the nanoenriched epoxy matrix and the laminates, towards characterising the process and to optimise the volume of nanofillers in order to achieve the enhancements targeted.

- Tensile test as per ASTM Standards D638
- Three point bending test as per ASTM Standards D790M
- Phase contrast microscopy
- High speed photography
- Surface tension measurement using the Drop shape method

3.3.1 Tensile test as per ASTM Standards D638

To measure the tensile strength of a nano-enhanced epoxy composite matrix, the samples as shown in figure 3.8 and figure 3.9 were stretched with a Hounsfield machine with a leading span of 600 mm. This machine simply clamps each end of the sample and it stretches the sample at the rate of 1.2 mm per min, when the machine is turned on. While it is stretching the sample, it measures the amount of force (F) that it is exerting. When we know the force being exerted on the sample, we then divide that value of force by the measured cross-sectional area (A) of the sample to arrive at the value of stress experienced by our sample as shown in the following page.

$$\frac{F}{A} = \text{stress}$$

Again using this machine, force on the sample was continued to increase until it breaks in order to find the ultimate tensile stress. Likewise, similar tests were conducted for compression or flexural strength too. In all these cases, the strength is the stress needed to break the sample or to get the maximum strain.

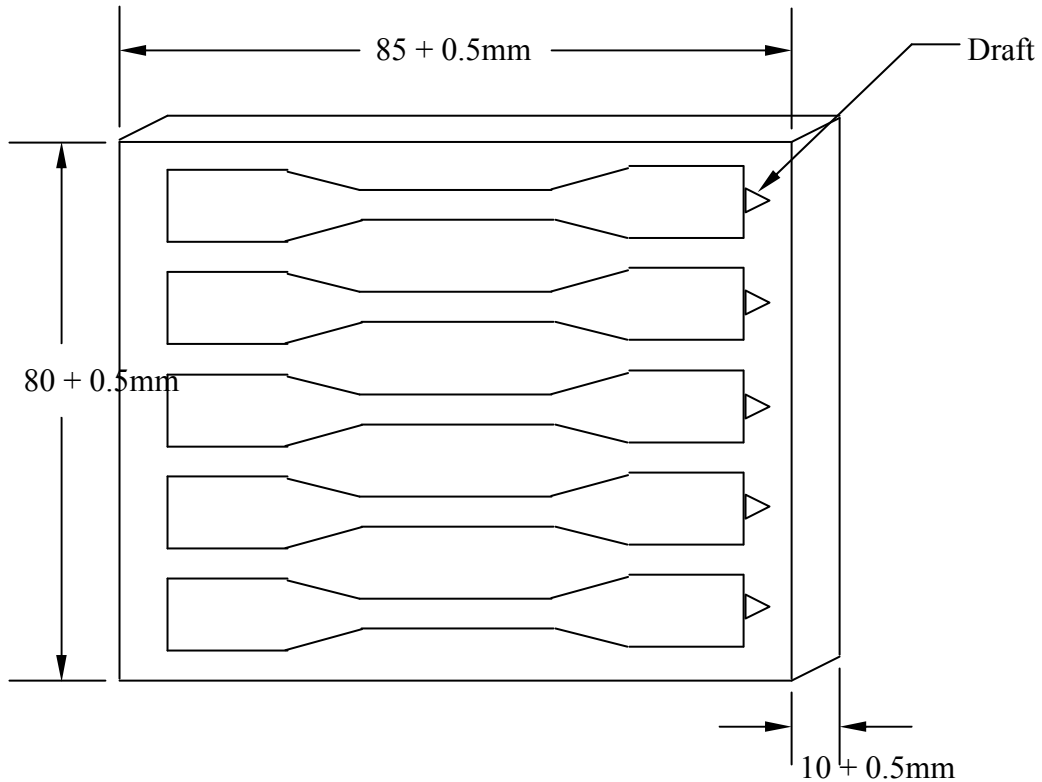


Figure 3.8: Mould design

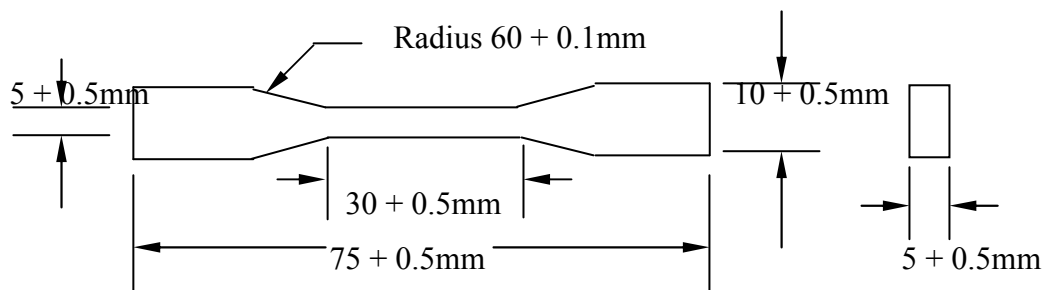


Figure 3.9: Layout of matrix sample for tensile testing based on ASTM Standards D638



Figure 3.10: Sample of 1% nanoclay/epoxy matrix for tensile testing

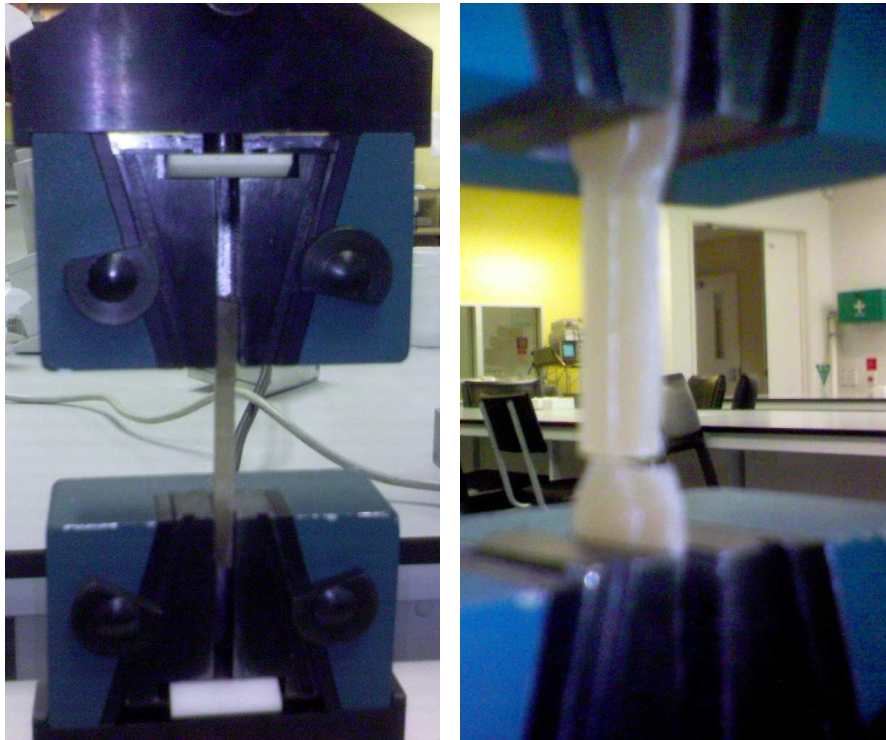


Figure 3.11: Tensile testing by Hounsfield machine

Since tensile stress is the force placed on the sample divided by the cross-sectional area of the sample, tensile stress can be measured and the tensile modulus can be calculated by dividing the stress by the elongation, which would be measured in terms of elongation. Modulus is therefore expressed in the same units as strength i.e. N/cm^2 . Normally, stress is measured in terms of mega pascals (MPa) or giga pascals (GPa). It is easy to convert the different units using the following conversion factors. $1\text{MPa} = 100 \text{ N/cm}^2$. If stress and strain are measured in the English units of pounds per square inch or psi, they can be converted from psi to N/cm^2 using the following conversion factor $1\text{N/cm}^2 = 1.45 \text{ psi}$.

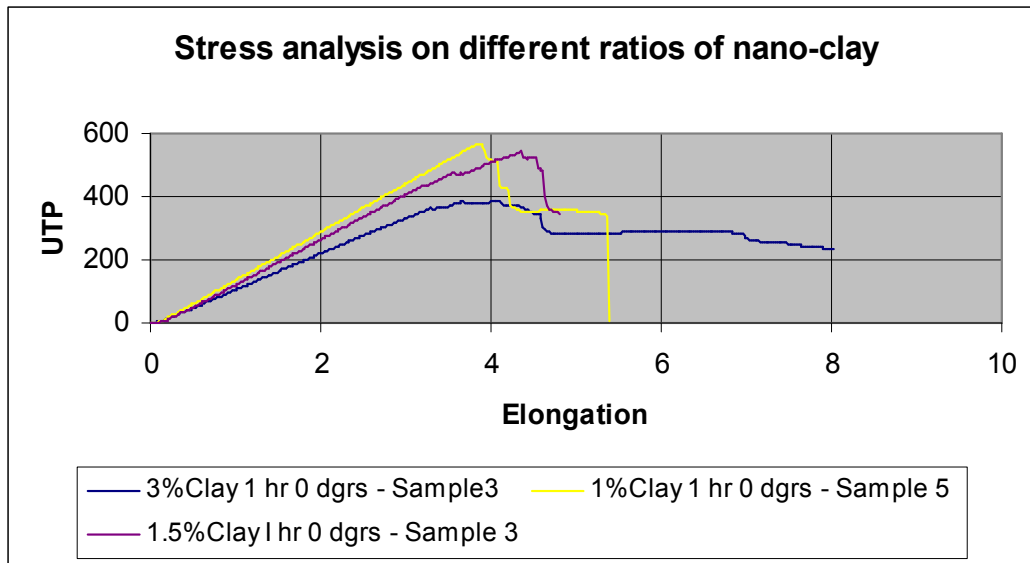


Figure 3.12: UTP Vs Elongation of various samples of nanoclay/epoxy composite matrix

The above figure 3.12 shows the stress-strain curves for various samples of nanoclay/epoxy composite matrix. Strain is a kind of deformation or elongation. Elongation is the word used specifically to tensile strain. The height of the curve at the time when the sample breaks is the ultimate tensile strength and the slope represents the tensile modulus. If the slope is steep, then it means that the sample has a high tensile modulus, which means it resists deformation. If the slope is gentle, then it means that the sample has a low tensile modulus, which means it can be easily deformed. The slope is not constant as stress increases. The slope or the modulus changes with stress. [70].

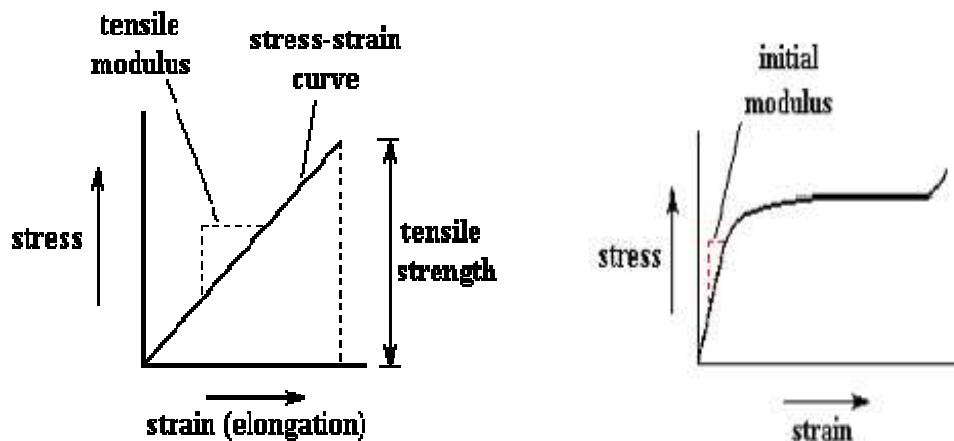


Figure 3.13: Stress-strain graphs [70]

To have a better understanding about the relationship between the stress and strain, the graphs in figure 3.14 show typical stress-strain curves for different kinds of polymers. The green plot shows that rigid plastics such as polystyrene, PMMA or polycarbonate can withstand relatively high stress but they cannot withstand much elongation before breaking. So materials like this are strong but not very tough. Also, the slope of the plot is very steep, which means that it takes a lot of force to deform a rigid plastic. So it is easily seen that rigid plastics have high moduli. In short, rigid plastics tend to be strong, resist deformation but they tend not to be very tough, which means, they are brittle [71].

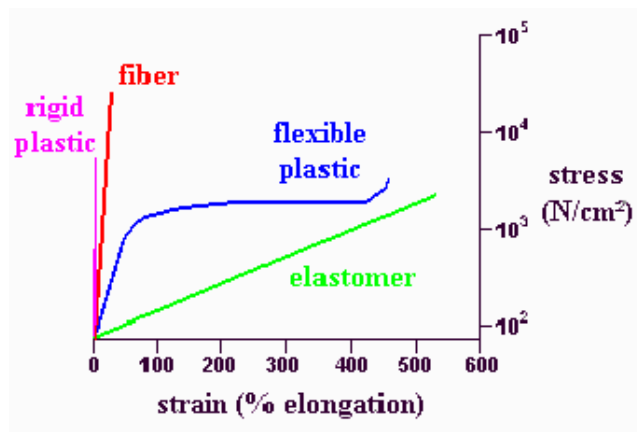


Figure 3.14: Stress-strain comparison for various materials

With the discussed tensile testing method, materials of thickness upto 14 mm can also be tested. However, the matrix samples were reduced to 5 mm uniformly by machining. Also, this testing method included the option of determining Poisson's ratio at room temperature. It was understood that the constant rate of crosshead movement for a desired theoretical value and the testing speed give important effects in characterising the behaviour of the composite material in its plastic state.

Table 3.4: Tensile test samples to ASTM D638

Batch and Sample nos.	Neat Epoxy grams	Percentage of Nanofillers		Dimension of the samples		UTP, MPa	Elongation, mm
		Nano clay	Nano carbon	Thickness, mm	Width, mm		
14B,1	20	No fillers		5.26	6.78	24.647	2.533
14B,2				5.20	6.88	26.759	3.129
15B,1	20	No fillers		5.24	5.82	24.232	3.141
15B,3				5.14	5.64	23.882	4.470
16B,1	20	1		5.52	6.32	14.360	2.288
16B,2				5.28	6.42	15.458	3.138
16B,3				5.74	6.20	12.288	3.953
17B,1	20	1.5		5.24	5.70	20.534	3.229
17B,2				5.12	7.70	28.189	3.537
11B,1	20	3		5.00	5.00	9.706	7.595
11B,2				5.00	5.00	8.653	4.121
11B,3				5.00	5.00	12.066	4.717
18B,1	20		1	5.56	6.50	25.677	5.814
18B,3				5.40	6.10	18.336	8.587
12B,1	20		1.5	5.00	5.00	14.720	1.963
13B,1	20		3	5.50	6.00	20.542	1.977

During this test, it was understood that variations in the thicknesses of the test specimens produce variations in the surface-volume ratios of such specimens, which in turn influence the test results. Hence, all the samples were carefully made to the same thickness as said above in order to allow reliable comparison of the end results for all the samples. This tensile testing method was used for testing laminated composites also.

3.3.2 Three point bending test as per ASTM Standards D790M

During a three point bending test, the composite lay-up is subjected to in-plane compressional stress. Each lay-up is made of three layers, called plies, of nanofiller/epoxy with nylon woven carbon fibre to a thickness of 1.5 mm. The lay-up is made to a size of 200 mm by 100 mm. Then that is cut into a length of 80 mm and a width of 15 mm as per ASTM D790M using a high-speed cutting tool. The samples of lay-up were loaded for compression in a Hounsfield three point bending machine, with a leading span of 600 mm. The crosshead speed was maintained at 1.2 mm per min. Six specimens were tested on each weight ratio of nanofiller/epoxy composite lay-ups. The tensile loads and the displacement were measured. Tensile modulus and yield strength were also calculated.

The three point bending test showed the effect of the nanofillers in the epoxy composite in comparison with the tensile strength tests. The summary of the experimental results from the three point bending test carried out on the nanocarbon/epoxy lay-up on carbon fibre is as shown in figure 3.15:

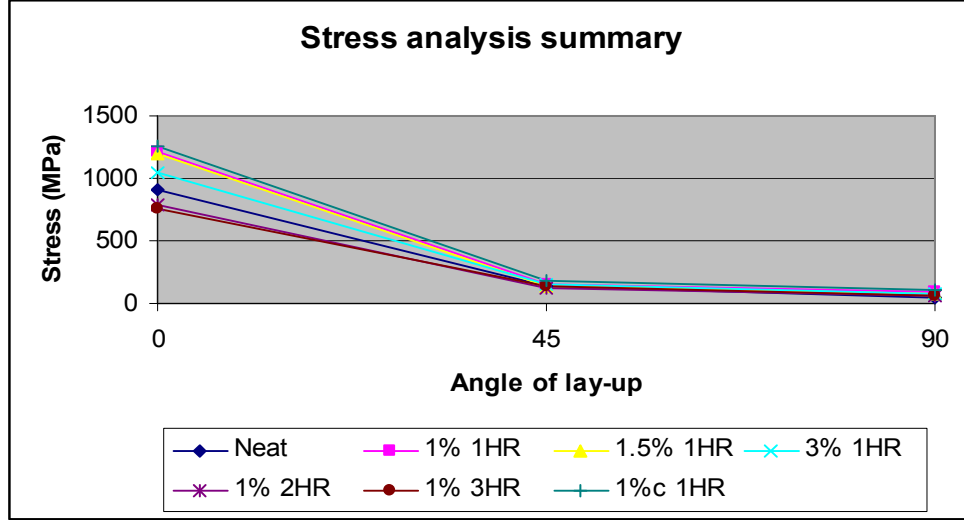


Figure 3.15: Stress analysis summary

The stress-strain curves obtained from the three point bending test for different compositions of nanofillers to epoxy matrix at different angle of lay-ups are shown as above. The fractural strength is represented as the ultimate tensile strength because the curvatures in the graph are too small. The modulus is calculated as the slope of the linear elastic regions from the stress-strain curves.

For a three point bending, at a given load P , the maximum tensile stress σ for a given span length L will be

$$\sigma = \frac{3PL}{2bt^2} \quad (3.1)$$

where b and t are the width and thickness of the lay-up respectively.

And the Shear stress τ can be represented by

$$\tau = \frac{3P}{4bt} \quad (3.2)$$

For a three point bending, at a given span length L , the Modulus of Elasticity E will be

$$E = \frac{L^3 m}{4bt^3} \quad (3.3)$$

where b is the width of the lay-up and t is the thickness of the lay-up again and m is the slope of the modulus.

Now the strain can be calculated using Hook's law. According to Hook's law, the stress experienced by the matrix is proportional to the strain or the deformation. Therefore as per Hook's law [76]

$$\sigma = E\varepsilon \quad (3.4)$$

Stress in a composite is the sum of the stress in the fibre and the matrix multiplied by their relative cross-sectional areas. The stress in the fibre and the stress in the matrix are generally not the same. Therefore,

$$F = F_f + F_m \quad (3.5)$$

$$\sigma.A = \sigma_f.fA + \sigma_m.(1-f)A \quad (3.6)$$

$$\sigma = \sigma_f.f + \sigma_m.(1-f) \quad (3.7)$$

Since the fibre and the matrix often have different elastic moduli, the stress in each must be different [72].

Since the force is applied perpendicular to the direction of fibre, the fibre deflects in the same direction. Therefore, the total deflection, d is the sum of the deflection of the fibre and the matrix.

$$d = d_f + d_m \quad (3.8)$$

The effect of nanoclay on the compressive properties of these nanocomposites was similar. At 1% of exfoliated nanoclay/epoxy composite, the compressive modulus increased by 30%, while exhibiting maximum strength over the neat epoxy matrix. While the neat resin matrix shows approximately 55% decrease in strength past the yield strength compared with the 1% nanoclay/epoxy composite, the other

composites did not show a similar decrease. The main compressive failure with the epoxy matrix is due to the initiation of cracks in the direction of compression, due to the lateral expansion of the lay-up resulting from the Poisson's ratio effect. Whereas, in the case of nanocomposites, the increase in the modulus had lead the lay-up to lateral expansion, which in-turn had initiated the crack along the matrix. When cracking is initiated i.e. when the yield point is reached, a sudden fall in strength was observed. It was also noticed that the increase in the proportion of nanoclay content has led to lesser compressive modulus resulting in the final failure at lower strain values.

3.3.3 Phase contrast microscopy

Phase contrast microscopy is often preferred when higher magnifications (i.e.) magnifications up to 1000X are needed and also when the samples to be examined are colourless or the needed details are so fine that the colours do not show up well. In this research, the images obtained from the Phase contrast microscopy were used to analyse the internal chemistry behind dispersion in order to understand the effect of various mixing processes. This Phase contrast microscopy was carried out on all the samples of composited nano-enhanced epoxy matrix as well as on the lay-ups.

Sample preparation being very important in any microscopical technique, the samples were first mounted in a round substrate of 30 mm diameter with an excess amount of low viscosity neat epoxy, to prevent rocking during grinding and polishing, as shown in figure 3.16 in the next page. This mounting process besides enabling us to handle the sample with ease during polishing and even during microscopy, also minimises the likelihood of any damage that could happen to the sample. Most of the time, the damage occurs, while the sample is cut and polished [73]. Cutting with abrasives could also cause a high amount of damage to the surface, but this has been drastically reduced by using a high-speed diamond saw and most importantly with a proper lubricant. It is also important to remove the cutting and grinding marks so that the microstructure of the cross section of the matrix and the lay-ups are exposed clearly. Since improper preoperational methods may obscure the result and would even lead to misinterpretation, utmost care was taken to attain a perfectly polished and flat surface for optimum imaging as shown in figure 3.16. In

order to get a highly polished smooth surface, the samples were ground and polished using a series of fine grades of diamond paste up to the particle size of 1 micron in diameter [74, 75]. Each time before changing the polishing wheel the samples were washed thoroughly with soap and warm water followed by a gentle rinse with alcohol to avoid contamination.

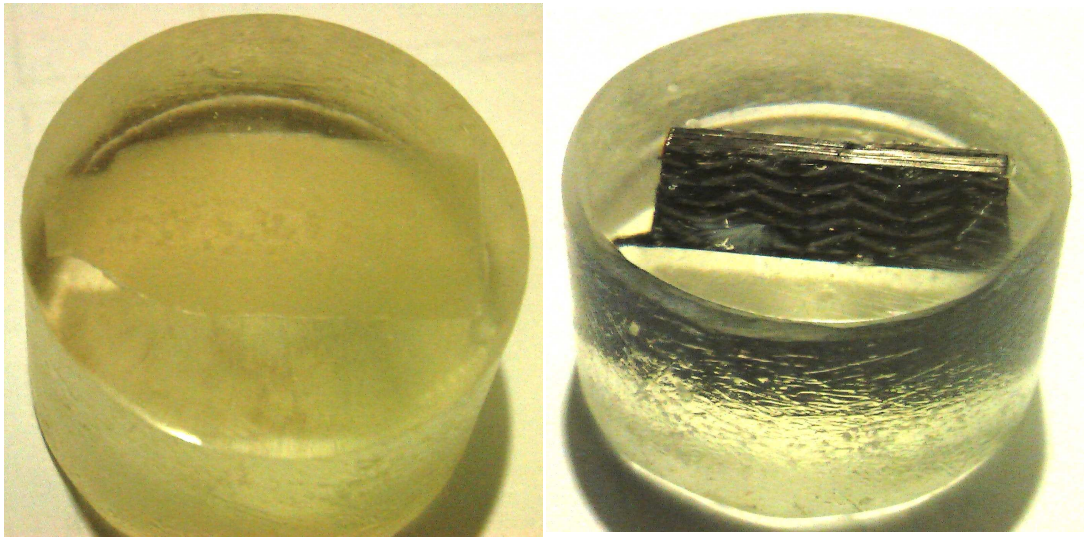


Figure 3.16: Mounted samples used during phase contrast microscopy

In order to use phase contrast during microscopy, the light path was aligned first. Then the element in the condenser was aligned with the element in the phase contrast lens by sliding a sample into the light path and by rotating a condenser turret. The elements were then lined-up to a fixed position by adjusting the eyepiece in the observer till the phase effect was obtained. Generally the phase contrast needs more light when compared to a bright light microscopy, since here the viewing technique is based on the diminishment of brightness of most objects [76].

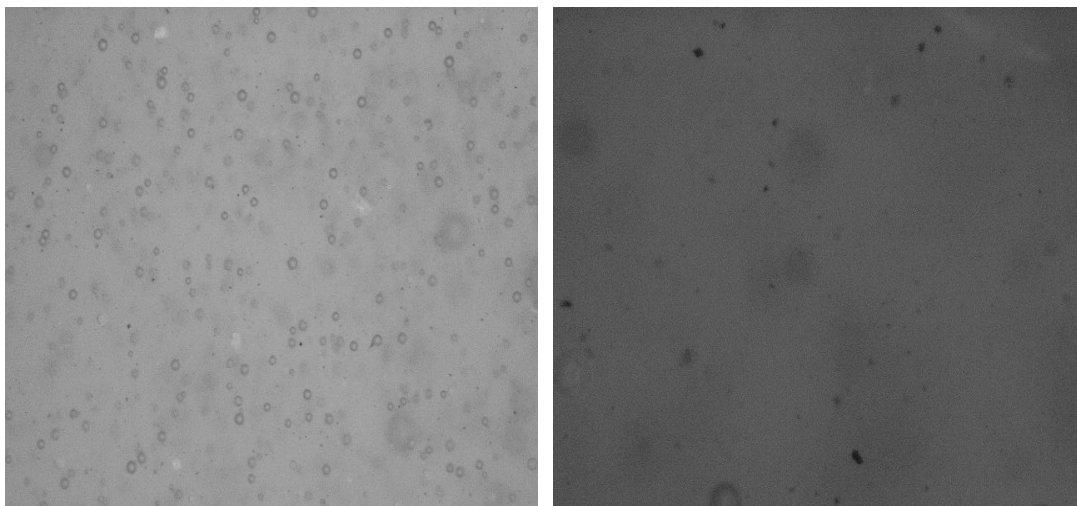
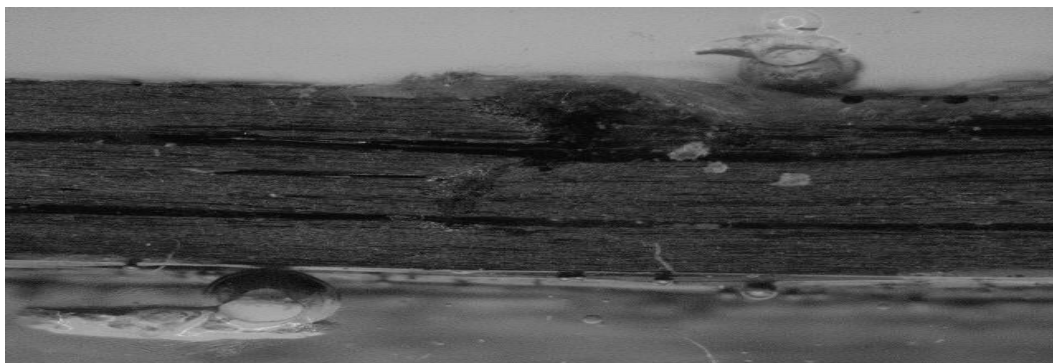
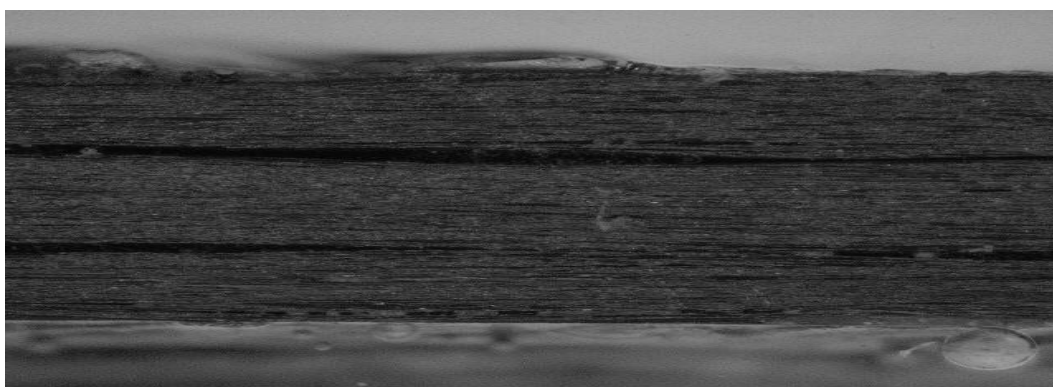


Figure 3.17: Phase contrast microscopy at 200X and 1000X of 3% nanoclay/epoxy matrix

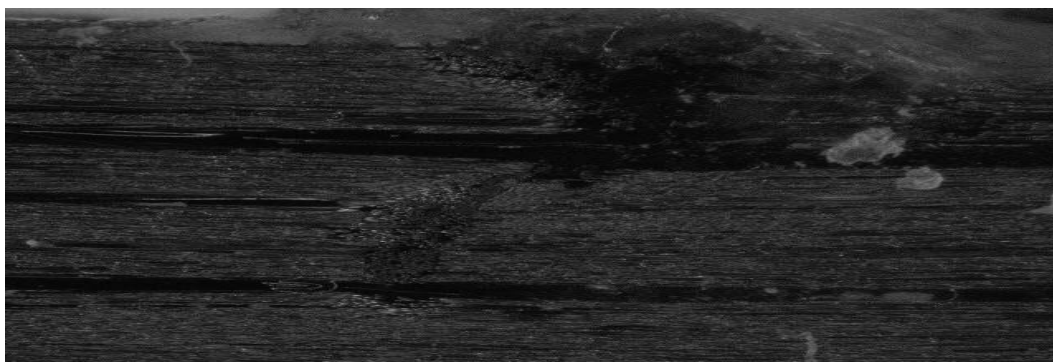
From the above shown figure 3.17, phase contrast images obtained from the samples of nanoclay/epoxy matrix, agglomerations of nanoclay particles were made visible. During this research, it was noticed that the amount of agglomerated nanoclay particles present in the sample decreased with the increase in the mixing duration up to an optimum level, which is 1 hour. But still there were tiny agglomerated particles visible even after an hour of ultrasonic mixing processing, indicating that not all the nanoclay particles were fully dispersed and were unlikely to be exfoliated. Again this microscopic analysis indicated that the exfoliation of nanoclay was greater when they are mixed ultrasonically, compared with other processing methods like mechanical mixing.



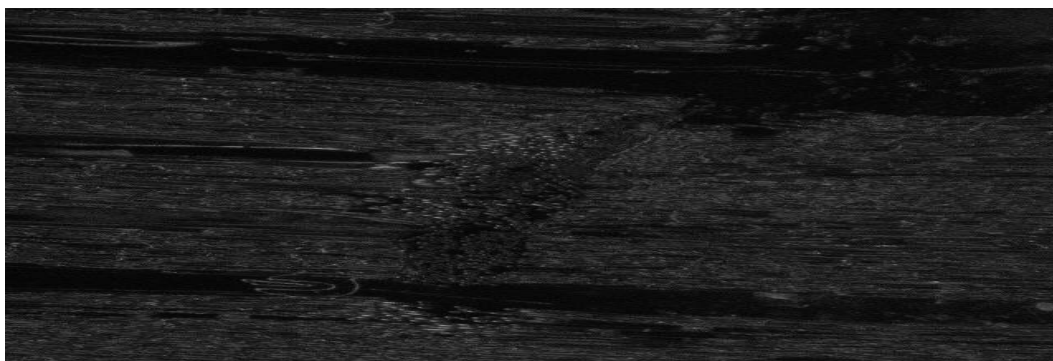
At 100X



At 200X



At 1000X



At 2000X

Figure 3.18: Phase contrast microscopic samples of 1% nanoclay/epoxy lay-ups at different magnifications

Cross-sectional images of the above samples in figure 3.18 show the cracking and tearing action of the microstructure inside the lay-up. In order to optimise the volume of nanofillers into the epoxy matrix, to get a stronger lay-up, the use of Phase contrast microscopy for lay-up crack analysis has become inevitable. This microscopy gave a clear view of the locus of failure and a good understanding about the progression of crack in the fractured surface, besides the effect of molecular dispersion resulting in crack formation and propagation. Interfacial debonding, which caused a reduction in the strength of these laminates, resulting in the yielding of the lay-up was also observed between the carbon fibre and the nanofiller/epoxy matrix.

The easiest way of measuring the size of an agglomerated particle under this microscopy is by relating it to the size of the field of view. The simplest way of achieving this is by measuring the size of the field of view at a low magnification and then scaling the size appropriately as the magnification is increased. The field of view can be measured approximately by looking at a ruler under the lowest magnification lens. Accuracy can be improved by using a graticule.

3.3.4 High speed photography

During this research, high-speed photography helped in studying the yielding process, besides providing a lot of information about the time taken to reach maximum yield each time as well [77]. Therefore, during each test, the high-speed camera was employed live. The frame speed at 1000 frames per sec, shutter speed at 60X and the contrast ratio at 10000:1 were set as standard during photography. Some of the frames are displayed as shown below in figure 3.20 to figure 3.22.

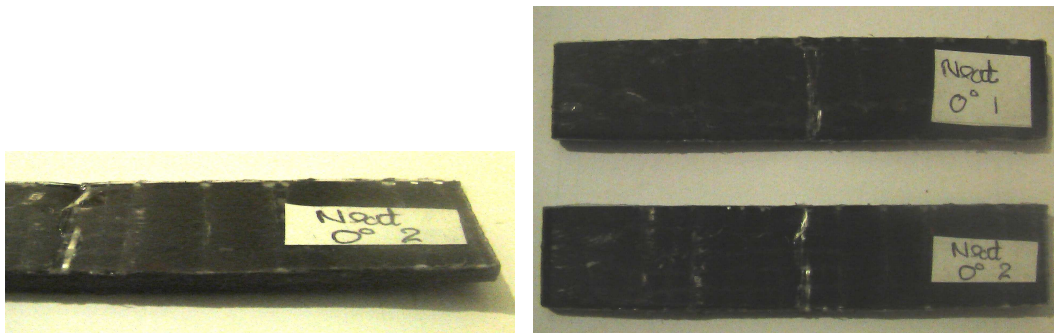


Figure 3.19: Lay-up samples used during high-speed camera photography



Figure 3.20: Samples of 1% nanoclay/epoxy composite lay-up at 0 degrees (1hr mixing)

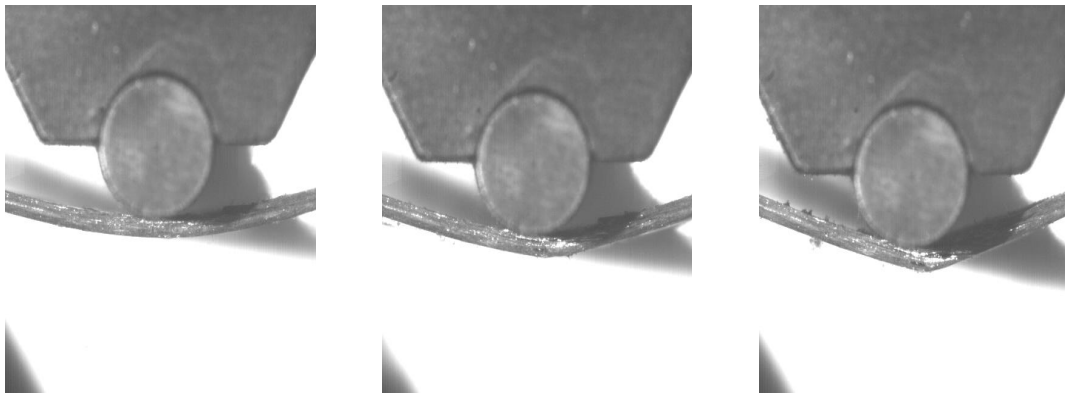


Figure 3.21: Samples of 1% nanoclay/epoxy composite lay-up at 45 degrees (1hr mixing)

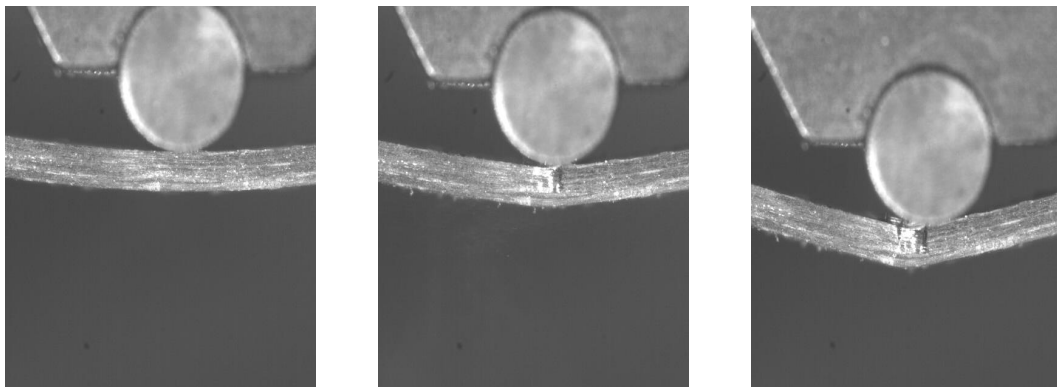


Figure 3.22: Samples of 1% nanoclay/epoxy composite lay-up at 90 degrees (1hr mixing)

It was made clear that continuous loading or continuous stresses during three point bending could cause the lay-up to separate at the interface between two layers resulting in delamination. This could also lead to fibre pullout or separation of individual fibres from the matrix lay-up. In order to achieve high reinforcement volume fractions and high stiffness and strength to weight ratios, through this research it is recommended that these nanofilled/epoxy composites can be laminated and cured under temperature and pressure [78].

3.3.5 Surface tension measurement using the Drop shape method

Solids have free surface energy because atoms in a bulk of solid are subjected to attractive forces from all directions while the atoms along the surface experience only inward forces. In case of liquids, the net inward force along the surface of a liquid makes the surface act as if it is an elastic skin that constantly tries to decrease its area. The way of looking at surface free energy in a liquid drop was first used by Young in 1805. In that, he had referred this phenomenon as ‘surface tension’. He also showed that the mechanical properties of an interface could be modelled as an imaginary membrane stretched over the surface [79]. The tension acting in this imaginary membrane is expressed as a force per unit length and in the units of Newtons per metre. Therefore, whenever dealing with liquids, the surface energy i.e. the force acting along the surface of the liquid is referred as surface tension even though the surface energy and the surface tension refer to the same dimensional quantity as shown in the equation below sharing the same symbol γ .

$$\text{surface energy} = \frac{\text{energy}}{\text{area}} = \frac{\text{joule}}{\text{m}^2} = \frac{\text{newton} \times \text{m}}{\text{m}^2} = \frac{\text{newton}}{\text{m}} = \frac{\text{force}}{\text{length}} \quad (3.9)$$

Drop shape analysis is one of the convenient ways to measure the surface tension of liquids. According to this drop shape method, by knowing the density of the liquid and by identifying the geometric parameters of the liquid droplet such as the droplet volume and the contact angle through an imaging system, one can compute the surface tension of the liquid [80]. In this research, this approach is adopted modelling and validation to understand the effect of the surface tension of epoxy in bonding.

3.3.5.1 Principle

The principal assumptions behind this analysis are

- The droplet should be symmetric to the central vertical axis. This means, it is irrelevant from which direction the drop is viewed [81].
- The droplet should not be in motion. Since the viscosity or the inertia plays a vital role in determining its shape, enough care should be taken to maintain the droplet away from any external forces other than the interfacial tension and gravity [82].

As long as the axisymmetric droplet profile may be precisely predicted by the direct method, which is by modifying and incorporating the droplet image system to build up a measurement system, one can determine the surface tension of the liquid. This principle acts as the basis of this analysis.

3.3.5.2 Procedure

1. A 20 SWG needle with an outside diameter of 0.914 mm was found to be a good size to start with. But 22 SWG needle with an outside diameter of 0.71 mm could have also been tried.
2. 20 μ l of epoxy was measured with the help of a pipette and then the same was sucked into the syringe through the needle. While doing so, adequate care was taken to ensure that there was no air trapped in the needle. Dispensing excess epoxy through the needle did this.
3. This was an iterative process, because one will not know how large the drop is going to be before setting magnification and one cannot calibrate until the magnification is set.
4. A camera was then aligned so that the line of sight of the droplet was made exactly horizontal or axisymmetric and in focus. Obviously focusing the drop was very important.
5. To obtain the best results, the image was precisely brought into focus by ensuring the backlight centred on the droplet so that the bright spot was at its maximum diameter as shown in the figure 3.23 in the next page.



Figure 3.23: Profile of the droplet under experiment

6. Mechanical standards were made to fit into the image and required external measurements were collected to one micron accuracy.
7. The vertical line was brought to the centre of the drop to ensure that the drop is axially symmetric. There was another horizontal line running at the bottom end of the drop i.e. at its maximum diameter.
8. The magnification standards were measured with the same lighting and aperture setting on the drop.

During this experiment, a high-speed camera was set up to take a movie till the drop reached its stability. This is to identify the shape of the drop from the initial stage. By this drop shape method, accuracy was also set by magnification, while the resolution was defined by electronic noise and mechanical vibration were controlled on the drop.

During this experiment, while using the Young-Laplace equation, it was noticed that the droplet required a small amount of internal energy to get distorted by the gravity. This distortion by the gravity was balanced against the restoring force called the surface tension. So it was made evident that the surface tension cannot be determined for a droplet, which is not affected by gravity [83]. Therefore to confirm the distortion, the drop height was ensured to have pressure difference between the top and the bottom end. This was done by trial and error method only, usually by deploying a dispenser with a wide tip to support the needed drop size.

However, as a continuation of this experimental process, a modelling was also carried out and the results were validated against a standard reference. Detail discussion about the relationship between the surface tension of the newly developed nano-enhanced epoxy matrix and bonding follows in the next chapter. This gave a lot

of valuable information about the effect of the inner chemistry upon adhesion of the altered matrix with the carbon fibre lay-up.

Chapter 4

Modelling and Validation

4.1 Introduction

In this research, the modelling was carried out to understand the influence of the surface tension in bonding and also to confirm the theory behind cracking and propagation of crack in the nano-enhanced epoxy reinforced carbon fibre laminations. The entire analysis was carried out using drop shape analysis with water and then with the nano-enhanced epoxy matrix and the results were validated with the standard reference.

During each experiment, six samples were taken for validation. Based on the measurement of surface tension of the newly developed epoxy matrix, the effect of its surface tension in bonding is analysed and discussed in the latter part of this chapter. Therefore this is carried out in two steps as mentioned below:

- Modelling.
- Validation and analysis on the influence of surface tension in bonding.

4.2 Modelling

As modelling is a vital part in an analysis, in this research, it was adopted to characterise the influence of surface tension of the nano-enhanced epoxy in bonding using drop shape analysis method. It was also carried out in order to confirm whether the theory behind cracking and propagation of crack has anything to do with the surface tension of the matrix. The entire results of the modelling were validated with

water as the standard reference and the results were considered during analysis and the take has been discussed in correlation with the bonding theories.

Primarily finding

Contact angle, θ_s in deg

Liquid droplet profile, $h(r)$ in m

Droplet radius, r in m or Droplet diameter, d in m

Droplet height, h in m

Mass of liquid droplet, m in mg

Volume of liquid droplet, V in m

Secondary findings

Liquid pressure at droplet surface in atm.

Ambient air pressure in atm.

Volumetric flow rate of the dispensed fluid

Droplet temperature, C

Radius coordinate, m

Reference temperature, C

And we have

Gravitational acceleration, g in m/s

Density of the liquid, ρ in kg/m

Objective function

Cartesian coordinates, m

Theoretical Surface tension, N/m

During this drop shape method, since measuring the contact angle of the liquid becomes the key indicator, as discussed in the previous chapter, the experiment was carried out to identify the profile in order to measure the contact angle. The contact angle is the angle enclosed between the tangent to the liquid surface and the interface between substrate and liquid at their line of intersection. Figure 4.1 illustrates this.

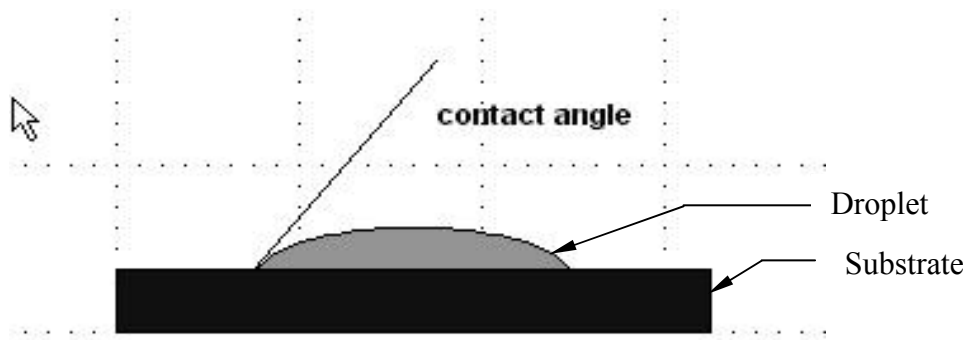


Figure 4.1: Schematic representation of a drop on a glass substrate

Stated above, from the measurement of contact angle, physical properties such as wettability, affinity, adhesiveness and repellency of the nano-enhanced epoxy droplet, besides an indication about the chemical bonding by the uppermost surface of the matrix can be inferred. Therefore the contact angle is seen as the physical manifestation of the more fundamental concepts of surface energy and surface tension as shown in figure 4.2.

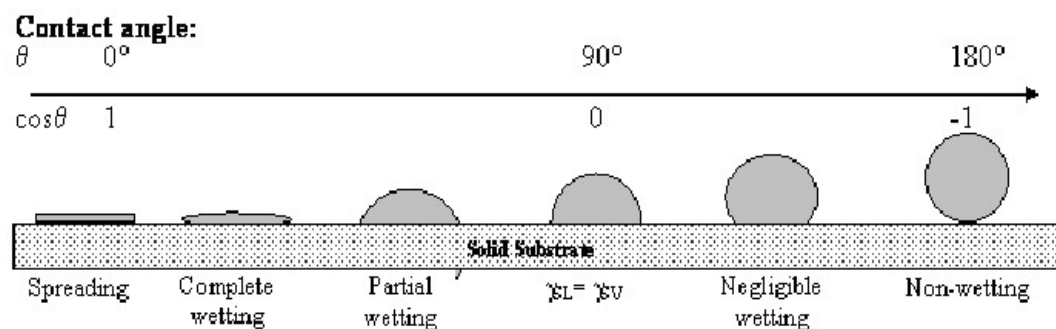


Figure 4.2: Liquid drop on solid surface

During a theoretical or empirical approach, surface energy values are calculated from the contact angle data. Both the approaches emphasize the concept that the contact angle is related to surface energy and surface tension. In order to measure the contact angle of the liquid droplet, complete wetting is recommended. Wetting is the extent

to which a liquid droplet spreads over the glass substrate, which is illustrated in the figure 4.3 below. For practical purposes, if $\theta_s > 90^\circ$, it is considered as non-wetting [84].



Figure 4.3: Effect of wetting on contact angle

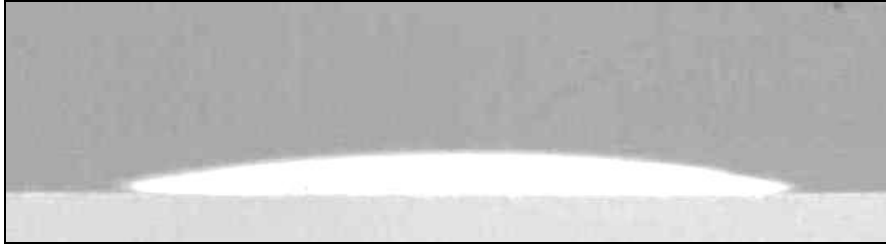


Figure 4.4: Profile of the droplet under experiment

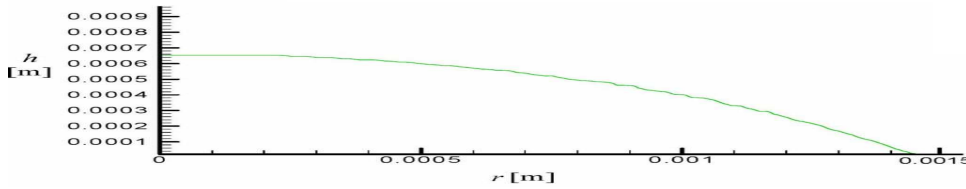


Figure 4.5: Graphical reproduction of the water droplet

When applying this surface tension measurement method, one needs to measure only the density of the liquid, ρ and identify the liquid droplet profile, $h(r)$ by a droplet image system. The identified droplet profile is analysed to calculate the geometric parameters such as the droplet volume, V whereas the contact angle, θ_s is measured by using an image analysis system. With the measured density, the droplet volume, the contact angle and the surface tension of the liquid, σ can be evaluated. In this research, an objective function in conjunction with the direct method is used as

$$J = (\rho - \rho_d)^2 + (V - V_d)^2 + (\theta_s - \theta_{sd})^2 \quad [4.1]$$

where ρ_d , V_d and θ_{sd} represent the predicted density, droplet volume and the contact angle respectively of the liquid from direct solver. Therefore, the obtained liquid droplet profile will be used to calculate ρ_d , V_d and θ_{sd} . And hence it becomes an objective function. In the successive steps the value of ρ is continuously updated. When the objective function reaches a minimum, the inverse process is completed and the searching procedure for ρ is then terminated. An initial approximation for surface tension γ will be made in the beginning and then with the liquid droplet profile $h(r)$. Accompanying the approximation value, the actual value of the surface tension γ will be then calculated. The accuracy of the measurement can be improved as long as a lower objective function is yielded [84].

Therefore to start, when the contact angle is less than 90° ,

$$\gamma = 0.25 \Delta \rho g Z_{180}^{20} C_{180} \quad [4.2]$$

where γ is the surface tension in N/m, ρ is the density in kg/m and g is the gravitational constant in m/s and Z_{180} is the experimental measure of the drop height.

In accordance with the existing information, it is understood that the size or the diameter of the droplet is greatly dependent on the surface tension of the epoxy resin, since this property has large influence on the dynamic behaviour of the liquid droplet formed on the glass substrate. Therefore, the direct method has been incorporated with a dynamic droplet imaging system to build-up a measurement system for the determination of the surface tension of epoxy resins as shown below.

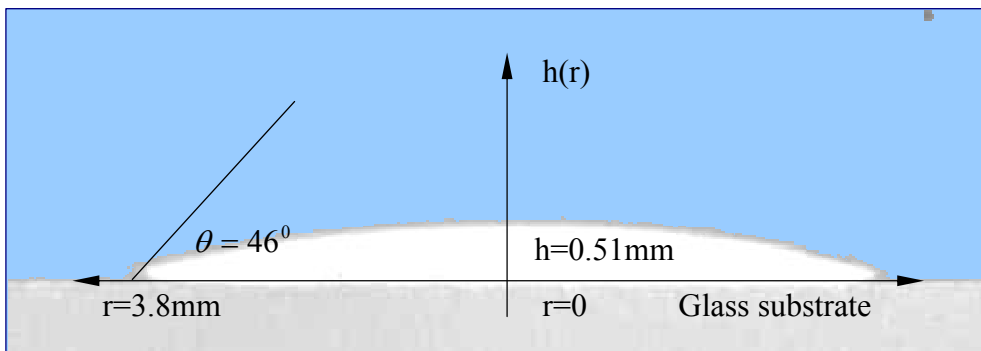


Figure 4.6: Analysis on a water droplet

$$\theta = 46^\circ$$

$$\rho = 0.072 \text{ N/m}$$

$$R_0 = 3.8 \text{ mm}$$

$$h(r) = 0.51 \text{ mm}$$

On getting the droplet on a glass substrate, the surface tension of the liquid can be determined by fitting the shape of the drop to the Young-Laplace equation, which relates the interfacial tension to drop shape. The shape of a drop is determined by its radii of curvature R_1 and R_2 . The relationship between the interfacial pressure, i.e. the pressure acting across the interface and the radii of curvature, are represented in the form of an equation called the Laplace equation

$$\Delta P = \gamma (1/R_1 + 1/R_2) \quad [4.3]$$

where ΔP = interfacial pressure difference

γ = interfacial tension

R_1, R_2 = radius of curvature of the surfaces

In a column of fluid density ρ with height h , the pressure can be written as

$$\Delta P = \rho g h \quad [4.4]$$

where g is the acceleration due to gravity, (9.8 m/sec^2).

Combining equation [4.3] and equation [4.4] to get Young-Laplace equation,

$$\rho g h = \gamma (1/R_1 + 1/R_2) \quad [4.5]$$

where h is normally measured from the apex of the drop, ρ and g are known, γ is what is desired and R_1 and R_2 can be measured from the profile. When the radii of curvature are expressed in X-Y coordinates of the drop profile (taking the height of the droplet h in the y direction), a differential equation results with no analytical solution. Therefore bringing the y coordinates in relation to the above equation,

$$\rho g h = \gamma \left[\{y'' / (1 + y'^2)^{3/2}\} + \{y' / (1 + y'^2)^{1/2}\} \right] \quad [4.6]$$

where $y' = \frac{dy}{dx}$ and $y'' = \frac{d^2y}{dx^2}$

Since the static profile of the axis-symmetric liquid is governed by the Young-Laplace equation, equation [4.6] can be rewritten as:

$$\gamma \frac{d}{dr} \left\{ r \frac{dh(r)}{dr} \left[1 + \left(\frac{dh(r)}{dr} \right)^2 \right]^{-\frac{1}{2}} \right\} = P_0 - P_a - \rho g h(r) \quad [4.7]$$

Boundary conditions were expressed as

$$\frac{dh(r)}{dr} = 0 \quad \text{at } r = 0 \quad [4.8]$$

$$\left. \frac{dh(r)}{dr} \right|_{r=a} = -\tan \theta_s \quad \text{at } r = a \quad [4.9]$$

where $h(r)$ represents the height of the liquid droplet as a function of radius r , P_a is the atmospheric pressure, P_0 is the liquid pressure at $z = 0$ and θ is the contact angle.

Also since the liquid is assumed to be incompressible, the mass conversion law can be written as

$$Qt = \pi \int_0^{h(0)} r(h)^2 dh \quad [4.10]$$

where Q is the volumetric flow rate of the liquid, t is the dispensing time and the function $r(h)$ is the inverse function of $h(r)$.

Numerically solving the equations using the fourth order Runge-Kutta method with the given values of θ , ρ and γ , $h(r)$ by substituting the values in equation [4.7]

$$\gamma \frac{d}{dr} \left\{ 3.8 * \frac{dh(r)}{dr} \left[1 + \left(\frac{dh(r)}{dr} \right)^2 \right]^{-1/2} \right\} = P_0 - 0.072 - (0.0728 * 9.81 * h(r)) \quad [4.11]$$

$$\text{where } \frac{d}{dr} = f_1 \text{ and } \frac{dh(r)}{dr} = f_2$$

$$\gamma \left(r f_2 + r f_2^3 \right)^{\frac{1}{2}} = P_0 - P_a - \rho g h(r) \quad [4.12]$$

$$\gamma \left(r f_1 f_2 + r f_1 f_2^3 \right)^{\frac{1}{2}} = P_0 - P_a - \rho g h(r) \quad [4.13]$$

$$\gamma \frac{d}{dr} \left\{ r \frac{dh(r)}{dr} \left[1 + \left(\frac{dh(r)}{dr} \right)^2 \right]^{\frac{1}{2}} \right\} = P_0 - P_a - \rho g h(r) \quad [4.14]$$

where $\frac{dh(r)}{dr} = Z$

$$\gamma \frac{d}{dr} \left\{ r Z \left[1 + (Z)^2 \right]^{\frac{1}{2}} \right\} = P_0 - P_a - \rho g h(r) \quad [4.15]$$

$$\gamma \frac{d}{dr} \left\{ \left[r Z + r Z^3 \right]^{\frac{1}{2}} \right\} = P_0 - P_a - \rho g h(r) \quad [4.16]$$

Following are the steps involved in analysing the drop shape of the droplet.

The drop height Z_θ , the equatorial radius X_{90} and the contact angle θ for the drop were measured.

For the value of θ , the coefficient of correcting factor $c_1 - c_8$ with respect to the contact angle can be obtained from the Paddy's table in Appendix A.

The initial calculation of $f \left(\frac{X_k}{X_k} \right)$ was carried out using the random value of X_k .

The ratio was compared with the measured $\frac{Z_\theta}{X_{90}}$.

An iterative technique was used to solve the equation $f \left(\frac{X_k}{X_k} \right) = \frac{Z_\theta}{X_{90}}$ for X_k , the only unknown value.

By substituting the random value to the equation $Z_k = \frac{Z_\theta}{X_k}$ the value of Z_k can be obtained from the equation [4.16].

Thus the surface tension becomes

$$\gamma = \Delta \rho g \frac{Z_\theta^2}{Z_k^2}$$

It is to be noted that the measurement of Z_θ , X_{90} and θ will also affect the accuracy of the actual surface tension, γ .

Since c_{180} is the function of the droplet shape, an iterative procedure is needed for different experimental values of X_{90} and Z_θ to get the value of θ in order to

measure the value of β which is the ratio of $\frac{Z_\theta}{X_{90}}$. The value of β is found when the two ratios of $\frac{Z_\theta}{X_{90}}$ match.

This was a time consuming process and needed a lot of interpolation between the tables. Since the approximation could be quite inaccurate and does not cover the whole range of the drop shape factor β or the contact angle θ , adopting a polynomial function would serve the purpose and the same could be solved easily as follows.

Therefore the polynomial equation can be written as

$$Z_k = 2 \sum_{i=1}^5 c_i X_k^i - \frac{\sqrt{\frac{1 - \cos \theta}{2}} + c_8}{X_k + c_8} e^{0.1c_6 X_k^{c_7}} + \frac{\sqrt{\frac{1 - \cos \theta}{2}} + c_8}{X_k + c_8}, \left(\frac{\gamma}{g\Delta\rho}\right)^{1/2} \quad [4.17]$$

where k is the meniscus coefficient

It was understood that the shape of a drop of the liquid lying on the surface of the glass substrate is determined from the balance of forces, which included the surface tension of that liquid as well. The surface or the interfacial tension at the liquid interface could then be related to the drop shape through the following equation

$$\gamma = \frac{\rho g R_0^2}{\beta} \quad [4.18]$$

where γ = surface tension in N/m.

ρ = density in kg/m.

g = gravitational constant in m/s⁻².

R_0 = radius of drop curvature at apex

β = shape factor.

β , the shape factor, can be defined through the Young-Laplace equation, expressed in modern computational methods. This was performed using iterative approximations, allowing the solution of the Young-Laplace equation for β to be performed. Thus, for any drop shape where the densities of the fluid and the vapour in contact, are known,

the surface tension may be measured, based on the Young-Laplace equation. This approach represented a significant improvement in both the ease and accuracy from other traditional methods.

Among other things, the Young-Laplace equation showed that the pressure is quite high in smaller drops. The weight of a drop can be described using Tate's Law as follows

$$W = 2 \pi r \gamma \quad [4.19]$$

where W = weight of drop

R = radius of wetted tip

γ = surface tension

4.3 Validation and analysis on the influence of surface tension in bonding

The measurement of the contact angle of the epoxy droplet through the drop shape method was found to be a quick and simple way to evaluate the surface tension of the epoxy in order to understand the effect of surface tension in bonding. For testing the accuracy of this approach towards validation, this experiment was first carried out with water and then repeated with six samples of neat epoxy and six samples of epoxy with 1% loading of nanoclay. The neat epoxy and the 1% nanoclay/epoxy samples were directly dispensed to a glass substrate to form a droplet like the water. In this research, it became critical to have an accurate measurement of the surface tension of epoxy and the nano-enhanced epoxy matrix, in order to compare and understand the forces acting between the matrix and the carbon lay-up, to determine the influence of such forces in bonding.

Table 4.1: Analysis results on the surface tension of water and epoxy using Drop shape approach.

Analysis summary						
Name of the liquid used	θ	ρ N/m	R_0 mm	$h(r)$, mm	Theoretical Surface tension, γ_t , N/m	Calculated Surface tension, γ , N/m.
Water	46°	0.998	3.8	0.51	0.072	0.71
Neat Epoxy	43°	1.10	4.3	0.39	0.047	0.045
1% Nanoclay/ Epoxy	38°	1.45	4.6	0.32	0.035	0.032

In nano-enhanced epoxy matrix, increasing a new surface area always requires an internal energy. This internal energy develops a crack along the surface and lets the crack to propagate and create new surfaces. With nanoclay/epoxy samples, it was interesting to notice that along the surface, the nanoparticles were pulled towards the rest of the nanoparticles embedded in the matrix. Since it is the intermolecular force, *Van der Waals* force, which draws the nanoparticles together to bind them along the surface [85]. It has been found that though these bonds were weak, they had enough internal energy to develop a weak bonding structure, which in turn had the potential to create a cavity in the matrix, resulting in developing a path to break the surface of the matrix along the direction of the lay-up, during testing.

Apart from the above correlation of the effect of surface energy in bonding, enlarging the area of contact for the epoxy matrix has the advantage of better adhesion over the wider area. While increasing the surface area by the addition of nanoparticles is one of the most attractive characteristics in a nano-enhanced epoxy composite during lay-ups, it also develops an internal force which, in turn facilitates bonding by taking advantage of the newly created large interface area by the addition of nanofillers into the epoxy matrix. Through earlier researches, it was found that an interphase of 1 nm thick of nanoparticle could occupy around 30% of the total volume, in case of nanofilled epoxy composites [86]. Therefore, the interphase contribution made by less than 5% loading of nanofiller into an epoxy matrix provided diverse possibilities and opportunities of altering the performance of the matrix, by influencing the properties of the matrix directly. Significant improvement

in the tensile performance of epoxy nanocomposites has also been reported in this research in terms of strength, stiffness and toughness with a low filler content of about 1% loading which was due to better adhesion due to optimal surface forces action along the matrix.

During wetting or spreading process, the contact area formed along the surface of contact between the epoxy matrix and the carbon fibre always depends on the surface tension and the viscosity of the epoxy. Therefore, in order to achieve a better bonding strength, increasing the surface energy becomes inevitable. And to achieve that, pre-treating the fibre with chemical adhesion enhancers like silicone and fluorocarbon becomes desirable. This pre-treating can also be done by physical processes like etching, flame treating etc. depending upon the nature of the materials used. But enough care should be taken to make sure that the matrix fills the grooves and valleys created by the above said processes. Therefore with relevance to bonding, it was also found that for the substrates like fibres, good wetting results in better adhesion.

Table 4.2: Effect of surface tension on adhesion

Properties	Liquid with smaller contact angle	Liquid with larger contact angle
Wettability	Better	Worse
Adhesiveness	Better	Worse
Solid surface free	Larger	Smaller

Further to this, to enable the adhesive bonding between the epoxy matrix and the fibre during lay-up, first the epoxy matrix was made to wet the surface evenly. Poor wetting would always allow the entrapped air to remain between the fibre and the matrix, which in turn will reduce the effective bonding area and create stress raisers along the interface [85]. During any practical applications, the area of the effective surface will be smaller than the true surface due to the existence of pores and uneven parts along the surface, which were not completely filled by the composite matrix.

Therefore adequate care was taken during the experiment to contain the surfaces from any external contaminations. Also these contaminants would tend to spread

readily on the fibre, because of their low surface tension, and prevent complete wetting. During this research, it was understood that a good wetting occurs only when the contact angle, θ , between the epoxy matrix and the fibre was less than 90° . Complete wetting occurs when the molecular attraction between the liquid and solid molecules are greater than that between similar liquid molecules.

From earlier researches, it has been found that adding pressure would enhance the adhesion [87]. Therefore, a set uniform pressure during wetting and an external continuous pressure of 30 kgs had been tried during the curing process. These pressures imparted better wetting, besides ensuring complete interfacial contact. Also it was made evident during this research that the lay-up with such pressure loading showed better bonding, which in turn resulted in higher adhesive strength than without pressure loading. This is evident through the results shown in the next chapter.

It was also noticed that the contact angle of the epoxy droplet changes with time. Therefore during this analysis, a curing time of 3 hours was employed uniformly during each experiment with all the epoxy samples. During lay-ups, a curing period of 24 hours was employed under pressure.

Chapter 5

Results and Discussions

5.1 Introduction

In this chapter, results of the various experiments carried-out so far through this research are analysed, discussed and substantiated in detail. This is aimed towards evaluating the effect of the different processing methods used during the synthesis, towards optimising the mixing processes and also to identify the optimum volume of nanofiller to epoxy in correlation with the adhesion of the nanofilled epoxy matrix to the lay-up. While doing so, it is also aimed to ascertain the enhanced achieved through this research. This chapter focuses on choosing the right nanofiller for varied applications, depending upon the property parameters required. While doing so, the tensile and compressive properties of epoxy matrix incorporating 1% nanoclay and 1% nanocarbon were considered individually for comparison. During this comparison, the commercial viability, in terms of producing bulk quantities for a commercial batch processing, was also considered. Since the combination of ultrasonic and mechanical mixing is capable of producing bulk quantities of nanofiller/epoxy nanocomposites in addition to other advantages in dispersion and consistency, they were identified as the right candidates for this synthesis.

Therefore, samples from various combinations of several nanofillers to the epoxy resin matrix, at various ratios, at a range of mixing durations and by different mixing methods were analysed. While doing so, samples from carbon lay-up laminates were also tested for their mechanical properties and the results were also analysed. During that process, the effect of complete exfoliation of nanoclay in bonding was discussed, in relevance to the bonding theories.

5.2 Results

Following is the summary of the analysis arrived after an extensive experimental work carried out on epoxy/nanocomposite matrix, as well as on carbon fibre lay-ups at various angles.

Table 5.1: Summary of the analysis on tensile test at 0° degree

	Sample no.	1 hour mixing				2 hour mixing	3 hour mixing		Neat Epoxy
		Nanoclay by weight			Nano carbon by weight	Nanoclay by weight	Nanoclay by weight		
		1%	1.5%	3%	1%	1%	1%	3%	
UTP MPa	Sample 1	463.000	555.333	416.000		315.000	260.666	217.666	558.000
	Sample 2	525.333	648.333	371.333	516.000	267.333	220.333	211.666	554.333
	Sample 3	484.667	542.000	389.333	557.000	352.666	318.333	231.333	577.333
Mean UTP MPa		591.000	481.888	392.222	563.222	311.666	266.444	220.221	536.500
σ_b MPa	Sample 1	1006.053	1126.651	1044.817		785.410	695.483	669.238	910.834
	Sample 2	1269.644	1323.954	943.801	1174.150	680.667	632.170	642.047	907.979
	Sample 3	1163.852	1136.625	1166.811	1332.110	886.314	942.902	764.212	910.979
Mean σ_b MPa		1206.44	1195.743	1051.81	1253.130	784.130	756.851	691.832	909.930

Table 5.2: Summary of the analysis on tensile test at 45° degree

	Sample no.	1 hour mixing				2 hour mixing	3 hour mixing		Neat Epoxy
		Nanoclay by weight			Nano carbon by weight	Nanoclay by weight	Nanoclay by weight		
		1%	1.5%	3%	1%	1%	1%	3%	
UTP MPa	Sample 1	64.667	53.000	59.666	79.000	52.000	53.666	36.333	54.000
	Sample 2	62.333	52.666	54.333	70.666	47.000	49.000	31.666	52.666
	Sample 3	62.666	46.333	63.000	68.666	50.333	43.666	30.000	45.333
Mean UTP MPa		63.222	50.666	58.999	72.777	49.777	48.777	32.666	50.666
σ_b MPa	Sample 1	160.663	150.418	153.976	199.287	129.004	155.744	116.435	140.518
	Sample 2	156.321	146.565	133.466	174.733	115.226	138.907	111.025	133.794
	Sample 3	155.691	120.202	157.336	188.772	122.436	125.870	109.689	117.965
Mean σ_b MPa		157.558	139.061	148.259	187.597	122.222	140.173	112.383	130.759

Table 5.3: Summary of the analysis on tensile test at 90° degree

	Sample no.	1 hour mixing				2 hour mixing	3 hour mixing		Neat Epoxy
		Nanoclay by weight			Nano carbon by weight	Nanoclay by weight	Nanoclay by weight		
		1%	1.5%	3%	1%	1%	1%	3%	
UTP MPa	Sample 1	34.000	52.666	26.666	38.000	21.333	20.000	16.333	32.333
	Sample 2	28.666	48.666	31.333	49.000	24.333	21.000	17.333	23.333
	Sample 3	33.000	50.333	30.000		24.666		15.666	32.333
Mean UTP MPa		31.888	50.555	29.333	43.500	23.444	20.500	16.444	29.333
σ_b MPa	Sample 1	94.524	78.475	72.474	78.758	52.232	67.411	60.252	51.533
	Sample 2	72.394	70.644	84.621	115.702	59.577	68.620	64.126	41.060
	Sample 3	97.086	74.999	74.534		59.536		62.004	56.270
Mean σ_b MPa		84.119	74.706	77.210	97.23	57.115	68.015	62.127	49.621

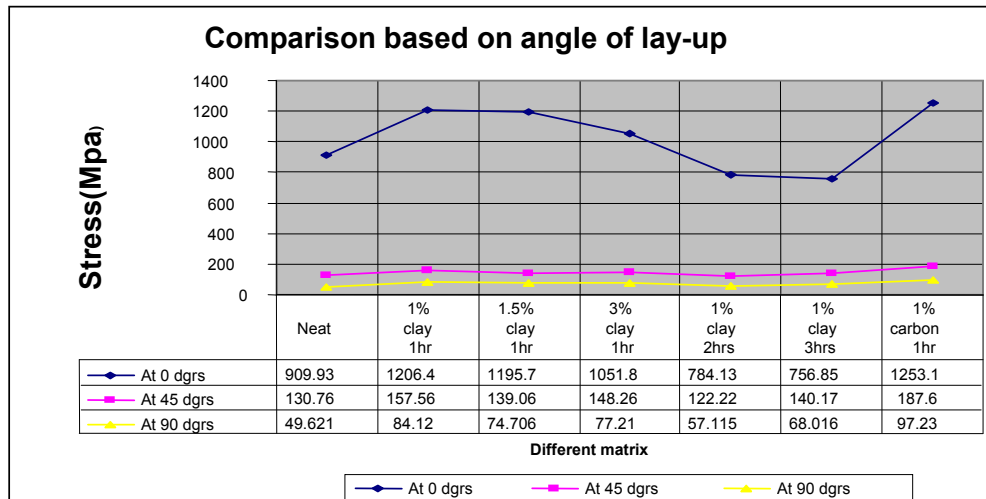


Figure 5.1: Comparison based on the angle of lay-up with various matrices

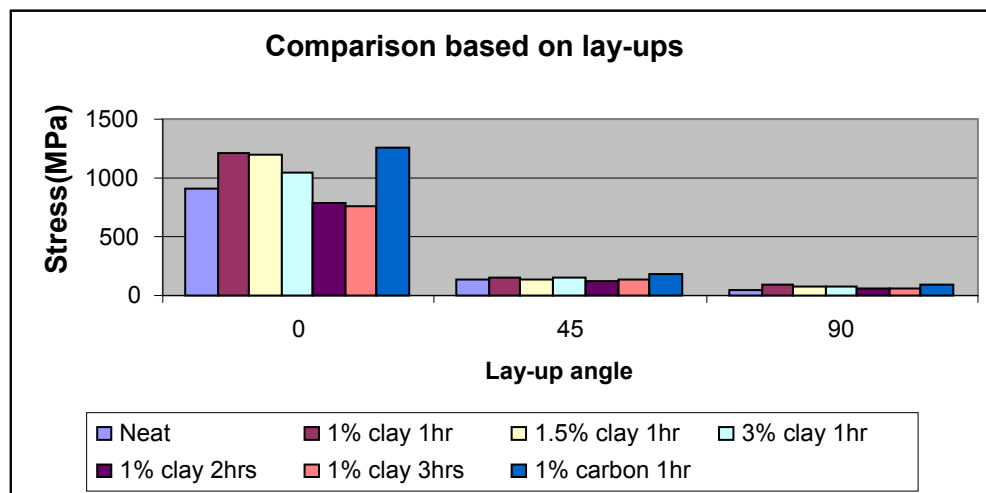


Figure 5.2: Stress comparison on different lay-ups

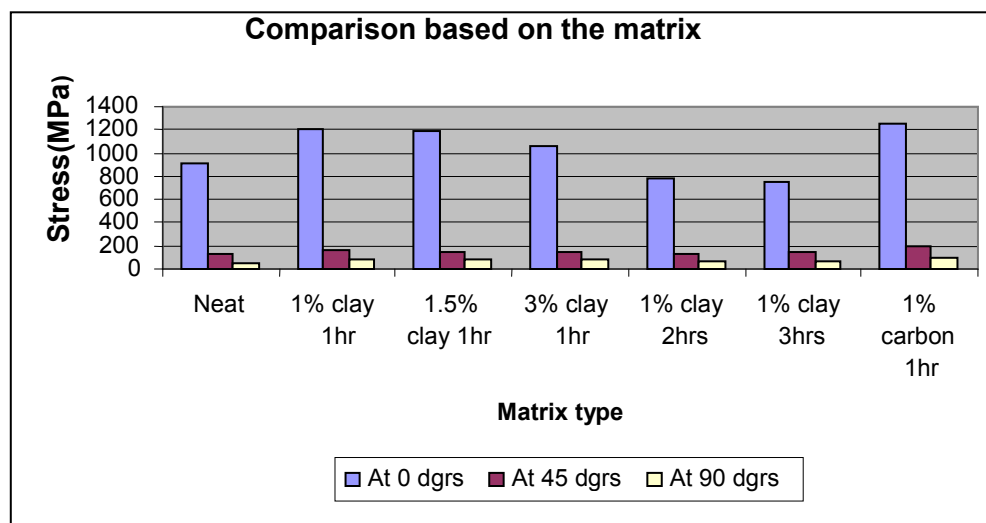


Figure 5.3: Stress comparison on various matrices

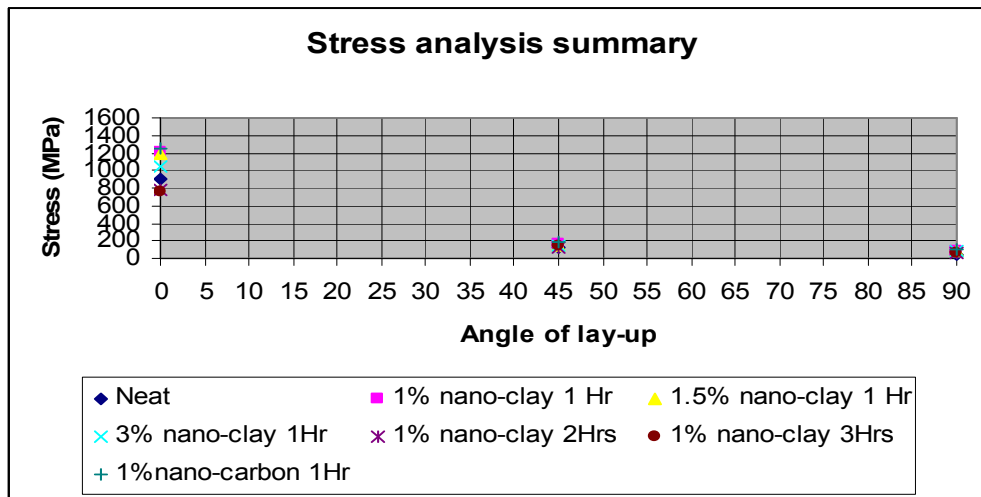


Figure 5.4: Summary of stress analysis

Table 5.4: Effect analysis on nanoclay lay-ups using factorial design method

	Duration of mixing T in hrs	Concentration C in %	Fibre orientation F in degrees
Low (-)	1 hr	1%	0°
High (+)	3 hr	3%	45°

Table 5.5: Effect analysis on nanoclay lay-ups based on UTP

SI no	Duration of mixing 'T' in hrs	Concentration of nanofillers 'C' in %	Fibre orientation 'F' in degrees	TC	TF	CF	TCF	UTP MPa
1	+	+	+	+	+	+	+	32
2	+	+	-	+	-	-	-	220
3	+	-	+	-	+	-	-	48
4	+	-	-	-	-	+	+	266
5	-	+	+	-	-	+	-	59
6	-	-	+	+	-	-	+	63
7	-	+	-	-	+	-	+	392
8	-	-	-	+	+	+	-	591
Effect	- 67	- 33	- 158	17	57	- 20	-20	

Therefore from the Table 5.5,

$$\begin{aligned}\text{the effect of duration of mixing, } T &= \frac{(32 + 220 + 48 + 266) - (59 + 63 + 392 + 591)}{8} \\ &= \frac{(566) - (1105)}{8} = \frac{-539}{8} \\ &= -67\end{aligned}$$

Similarly,

the effect of concentration of nanofillers,

$$\begin{aligned}C &= \frac{(32 + 220 + 59 + 392) - (48 + 266 + 63 + 591)}{8} \\ &= \frac{(703) - (968)}{8} = \frac{-265}{8} \\ &= -33\end{aligned}$$

And

$$\begin{aligned}\text{the effect of fibre orientation, } F &= \frac{(32 + 48 + 59 + 63) - (220 + 266 + 392 + 591)}{8} \\ &= \frac{(202) - (1469)}{8} = \frac{-1266}{8} \\ &= -158\end{aligned}$$

Also the combined effect of duration, T and concentration, C will be,

$$\begin{aligned}TC &= \frac{(32 + 220 + 63 + 591) - (48 + 266 + 59 + 392)}{8} \\ &= \frac{(906) - (765)}{8} = \frac{141}{8} \\ &= 17\end{aligned}$$

Similarly the combined effect of duration, T and fibre orientation, F will be,

$$\begin{aligned}TF &= \frac{(32 + 48 + 392 + 591) - (220 + 266 + 59 + 63)}{8} \\ &= \frac{(1063) - (608)}{8} = \frac{455}{8} \\ &= 57\end{aligned}$$

And the combined effect of concentration, C and fibre orientation, F will be,

$$\begin{aligned}
 CF &= \frac{(32 + 266 + 63 + 392) - (220 + 48 + 59 + 591)}{8} \\
 &= \frac{(753) - (918)}{8} = \frac{-165}{8} \\
 &= -20
 \end{aligned}$$

Finally the combined effect of duration, T, concentration, C and fibre orientation, F will be,

$$\begin{aligned}
 TCF &= \frac{(32 + 266 + 63 + 392) - (220 + 48 + 59 + 591)}{8} \\
 &= \frac{(753) - (918)}{8} = \frac{-165}{8} \\
 &= -20
 \end{aligned}$$

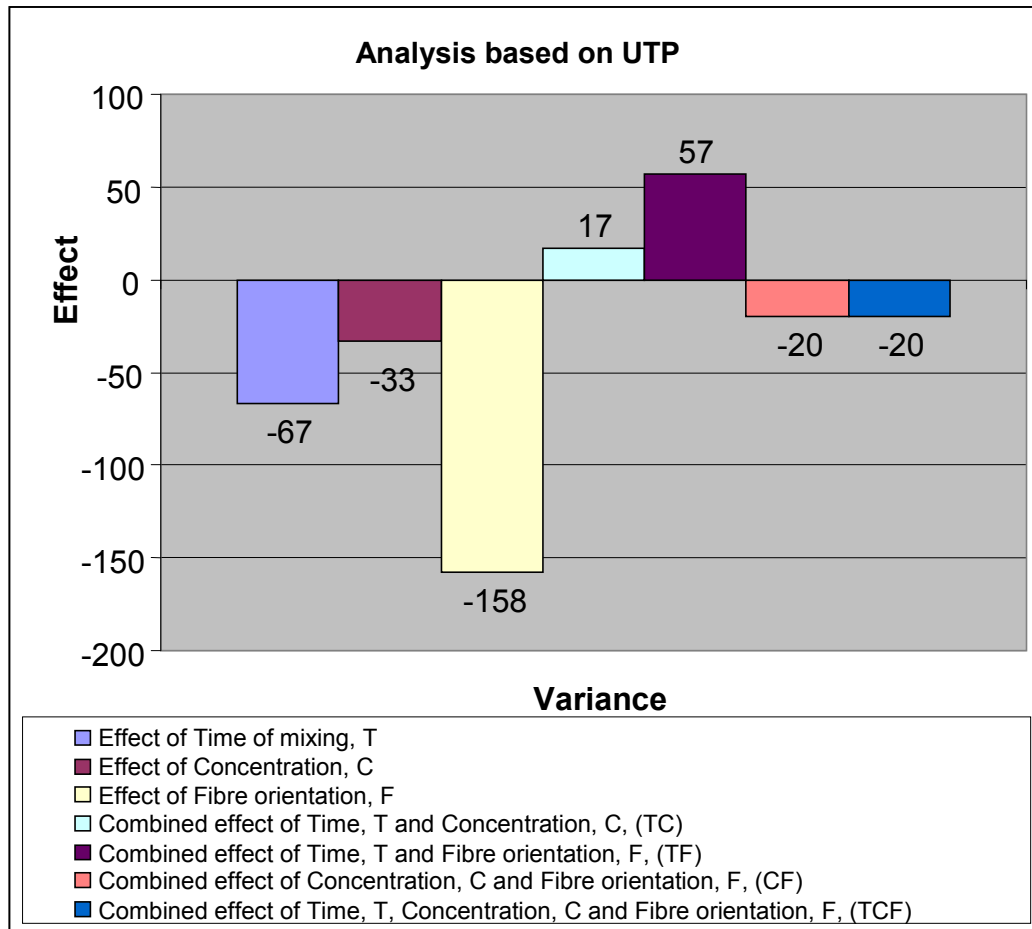


Figure 5.5: Summary of effect analysis on nanoclay lay-ups based on UTP

Table 5.6: Effect analysis on nanoclay lay-ups based on Stress

Sl no	Duration of mixing 'T' in hrs	Concentration of nanofillers 'C' in %	Fibre orientation 'F' in degrees	TC	TF	CF	TCF	Stress σ_b MPa
1	+	+	+	+	+	+	+	112
2	+	+	-	+	-	-	-	691
3	+	-	+	-	+	-	-	140
4	+	-	-	-	-	+	+	757
5	-	+	+	-	-	+	-	148
6	-	-	+	+	-	-	+	157
7	-	+	-	-	+	-	+	1052
8	-	-	-	+	+	+	-	1206
Effect	- 108	-32	-393	8	94	23	- 13	

Therefore by referring to the Table 5.6, the effect of duration of mixing,

$$\begin{aligned}
 T &= \frac{(112 + 691 + 140 + 757) - (148 + 157 + 1052 + 1206)}{8} \\
 &= \frac{(1700) - (2563)}{8} = \frac{-863}{8} \\
 &= -108
 \end{aligned}$$

Similarly, the effect of concentration of nanofillers,

$$\begin{aligned}
 C &= \frac{(112 + 691 + 148 + 1052) - (140 + 757 + 157 + 1206)}{8} \\
 &= \frac{(2003) - (2260)}{8} = \frac{-257}{8} \\
 &= -32
 \end{aligned}$$

And the effect of fibre orientation,

$$F = \frac{(112 + 140 + 148 + 157) - (691 + 757 + 1052 + 1206)}{8}$$

$$\begin{aligned}
&= \frac{(557) - (3706)}{8} = \frac{-3149}{8} \\
&= -393
\end{aligned}$$

Also the combined effect of duration, T and concentration, C will be,

$$\begin{aligned}
TC &= \frac{(112 + 691 + 157 + 1206) - (140 + 757 + 148 + 1052)}{8} \\
&= \frac{(2166) - (2097)}{8} = \frac{69}{8} \\
&= 8
\end{aligned}$$

Similarly the combined effect of duration, T and fibre orientation, F will be,

$$\begin{aligned}
TF &= \frac{(112 + 140 + 1052 + 1206) - (691 + 757 + 148 + 157)}{8} \\
&= \frac{(2510) - (1753)}{8} = \frac{757}{8} \\
&= 94
\end{aligned}$$

And the combined effect of concentration, C and fibre orientation, F will be,

$$\begin{aligned}
CF &= \frac{(112 + 757 + 148 + 1206) - (691 + 140 + 157 + 1052)}{8} \\
&= \frac{(2223) - (2040)}{8} = \frac{183}{8} \\
&= 23
\end{aligned}$$

Finally the combined effect of duration, T, concentration, C and fibre orientation, F will be,

$$\begin{aligned}
TCF &= \frac{(112 + 757 + 157 + 1052) - (691 + 140 + 148 + 1206)}{8} \\
&= \frac{(2078) - (2185)}{8} = \frac{-107}{8} \\
&= -13
\end{aligned}$$

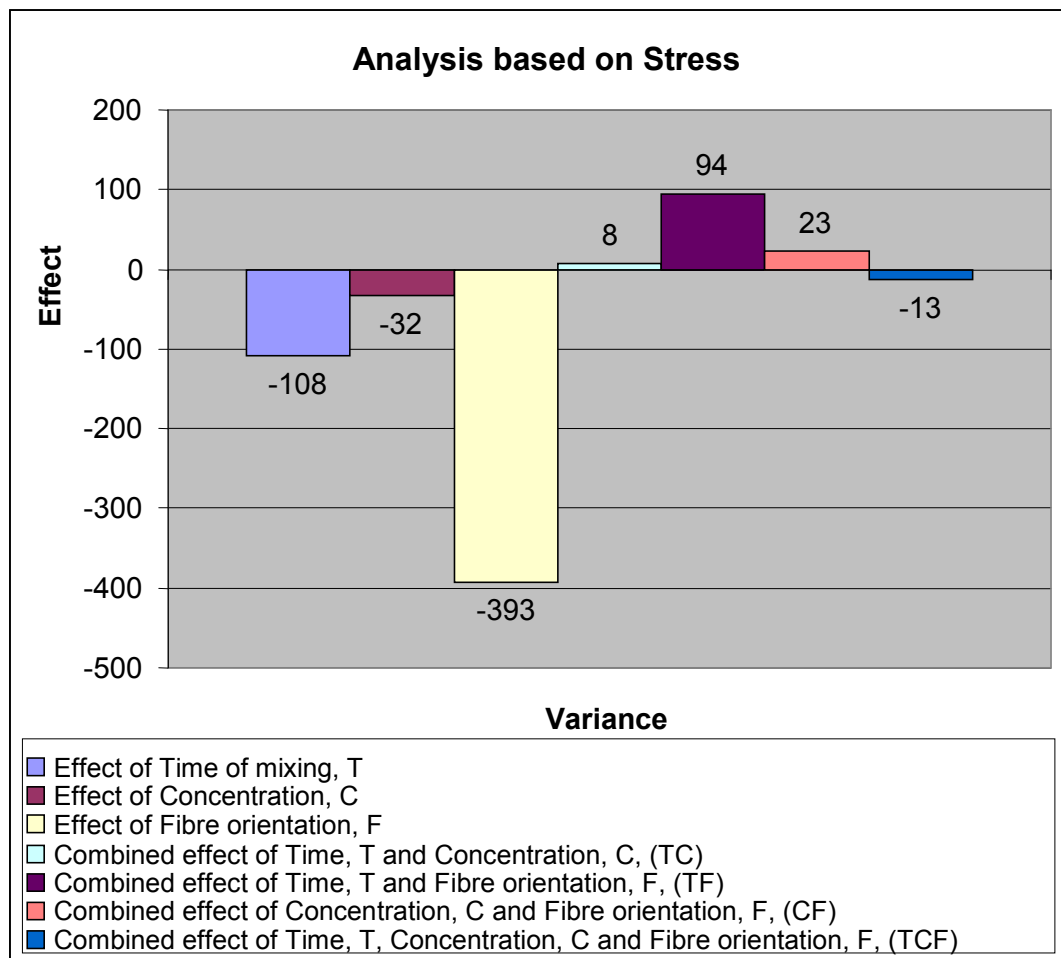


Figure 5.6: Summary of effect analysis on nanoclay lay-ups based on Stress

5.3 Analysis

The broadening field of nano-science has led the ability to characterise the nanocomposites through various analytical techniques. During this research, the entire analysis was carried out in four segments. They are:

- Analysis based on various nanofillers used.
- Analysis based on various ratios or concentrations of the nanofillers used.
- Analysis based on various duration of mixing.
- Analysis based on nature of mixing.

5.3.1 Analysis based on various nanofillers used

As the tensile property of these composite materials is directly related to their overall toughness, the composites fracture toughness is related to its interlaminar and interfacial strength parameters as well. It was noticed that, while nanocarbon and nanoclay show a higher tensile strength at 1% composition, the nanocarbon composite yielded earlier than the latter one during tensile testing. This indicates that the density of the nanocarbon particle, due to its closer molecular arrangement, could have had an effect on the strength of the matrix even though it bore a higher load than other samples. It deformed less until maximum load, which indicates a higher flexural modulus. On the other hand, composites with 1% loading of nanoclay showed higher values of tensile strength and tensile modulus compared with the nanocarbon composites.

Table 5.7: Comparison of tensile properties based on various nanofillers

Batch details	At 0 degree	At 45 degrees	At 90 degrees
	Mean UTP* MPa	Mean UTP* MPa	Mean UTP* MPa
A - Neat Epoxy	536.500	50.666	29.333
B - 1% Clay for 1 hour	591.000	63.222	31.888
G - 1% Carbon for 1 hour	563.222	72.777	43.500

UTP* - Ultimate Tensile Property

From the above Table 5.7, it is understood that, besides high tensile modulus, nanoclay possesses some extraordinary characteristics like excellent electrical properties in terms of insulation, good thermal stability and chemically inertness, high wear resistance, resistance against high-energy radiation. But it also has high friction coefficient. For these reasons, fillers like nanocarbon were also tested during this research to modify epoxy composites.

The in-built self-lubricating property of nanocarbon resulted a slide over between the lay-ups, which in turn resulted in developing a weaker bonding of matrix over the lay-up. This confirmed that the wear of the composite was mostly due to the fibre

matrix adhesion, which in-turn was due to the nature of the ingredients of the composite. While investigating at the laminar surface of the composite with 1% nanocarbon, the yielded surface displayed cracks and micro grooves and the surface was quite rough. This gave an indication that, during the test, the fibre had fractured into cracked fragments detaching many smaller filler particles from the composite, leaving cavities along the surface. These cavities were themselves stress concentrators, resulting in more cracks and a higher friction coefficient. This was also made evident when comparing the nanoclay/epoxy composite lay-ups with higher loading of nanoclay. This also gave an indication about the adverse effect of loading excess nanofillers into the matrix.

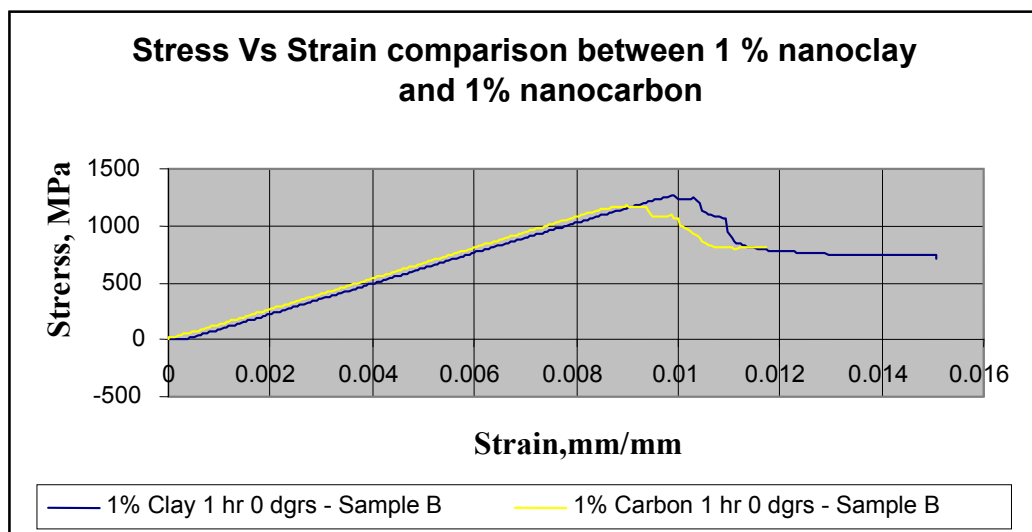


Figure 5.7: Stress analysis between 1% nanoclay and 1% nanocarbon

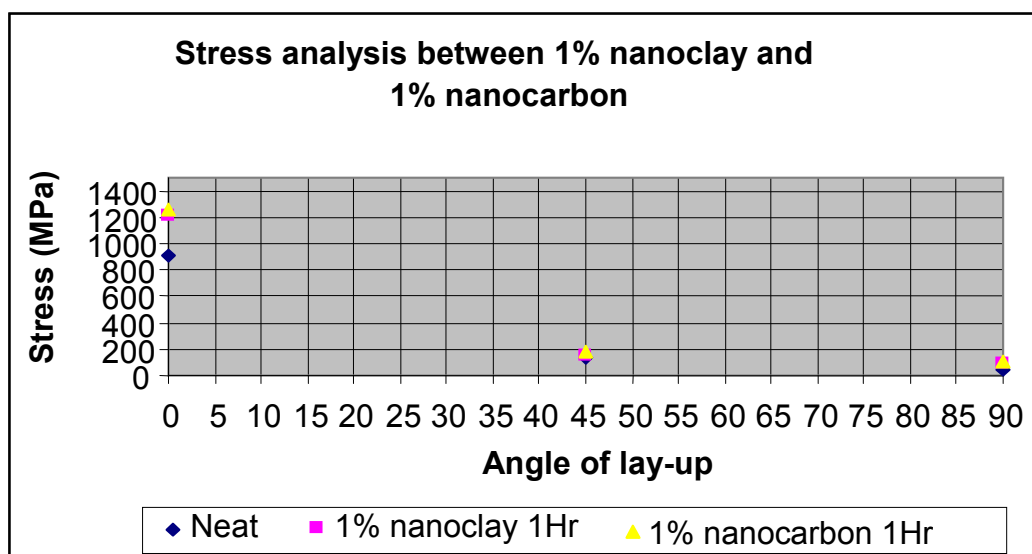


Figure 5.8 Stress analysis between 1% nanoclay and 1% nanocarbon at different lay-up angles

At the same time, the hydrophilic and hydrophobic property of the nanoclay had their effect on adhesion of matrix to the lay-up, during low percentage of loading. But the same also had an adverse effect during higher percentage of loading, by attracting excessive moisture into the matrix. In spite of that, nanoclay filled epoxy composite is identified as a potential candidate for structural applications in biomedical engineering, boat building, aerospace and sports gear due to its higher tensile strength and tensile modulus.

5.3.2 Analysis based on various ratios or concentrations of nanofillers used

As discussed earlier, experiments were carried out at various ratios of nanofillers to the epoxy resin base, 1%, 1.5% and 3%. In all these, composites with 1% loading of nanofillers offered a clear advantage with higher tensile strength than others. There was an observable decrease in the strength of the composite with the reduction of nanoclay by 0.5% loading. It can be observed from the Table 5.8 that the lay-up with 1% nanoclay was stronger and had higher tensile strength than the 1.5% and 3%. Therefore it was understood that loading of excess nanofillers (i.e. anything more than 1%) results in a weaker matrix. This deterioration in the physical property was noticed due to the agglomeration of excess particles along the matrix. During microscopy, this agglomeration of excess particles along the matrix was clearly visualised and the same was proven to be a weaker matrix during testing.

Table 5.8: Comparison of tensile properties at various ratios of nanoclay

Batch details	At 0° degree	At 45° degrees	At 90° degrees
	Mean UTP MPa	Mean UTP MPa	Mean UTP MPa
B - 1% Clay for 1 hour	591.000	63.222	31.888
C - 1.5% Clay for 1 hour	481.888	50.666	50.555
D - 3% Clay for 1 hour	392.222	58.999	29.333

It can be observed from the figures shown below that the tensile modulus increases with increasing nanoclay to 1% of loading and then it falls by up to 22% in ultimate yield strength with every increase of 0.5% loading of nanofillers into the epoxy matrix.

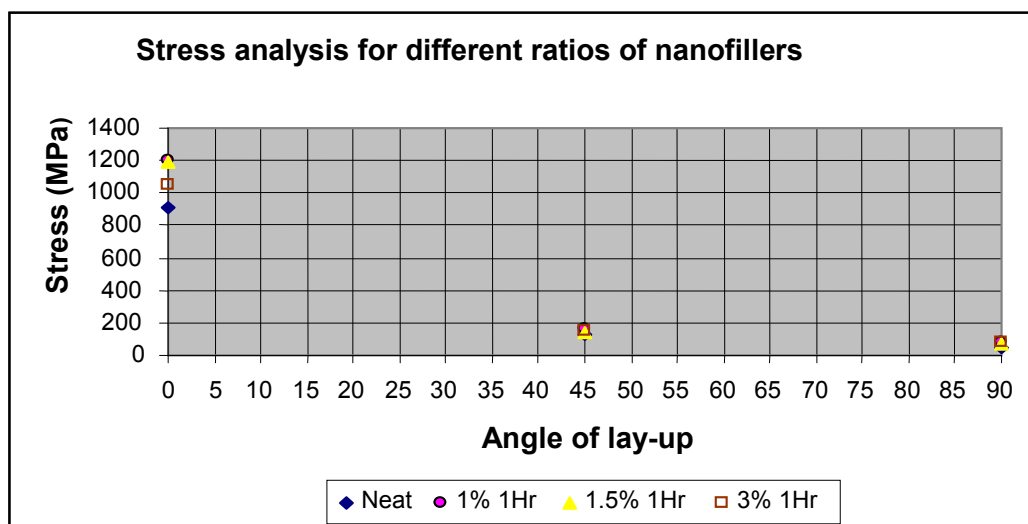


Figure 5.9: Stress analysis on different ratios of nanoclay/epoxy composites

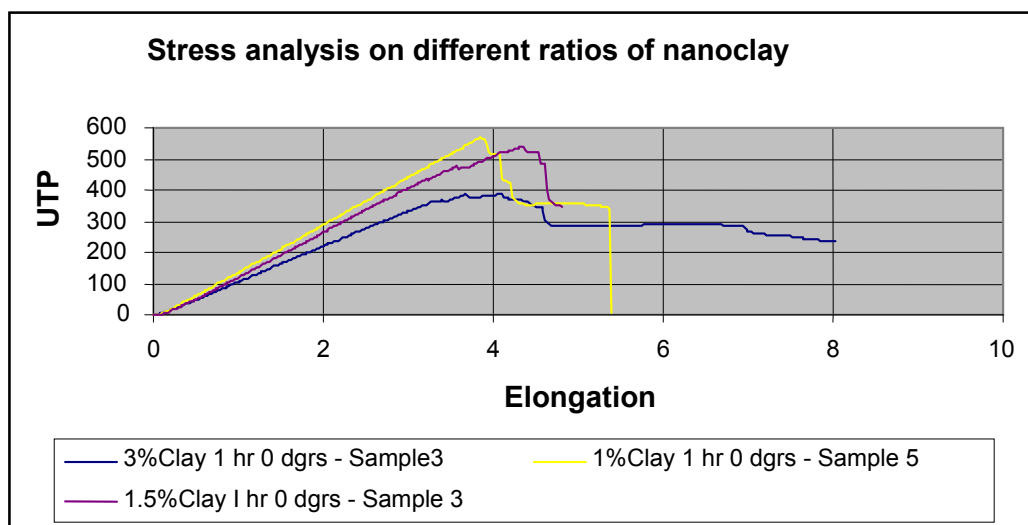


Figure 5.10: Stress analysis for different ratios of nanofillers at different angle of lay-ups

While discussing the mechanical strength of a composite, through earlier researches it was found that the interfacial frictional stress and the chemical bond between the matrix and the fibre plays a vital role which is shown in the figure 5.11 [87]. And again the physical properties are influenced by many factors including the matrix

fracture, the fibre/matrix de-bonding and the fibre pull out. This was observed to be higher with the lay-ups made from 1% loading when compared to other samples. However, the matrix material adjacent to the fibre controls the interfacial strength. This phenomenon was made clearly demonstrated during the analysis of the matrix and the lay-up in this research. It was understood that this was because of good covalent bond exhibited at 1% loading of nanoclay to the epoxy matrix. As discussed earlier, this bonding gets weaker in other epoxy composites with increased loading, due to the agglomeration effect, which was likely to be the cause of the drop in the tensile strength. This explained why it was much lower when the loading of nanofillers was high. It was also noticed that the interspaces developed due to the agglomeration of particles create and amplify the stress concentration.

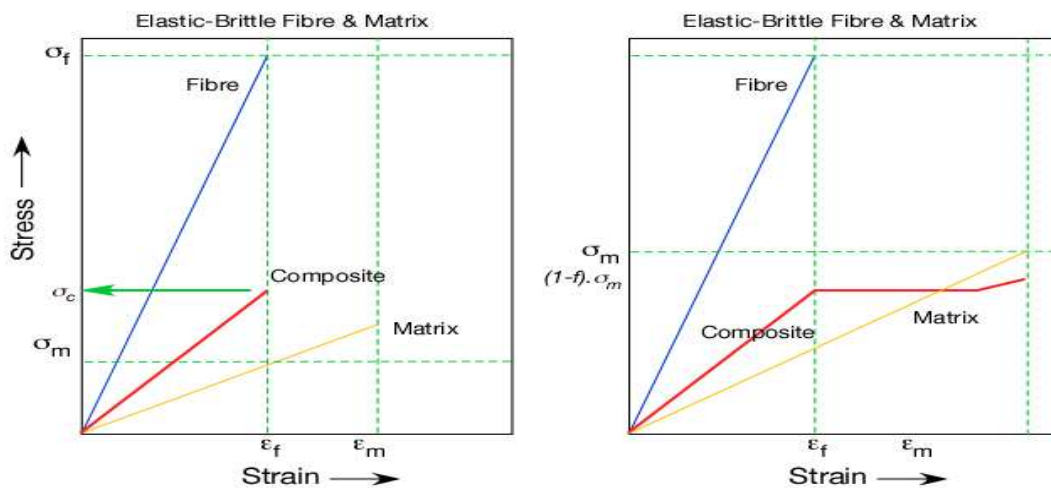


Figure 5.11: Effect of interfacial strength between the composite matrix and the fibre [92]

Moreover, the superior strength of the composite was associated with the proper interfacial adhesion between the fibre and the matrix. This was due to the fact that the fibres showed a reasonable amount of strength while acting as a stress transferring media, while the matrix act as crack initiating points during impact when the adhesion was weak. This was also partly due to the brittle nature of the epoxy matrix at high loading of nanofillers. Therefore it was concluded that the lay-up made from higher loading of nanofillers yielded faster than the one with 1% loading. The yielding of the fracture mainly happened in the matrix since it was already weak, whereas the fibres only enhanced the propagation of the crack along the matrix.

Further to that, the effect analysis using factorial design method also confirms the adverse effect of higher loading of nanoclay. Combined with mixing duration, increased loading of nanoclay had an adverse effect on the strength of the 0° degree lay-ups.

5.3.3 Analysis based on various duration of mixing

With respect to the duration of mixing, experiments were carried out at various mixing durations to ascertain the duration at which a maximum exfoliation is observed, in order to have a complete dispersion of the nanoclay particle in the epoxy matrix. Exfoliation is a process aimed to increase clay gallery distance in the matrix in order to have an even dispersion of the particle along the matrix. This can be better achieved during ultrasonic mixing by cavitation. It was made evident through the results shown below that 1 hour of ultrasonic mixing at 20°C with the combination of 20 mins of mechanical mixing gave better results in terms of dispersion than other mixing durations with the chosen 1% loading of nanoclay matrix. In fact, it was observed during the experiment that increasing the duration of mixing had only resulted in the degradation of the composite, which in turn had weakened the matrix. This is evident through the results in Table 5.9.

Table 5.9: Comparison of tensile properties at various mixing durations

Batch details	At 0° degree	At 45° degrees	At 90° degrees
	Mean UTP MPa	Mean UTP MPa	Mean UTP MPa
B - 1% Clay for 1 hour	591.000	63.222	31.888
E - 1% Clay for 2 hours	311.666	49.777	23.444
F - 1% Clay for 3 hours	266.444	48.777	20.500

The internal heat generated over a lengthy period of time during mixing had an adverse effect on the strength of the matrix. It was understood that this internal heat might have triggered internal polymerisation, in turn affecting the viscosity of the matrix. During lay-ups, this change in the viscoelastic nature of the epoxy composite

matrix might have imposed restrictions on the stiffening effect on the fibre material, which is adjacent to the matrix material, resulting a weaker bonding. Although the fibre/matrix interphase for the composites made from longer duration of mixing was expected to have a lower strength than the other matrices, the stiffening effect remained higher.

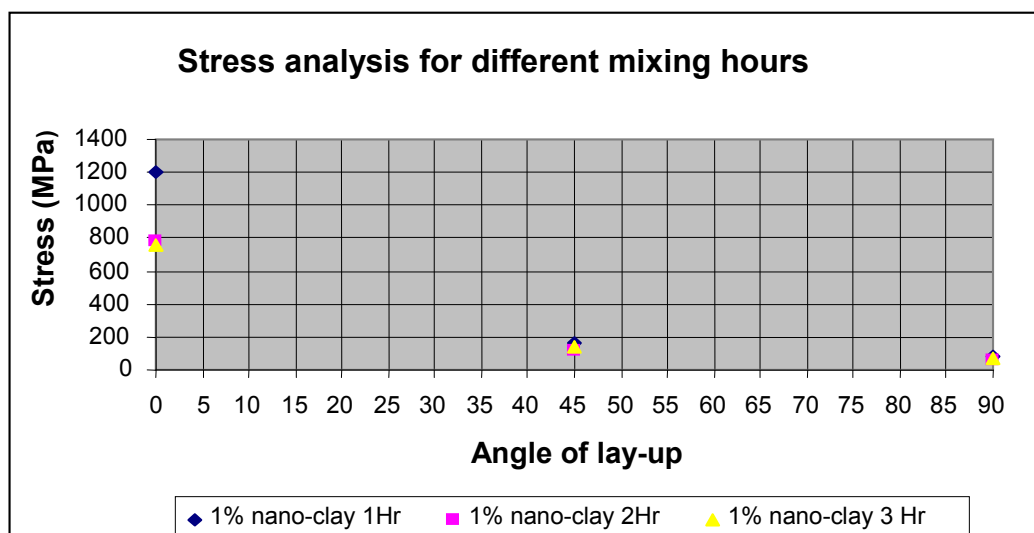


Figure 5.12: Stress analysis for different mixing durations of nanofillers at different angle of lay-ups

Further to that, the effect analysis using factorial design method also confirms the adverse effect of increasing the mixing durations. The combined effect of increased duration of mixing with higher loading of nanoclay had an adverse effect on the strength of the 0° degree lay-ups as shown in figure 5.12.

However, this different duration of mixing had helped in understanding the process and the system of interphase was expected to form between the polymer and the nanoparticles. Different composites with different mixing durations incorporating carbon fibres in a lay-up showed wide property variations. However, the maximum strength was exhibited by the 1% nanoclay and nanocarbon specimens at 1 hour sonication, where the tensile strength decreased with further increase in the nanoclay content and sonication period to a greater extent.

5.3.4 Analysis based on nature of mixing

While ultrasonic mixing ensures even dispersion, besides eliminating impregnation of air bubbles into the matrix to a larger extent, longer duration of mixing had only weakened the matrix as discussed above. While mechanical mixing breaks the layers of nanoclay particle, to exfoliate them into the matrix, ultrasonic mixing enhances the particle movement, thereby controlling particle agglomeration. Excess use of mechanical mixing also resulted a matrix with lots of micro bubbles impregnated in it.

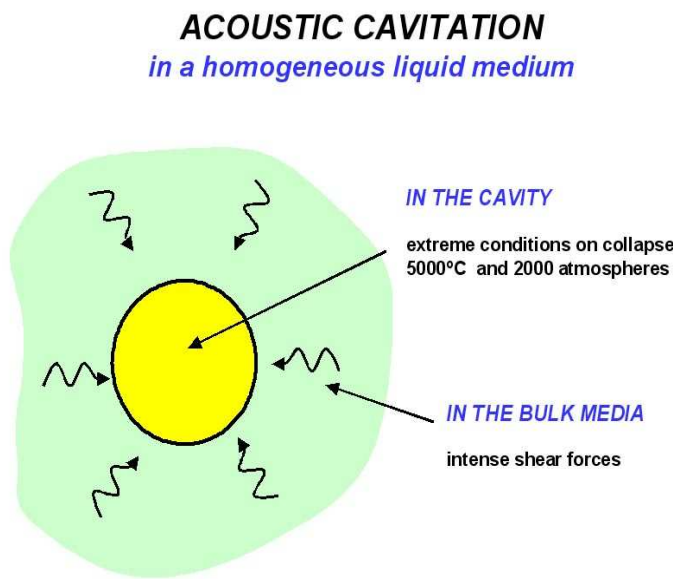


Figure 5.13: Schematic representation of acoustic cavitation.

The purpose in ultrasonic mixing has been emphasised as the core process during this synthesis and this can be substantiated in detail through the following discussion. Since the matrix is considered as an homogenous system, the ultrasonic process enhanced mass and heat transfer by acoustic streaming, while disintegrating the nanoclay platelets due to shear forces induced by shock waves through acoustic cavitation as shown in figure 5.13. In the liquid epoxy matrix, during the rapid collapse of the bubbles, the shear force generated produced mechanical effect, which led to a chemical effect in the matrix. This effect will be similar to high pressure jetting which can be visualised during ultrasonic cleaning. This effect can also activate and catalyse the chemical reaction by increasing mass and heat transfer to the surface, by disruption of the interfacial boundary layers. The drastic conditions

inside the bubble stimulate the generation of radicals. The source of the radical formation may be by the vapour developed inside the epoxy matrix. Subsequent to that, these primary radicals induced secondary reactions, which might initiate a radical chain, which could react with the polymer base containing nanofillers. These radical reactions, which occur in the bubble's interior in the epoxy matrix, accelerate the initiation of radical polymerisation, which in turn ensures uniform distribution of nanoparticles along the matrix, when the optimal volume of nanofillers was employed.

The physical effects generated inside the epoxy matrix during sonication process by the way of collapsing the bubbles had only affected the movement of the nanoparticles in suspension as well as in the surface. This effect did not affect the ionic chemical reaction inside the matrix. Thus power ultrasound provides one of the most exciting ways to synthesise nanomaterials for research and industry. The other reason for employing ultrasound excitation is also due to the high temperatures and pressures created during the collapse of an acoustic cavitation bubble. This is on a microsecond time scale and is associated with a rapid cooling rate ($>10^9$ K/s). This is very much greater than that obtained by conventional rapid cooling techniques (105-106 K/s).

Table 5.10: Comparison on mixing processes with 1% nanoclay/epxy matrix

Physical parameters	Method of mixing	
	Mechanical mixing	Ultrasonic mixing
Yield stress, MPa	960.05	1206.44 (25% increase)
Tensile modulus, N/cm ²	1095.25	1206.44 (10% increase)
UTP, MPa	408.015	591.000 (45% increase)

Even though through earlier researches, it was learnt that the nanocomposites prepared by the ultrasonic method show advantages over other mixing techniques, by this research it was made evident through the results. It was demonstrated that even dispersion of the nanofillers in the matrix ensured better bonding of the particles in the matrix, resulting directly in enhancing the material property of the composite. In this research, by using ultrasonic mixing, there was a 45% increase in ultimate tensile strength, a 25% increase in yield stress and a 10% increase in tensile modulus at 1% nanoclay by weight over mechanical mixing techniques. This is recorded in Table 5.10. This increase in strength and modulus might be attributed by the fact that the force generated by the ultrasonic wave has been transferred into the clay layers as stated before. It also developed an internal movement of particles along the matrix, to ensure even dispersion. This uniform mixture of nanoclay particles would have enhanced the formation of the covalent bonding between the particles in the matrix at 1% loading.

5.4 Discussion

In this section, the discussions are focussed towards understanding the effect of bonding resulting between the matrix and the fibre material during lay-up, based on the results obtained and through various theories on composite bonding. These discussions are made in correlation with the above analysis, as well as to support the conclusions made by this research.

5.4.1 Bonding theories to support crack analysis

During the three point bending test on the nanofilled epoxy/carbon lay-up, the ultimate or the breaking strength is the point at which the lay-ups exhibited catastrophic breakdown, or the breakage of fibre reinforcement. However, before this ultimate strength was achieved, the laminate reached a stress level where the matrix began to crack and the cracks propagate through the fibre reinforcements. The initial yield developed in the matrix to generate crack is called microcracking, which is the cause for debonding of the carbon fibre from the nanofilled epoxy matrix resulting in ultimate yield, which can be clearly seen in the figure 5.14. The epoxy based resin matrices help the laminates to achieve higher micro cracking strains [93].

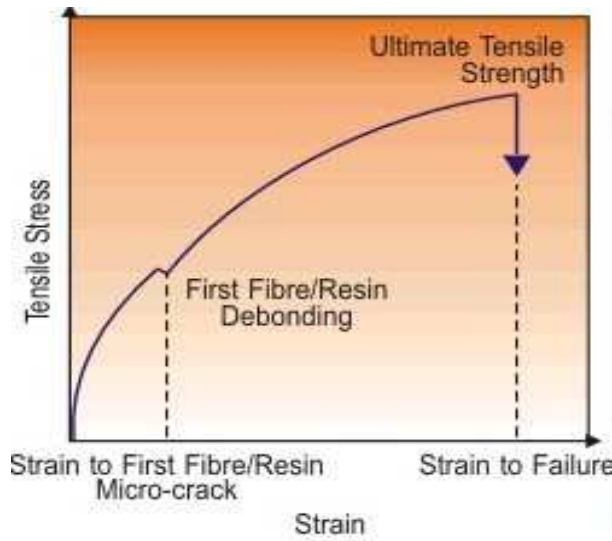


Figure 5.14: Typical tensile testing graph showing a lay-up yielding

Crack analysis on these structural laminates, with nano-infused epoxy resin base, in context with the various bonding theories defines such problems. No longer can traditional fibrous composites fulfil these stringent requirements, nor can they be engineered to control properties at the molecular or atomic level. However, it is known that molecular forces in bonding and the interaction between the interfaces along with the physical phenomena at this micro level, will dictate the aggregate properties of materials.

Adhesion theory

In order to understand the relation between the critical stress and the energy of fracture, according to the Griffith-Irwin theory of fracture applied to an adhesive bond, the fractural stress σ_f will be,

$$\sigma_f = k \sqrt{\left(\frac{EG}{l}\right)}$$

where E is the Modulus of Elasticity, l is the length of the critical crack and G is the work of fracture per unit area while k being the constant factor.

Where G will be

$$G = W_A(\text{or } W_C) + \psi$$

where w_a will be the work of adhesion and w_c will be the work of cohesion and ψ will be the other energy dissipated.

Bonding theory

The forces that act between the atoms and the molecules in the structure of a matrix are commonly known as ‘valence forces’. These forces and the created bonds are short range and they are presenting usually a continuous chain of covalent bonds. The dispersion can exert a significant influence at greater distances than primary chemical bonds, because of the additive effects of all the atoms in the body. These dispersion forces in many instances combine dipolar or polar forces at the interface.

Contact theory

When the molecules of epoxy/nanoclay composite make contact with the carbon fibre, *Van der Waals* forces acting between the polymer matrices give the adhesive bond its strength. In general, epoxy with higher viscosity would oppose the adhesive force and slow down the bonding [94].

For the isolated molecules with polarisabilities α_1 and α_2 as well as the ionisation energies I_1 and I_2 separated by a distance r , the energy of interaction will be,

$$U = -\frac{3}{2} \frac{\alpha_1 \alpha_2}{r^6} \cdot \frac{I_1 I_2}{I_1 + I_2}$$

where U is the potential energy. Therefore this can be written as

$$U = -\frac{A}{r^6}$$

where A is the *Van der Waals* dispersion attractive constant.

During the study on the crack formation and propagation in a carbon fibre lay-up, it was revealed that the nanoclay dispersion in epoxy influenced the strength of the matrix, which was evident by the test results shown in the earlier part of this chapter. It is also evident that certain toughening mechanism coexisted during the toughening process, which also contributed a synergetic effect on the matrix. However, carbon fibre debonding and the deformation of the fibre leading to microcracking, fracture

and splitting of fibres during tensile testing of the laminates are shown below in figure 5.15 through frames from high-speed photography.

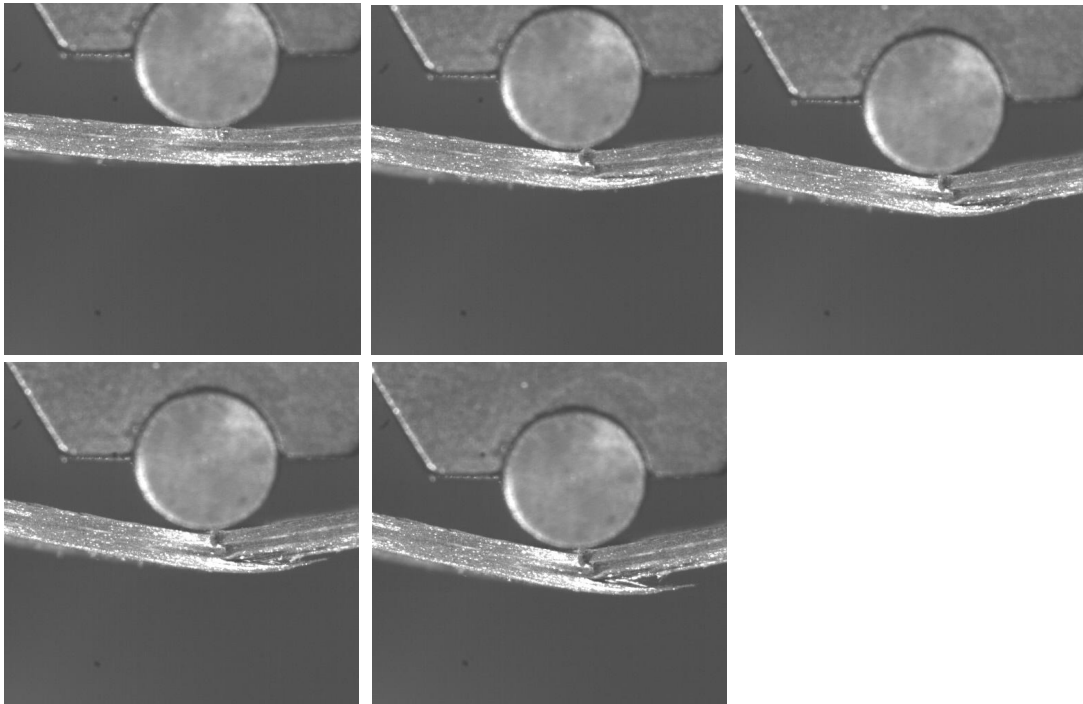


Figure 5.15: Crack analysis on 3% nanoclay/epoxy composite lay-up at 0° (1 hr mixing)

The independent properties of the epoxy nanocomposite matrix and the carbon fibre make a critical contribution to the quality of the reinforcement of the lay-up. In addition, the physical and chemical interaction between the fibre/matrix interface play an important role in improving the mechanical properties of the fibre reinforced composite lay-up. Following were some of the assumptions derived from the results, in conjunction with various bonding theories discussed earlier, in order to support the conclusions made from this research. A clear knowledge about physical and chemical bonding was evolved through the understanding of inter molecular kinetics, in correlation with the phenomena explained by the above theories.

- Electrostatic force explained by the Bonding theory emphasizes and confirms the adhesion energy generated between the nanoparticles in the embedded epoxy matrix, in terms of the molecular forces. This micro level force plays a crucial role in determining the degree of adhesive bonding in a macro level [94].

- The static development around the carbon fibre, due to its nature of affinity for micro particles, was quite unavoidable in enhancing the agglomeration of excess particles.
- It was observed that the physical and chemical absorption of the nanoenhanced matrix by the carbon fibre was proportionate to the strength of the lay-up, which was made evident by the effect of the *Van der Waals* forces.
- It was also observed that higher adhesion yielded higher strength and lower adhesion only resulted lower strength and greater failure energy.
- From the adhesion theory, the texture of the carbon fibre surface plays an important role in bonding, which is again partially due to the enhancement of the absorption area to increase the static force acting between the fibre layers.
- Rough surfaces create cavities and spaces in the form of canals to accommodate more matrices, which in turn enhance the bonding energy. But this could also accumulate excess nanoparticles into the cavity. Enough care should be taken to control excess flow of matrix into these canals. Rough surfaces always have the advantage over the smooth ones in terms of adhesion.
- The number of the fibres, the thickness of each fibre and its compactness are always important. The thickness of the fibre used in the lay-up affects the strength of the material in direct proportion.
- The alignment of carbon fibre during lay-up is important for improved mechanical properties. It was found that the alignment of fibres at 0° angle provided better yield strength, when compared with 45° and 90° .
- Penetration of the matrix into the carbon fibre relates directly to the bonding forces according to Adhesion theory, explaining the Griffith-Irwin theory, which is often controlled by the process.
- Incorporating more volume of nanoclay, i.e. the addition of nanoclay beyond the optimum level of 1% loading, would encourage the matrix to absorb moisture due to the hydrophilic nature of the clay. As water, under saturated condition is known for a significant decrease in the bonding strength of the adhesive in general, it weakens the lay-up to a larger extent.

This phenomenon was experienced with the lay-ups made from 3% loading of nanoclay.

- Agglomeration of nanoparticles in the form of clusters of whiskers along the matrix was because the particles were dispersed randomly. This clustered dispersion would have resulted because the volume of nanoparticles dispersed would have been more than the identified optimal volume, which is 1%. These locally clustered particles would have accumulated in the pores during lay-ups, which in turn would have resulted in developing loose bonding. This loose bonding would have occurred by the way of molecular intermixing or physical polarity interactions of the particle between the fibre and the epoxy matrix. Ultimately this has resulted in weak chemical bonding [93]. This was clearly evident during microscopy.
- During excess loading of nanofillers in the matrix, these loosely packed particles result in shear yielding initially in the plastic zone and then build-up a shear strain to a critical value, to make the matrix to undergo a shear yield to develop a crack that can propagate along the fibre, leaving the damage zone to grow unstably, resulting in a complete yield of the matrix [95].
- This suggests, that the cavitations created by the agglomeration of excessive nanoclay particles help the plain strain to induce the lay-up to make a sharp crack, which in turn develops a synergetic shear force along the direction of the fibre orientation, resulting in shear yield of the lay-up matrix.
- While using the nanocarbon fillers, the lubricating nature of the carbon particles could result in formation of micro conduits along the fibre, resulting a weak matrix.
- The size, shape, density and orientation of the pores (if any) due to the poor workmanship during lay-up/ moulding process contribute directly to the yield strength and hence the final mechanical properties.
- The interlocking pattern between the epoxy matrix and the lay-up fibre is an important factor in determining the bonding. Most of the time it depends upon whether it is a mechanical or a chemical bonding.
- The brittle nature of the epoxy capable of restricting the plastic deformation is made clear from the results of the lay-up with neat epoxy. This is because the matrix gets quite rigid at room temperature, after complete curing.

- Cross-link density of the resin is an important factor in determining the adhesive strength of the matrix in total.
- The viscoelastic property of epoxy influences inversely the bonding, according to the contact theory explained above. Therefore, good wetting results in better adhesion.

The viscosity and the surface tension of the resin play an important role in determining the forces exerted on nanoparticles during the mixing process. This in turn has a greater impact in bonding during lay-up with the carbon fibre. Therefore, during this research a medium viscous epoxy was employed.

The enhancement of mechanical properties in this nanoclay/epoxy composite depended on the exfoliated content of nanoclay in the epoxy matrix, as discussed earlier. Nanoclay has a layered structure in which an individual layer of 1nm thickness can typically extend up to 0.1 μ m to 2 μ m length and width with an interlayer spacing of 2 nm to 3 nm [91]. These layers are bonded together by *Van der Waals* forces. In the exfoliated condition, their surface area can be as high as 750 m²/g [92]. Since these nanoparticles possess enormous surface area, the interfacial area between the two intermixed phases in a nanocomposite is substantially larger than the traditional composites. This results in increased bonding between the nanoparticles and the matrix. That is why several mechanical, thermal and electrical properties of nano-composites are observed to be better than those of conventional composites. There are many ways to improve the final mechanical, physical and chemical properties of nanoclay/epoxy nanocomposites. One of the most important ways employed during this research was by dispersing the clay into the matrix evenly, to reach maximum exfoliation of clay layers in the epoxy matrix.

During this research, this phenomenon was studied, tried in detail to develop a system to reach optimum results through experimentation. It was also proved by the test results. Even by the combination of ultrasonic and mechanical mixing, obtaining the complete exfoliation of nanoclay at low loading percentages in the epoxy matrix was a significant challenge. The combination of these two different mixing techniques had ensured even dispersion under standard conditions, which is quite promising. This in-turn had improved the mechanical and physical properties of

nanocomposites lamina to a greater degree. However the mixing speed and the time were optimised for both the mixing techniques, based on preliminary investigations. It was found that good exfoliation could be obtained when the mixing is carried out for 1 hour using ultrasonic mixing at 20°C.

Through this research, by combining a few traditional approaches as discussed, nano-enhanced fibre reinforced composite materials with excellent in-plane properties have been developed. It has been found that optimum loading of nanofillers like nanoclay and nanocarbon will boost elastic or tensile modulus by 22%, while adding another 50% elongation compared to the one without such nanoparticles. Tensile strength of this nano-enhanced epoxy nanocomposite samples were 11% higher than neat epoxy matrix. These results have laid paths for the potential of using this nano-enhanced matrix in a traditional carbon fibre layering method for commercial applications with adequate importance to uniform distribution besides ensuring good interconnectivity between the carbon fibre and the matrix.

Also during this research, a high-speed video photography during mechanical testing and crack analysis through microscopy were employed. These were carried out not only to study the entire morphology but also to look for a possibility to propose changes to the matrix to improve it. With the layered-up three-dimensional composites containing right proportion of nanofillers, remarkable improvements in the interlaminar fracture toughness, hardness, delaminating resistance and in-plane mechanical properties were demonstrated making these lay-ups truly multifunctional.

Chapter 6

Conclusions and Recommendations

6.1 Conclusions

Through this research, it is demonstrated that incorporating the right amount of nanoparticles into an epoxy resin matrix poses a remarkable strength and flexibility. Industries could now be able to integrate the outcome of this research widely in high performance applications in the fields of biomedical engineering, aerospace, marine, high speed parts in engines, packaging and in sports goods. The ultimate goal of this project to characterise the physical and mechanical properties of enhanced nanocomposite was met, after a wide range of experiments. This was conducted on the reinforced polymer composite as well as on the carbon fibre laminations. Although carbon fibres are widely used in sports gear and boating industry because of their strength and lightness, they will show a tremendous potential when they are layered-up with an epoxy matrix enriched with 1% of nanoclay in a temperature controlled atmosphere.

During this research, the response of these nano-enhanced composites and the laminates to external deformations like bending were also tested, analysed and characterised as per the objective mentioned earlier. Based on the results, it is established that epoxy reinforced with a 1% of nanoclay can significantly improve the mechanical properties, without compromising the weight or the processability of the composite. This is made evident from the results shown in Chapter 5. Moreover, all these improvements have been achieved by making few changes to the conventional processing techniques, without any detrimental effects on processability and the appearance of the matrix.

Establishing the optimal method for dispersing nanoparticles completely in an epoxy matrix often required experimentation. The challenge of dispersing nanoparticles in the matrix was large, primarily because of several competing factors. On a smaller scale, controlling the interfacial free energy associated with the nanoparticles and electrostatic energy developed by the carbon fibre tending to cause the nanoparticles to clump together or keep them far apart in the matrix. This phenomenon was quite challenging. Also the hydrophilic and hydrophobic properties of the nanoparticles developing an internal force between the dispersed nanoparticles to cause agglomeration were substantial too. Through this research, an optimal way of dispersing the optimised volume of nanofillers into the epoxy matrix has been successfully identified to counter the above said challenges to meet the objectives of this research.

Nanoclay/epoxy composites, as they have attracted considerable technological and scientific attention because of their wide array of applications through property improvements even at very low filler content, developing a viable method to combine and optimise simple and cost-effective processing techniques like ultrasonic mixing and mechanical mixing, maximum exfoliation of nanoclay particles was achieved. This in turn maximised the dispersion of nanoclay particles along the matrix resulting in the enhancement of the neat epoxy matrix. From the outcome of these results, a nano-enhanced epoxy composite has been successfully made ready for commercialisation.

6.2 Recommendations

Following are the recommendations from the experimental work carried out on epoxy nanocomposite lay-up for future research. All these recommendations are carefully made after being suitably substantiated by the results, in correlation with the theories discussed.

6.2.1 Material selection

- Nanoclay of 10 nm to 30 nm at the proportion of 1% by weight.
- Medium viscous epoxy (9400 - 11000 Centipoise (cps) at 25°C)
- Epoxy to hardener ratio 4:1 by weight.

6.2.2 Process selection

- Successful even dispersion was achieved while processing the nanoclay/epoxy mixture by the combination of 1 hour of ultrasonic mixing at amplitude of 40 Watts followed by 20 minutes of mechanical mixing. The mechanical mixing has to be carried out at a slow speed of 650 rpm after the addition of hardener into the matrix.
- While employing a pulse rate of 9 seconds ON and 9 seconds OFF during ultrasonic mixing in order to maintain the temperature at 20°C to avoid self-polymerisation reaction, an external cooling set-up is also highly recommended.

6.2.3 Lay-up techniques

- Unidirectional carbon fibre lay-up gives a better yield strength compared to other lay-ups.
- Moulding has to be completed within 40 minutes of mixing with the hardener.
- With relevance to bonding, it was found that for the substrates like fibres, complete and uniform wetting is highly recommended. Poor wetting would always allow the entrapped air to remain between the fibre and the matrix, which in turn would reduce the effective bonding area to create stress raisers along the interface.
- Pre-treatment of lay-up material is also encouraged depending upon the application and the nature of the lay-up material used. Pre-treating the lay-up material with an adhesion promoter like silicons and fluorocarbon or by physical processes like etching, flame treating etc would enhance adhesion.
- Adequate care is to be taken during the experiment to prevent the surfaces from any external contaminations.
- As curing plays a vital role in adding strength to the matrix, complete curing under pressure of 30 Kgs for at least 24 hours is recommended. Pressure imparts better wetting, besides ensuring complete interfacial contact. Epoxy cured with heat will be more heat and chemical resistant than if cured at room temperature.

- Finally, while cutting the lay-up, high-speed cutting tool with appropriate lubricant depending upon the lay-up material will be the right choice.

From the outcome of the experimental results and the analysis, it has been identified that there is a tremendous functional potential for these nano-enhanced composites for structural applications in the area of Biomedical Engineering. Further to that, as a part of continuing this research, future researches can be tried to develop an eco-friendly nano-enriched composite towards functional applications in biomedical engineering besides looking at the possibilities of reducing the pollution problems in handling and processing these nanofillers.

The newly developed nano-enhanced epoxy composite and the outcome of this research will revolutionise the composites industry and benefit the mankind at large.

References

1. Wilkes G L, Maxwell B. Recent Advances in Polymer Science. In: Polymer Symposium; New York; 1974. Series Vol. 46; p. 15-58.
2. Giannelis E P. *Advanced Materials*. 1996. Vol. 8; p. 29.
3. Carl W, John Y. *Commercializing Nanotechnology*. 2004. p 2-11.
4. Pietro M. *Carbon Nanotubes - Overview of Properties, Classification, Fabrication and Synthesis*. Xlab Materials and Microsystems Laboratory; The Polytechnic of Turin and the National Institute for Physics of Matter; 2002.
5. Harry S. *Carbon Nanotube Manufacturing on a Commercial Scale - Ready for Mass-Markets*. The European Coatings Journal; November 2004.
6. Morinobu E, Takuya H, Yoong K A, Hiroyuki M. *Development and Application of Carbon Nanotubes*. *Institute for Carbon Science and Technology*; 2006. Vol. 45; No. 6A.
7. Lau K T, Lu M, Hui D. *Coiled Carbon Nanotubes: Synthesis and Their Potential Application in Advanced Composite Structures*. Composites Association; 2006. Part B. 3, 6; p. 400-450.
8. Guggenheim, Stephen, Martin R T. *Definition of clay and clay mineral. Journal report of the Clays and Clay Minerals Clay mineral nomenclature*; American Mineralogist; 1995. Vol 43: p. 255-258.

9. Dagani R. Nanostructural materials promise to advance range of technologies. *Chemical Engineering News*; 1992. p.18–24.
10. Shukla P R, Pandey O P, Narain G. *Characterisation of Clay/Polymer Composite*. *Journal in Indian Chemical Society*; 1985. 62: p. 175.
11. Wang L. Article on Preparation, Morphology and Thermal/ Mechanical Properties of Epoxy/Nanoclay Composite. *Composites Association*; 2006. Vol. 11; p. 37- 41.
12. Gilman J W, Kashiwagi T, Beall G W. *Polymer-clay nanocomposite*. Pinnavaia editors; Wiley; New York; 2000. p.100-125.
13. Lagaly G. *Characterisation of Clay for Structural Applications*. *Journal on Applied Clay Science*; 1999. 15, p. 5-9.
14. Lam C K. *Cluster Size Effect in Hardness of Nanoclay/ Epoxy Composites*, *Composites*; 2005. Part B, 36, p. 250-280.
15. Lilli S M. Chasing Nanocomposites. *Article on Plastic technology*; 2007.5.
16. Pinnavaia T J, Lan T, Wang Z, Shi H Z, Kaviratna P D. Clay-Reinforced Epoxy Nanocomposites: Synthesis, Properties and Mechanism of Formation: Nanotechnology-Molecularly Designed Materials. In: *ACS Symposium Series 622*; American Chemical Society; Washington, DC; 1996. p. 125-134.
17. Wang L. et al., Preparation, Morphology and Thermal/ Mechanical Properties of Epoxy/Nanoclay Composite; 2006. Part A, 37; 11 p. 1890-1896.

18. Senese, Fred. Who discovered carbon? Frostburg State University; Retrieved on 12, 2006.
19. Nasibulin A G, Pikhitsa P V, Jiang H. *A novel hybrid carbon material. Nature Nanotechnology*; 2007. Vol. 2, p. 156-161.
20. MatWeb-Material Property Database; retrieved on 01/2007.
21. Alumina (Aluminium Oxide) - The Different Types of Commercially Available Grades. The A to Z of Materials; Retrieved from Azom on 01, 2007.
22. Hu Y, Tsai H L, Huang C L. *Materials Science and Engineering*. Wiley & Sons; 2003. p. 209.
23. Zhu H L, Averback R S. *Materials and Manufacturing Processes*; 1996, 11; p. 800-805.
24. Periodic Table. Retrieved from chemical elements on 11, 2006.
25. Weast C. CRC Handbook of Chemistry and Physics. Boca Raton; Florida; 1982. p. 145-149.
26. Chen J S, Poliks M D, Ober C K, Zhang Y M, Wiesner U, Giannelis, E. Polymer Science. Wiley & Sons; 2002. Vol.43, p. 48-95 and p.185-201.
27. Kornmann X, Lindberg H, Berglund L. Article on Polymer synthesis, 2001. 42: p. 85-93.
28. Schultz J, Nardin M, Mittal K L, Pizzi A. *Handbook of Adhesive Technology*. Marcel Dekker Inc.; New York; 2003. p. 25-57.

29. Kornmann X, Lindberg H, Berglund L. Structural laminates of epoxy composites. Article on Polymer; 2001. 42:1303.
30. Sam S, Alfons V, Etienne S, Ulric D, Andre C V. Epoxy polymer surface modification through wet-chemical organic surface synthesis for adhesion improvement in microelectronics. In: Department of Solid State Sciences; Universiteit Gent; Krijgslaan; 2005. 281: p. 90.
31. Grezlak J H. The *Preparation and Physical Properties of Polyester-Poly(methyl methacrylate) Triblock Copolymers*; Journal of Applied Polymer Science; 1975. 19; 769.
32. Wilkes G L. *Rheo Optical Techniques and Their Application to Polymeric Solids*. Journal of Macromolecular Science (Review Paper); 1974. C10(2); 149.
33. Wilkes G L, Ian Brown, Wildnauer R H. Biomechanical Properties of Skin. Critical Reviews in Bioengineering; 1973. Vol.1; No. 4; p. 453.
34. Kenji O, Hiroji O, Keiko K. *Properties and Structural Applications of Poly Vinylidene Fluoride*. Journal on Applied Physics; 1996. 2760.
35. Zhang Q M, Bharti V, Kavarnos G, Schwartz M. *Poly Vinylidene Fluoride (PVDF) and its Copolymers*. Encyclopedia of Smart Materials; John Wiley & Sons; 2002. Volumes 1-2, p. 1-8, p. 12-55, p. 77-82, p. 253-267, p. 800-825.
36. Oertel, Gunter. *Polyurethane Handbook*. MacMillan Publishing Co. Inc.; New York; 1985. p.15-37.
37. Harrington, Ron, Hock, Kathy. Flexible Polyurethane Foams. The Dow Chemical Company Publication; Midland; 1991. p 255 -272.

38. Grillo D J, Housel T L. *Physical Properties of Polyurethanes from Polyesters and Other Polyols*. Journal of the Society of the Plastics Industry, Inc.; 1992. p. 52-67.
39. Frank M. Research Report, Nanotechnology: Impact of Nanoelectronics on the U.S. Electronics Industry. Naanotech IC Forecasts; 2006. FTM5010.
40. McWilliams A. Nanocomposites, Nanoparticles, Nanoclays, and Nanotubes. BCC; Norwalk; CT: Business Communications Company; 2006. retrieved on 02, 2007.
41. Research Report; Nanocomposites - A Global Strategic Business Report. Global Industry Analysts; 2007. GIA-MCP1526; retrieved on 05, 2007.
42. McWilliam A. Research Report, Nanotechnology for Consumer Products. 2005. GB319; retrieved on 02, 2007.
43. Research Report, World Nanomaterials. Freedonia Research Group; 2007. FR2215; retrieved on 03, 2007.
44. Research Report, Nanomaterials to 2008-Market Size, Market Share, Demand Forecast, and Sales. Cleveland; OH: Freedonia Group; 2006. retrieved on 02, 2007.
45. McWilliams A. Research Report, Nanotechnology - A Realistic Market Evaluation. 2007. GB-NAN031B; retrieved on 04, 2007.
46. Krishnamoorti R, Vaia R A. *Polymer nanocomposites: synthesis, characterization, and modelling*. American Chemical Society Meeting, American Chemical Society; Division of Polymeric Materials: Science and Engineering; Oxford University Press; 2002. p.7-13.

47. Wang H, Hoa S V, Wood-Adams P M. *New Method for the Synthesis of Clay/Epoxy Nanocomposites*. Department of Mechanical and Industrial Engineering; Concordia University; Montreal; Wiley InterScience; 2005. Vol. 10.1002.
48. Lam C K. Effect of *Ultrasound Sonication in Nanoclay Clusters of Nanoclay/Epoxy Composites*. Materials Letters; 2005. 59; p.1369-1372.
49. Joung G R, Hyung Su K, Jae W L. *Polymer-Clay Nanocomposites Prepared by Power Ultrasonic Wave - Synthesis and Rheological Properties*. Applied Rheology Center; Department of Chemical Engineering; 2004. p.121-742.
50. Joung G R, Hyung Su K, Jae W L. *Ultrasonic degradation of polypropylene and nanocomposites*. SPE-ANTEC Tech. Papers; 2001. p. 55-125.
51. Joung G R, Hyung Su K, Jae W L. *Rheological Properties of nanocomposites*. 2002. p.140-714.
52. Campbell C T, Parker S C, Starr D E. *The Effect of Size-Dependent Nanoparticle Energetics on Catalyst Sintering*. Journal of Department of Environmental Sciences and Engineering; 2002. Vol. 298: 25.
53. Coblenz W S, Dynys J M, Cannon R M, Coble R L. *Initial stage solid state sintering models: A critical analysis and assessment*. Journal of Material Science Research; 1980. Vol.13: p. 141-157.
54. Chaim R, Marder-Jaeckel R, Shen J Z. *Transparent YAG ceramics by surface softening of nanoparticles in spark plasma sintering*. Journal of Materials Science and Engineering; Elsevier; Department of Materials

Engineering; Technion; Israel Institute of Technology; Haifa; 2006. A429: 04.072, p. 74-78.

55. Maria V G, Luca I, Paolo M. *Design and production of fixtures for free-form components using selective laser sintering*. Journal on Rapid Prototyping; Emerald Group Publishing Limited; 2006.13:1.
56. Dusan G, Jaroslav S, Peter S, Ralf R, Raphaelle S, Michael H. *The influence of post-sintering HIP on the microstructure, hardness, and indentation fracture toughness of polymer-derived Al₂O₃-SiC nanocomposites*. Journal of Institute of Materials Science; 2006.
57. Ishida H, Campbell S, Blackwell J. *General Approach to Nanocomposites Preparation*; Journal in Chemical Matter; 2000. Vol.12: p. 260-267.
58. Carbon Nanotubes - *Overview of Properties, Classification, Fabrication and Synthesis*. Journal of Xlab Materials and Microsystems Laboratory; National Institute for Physics of Matter; 2001.
59. Vacuum Infusion - The Equipment and Process of Resin Infusion. Journal of Flow Media publication; 2006. retrieved on 05/2007.
60. Daniel R. Solid Particle Stabilization of Emulsions - Characterisation, Processing Methods and Applications. In: Skin Care Forum; 2005. Issue 25; p. 3.
61. Teishev A, Incardona S, Migliaresi C, Marom G. *Polyethylene fibers-polyethylene matrix composites: preparation and physical properties*. Journal of Applied Polymer Science; 1993. 50:503; p. 12- 24.
62. Munro W J, Richards H S, Edwards R W, Van Oss C. *Polymer Surfaces and Interfaces*. Journal of Polymer Science; 1993. Vol. 2: p. 57-65.

63. Van Oss J, Good R J, Busscher H J. *Polymer Science and Dispersion Technology*. Journal of Polymer Science; 1990. 11, p.75-81.
64. Wu S. Journal of Polymer Interface and Adhesion; New York; 1982.
65. Park J H, Jana S C. The Relationship between Nano and Microstructures and Mechanical Properties in PMMA-Epoxy-Nanoclay Composites. Article on Polymer Research; 2003. 44, p. 5-11.
66. ASTM Standard Test D 790M: Standard Test Method for Compressive Properties of Rigid Plastics. RA:ASTM International; August 10, 2002.
67. Nathaniel C, Hassan M, Vijaya K R, Adnan A, Shaik J. *Fabrication and mechanical characterization of carbon/SiC-epoxy nanocomposites*. Center for Advanced Materials; USA; 2004.
68. ASTM Standard Test D 638: Standard Test Method for Tensile Properties of Reinforced Thermosetting Plastics using Straight-Sided Specimens. RA:ASTM International; April 10, 2002.
69. Gupta N, Lin T C, Shapiro, Michael. Clay-Epoxy Nanocomposites: Processing and Properties. Article on Metals & Materials Society; 2007.
70. Luo J J, Daniel I M. *Characterization and Modelling of Mechanical Behavior of Polymer/Clay Nanocomposites*. Journal of Composites Science and Technology, 2003. 63:11, p. 1607-1616.
71. Sperling L H. *Introduction to physical polymer science*. 2nd edition; John Wiley & Sons Inc.; New York; 1992. p. 100-152.

72. Ke Y C, Lu J K, Yi X S, Qi ZN. *Synthesis and Characterisation of Clay/Epoxy/PMMA Composites*. Journal on Applied Polymer Science; 2002. 78: 808.
73. Haynes R. *Optical microscopy of materials*. Kluwer Academic Publishers; 1984. p. 72-86, p. 126-148.
74. Feldman L C. *Fundamentals of Surface and Thin Film Analysis*. 2nd Edition; 1986. p. 352- 367.
75. West P, Starostina N. *Advanced Materials & Processes*. 2004. p. 35-37.
76. Delly J G. *Photography through the Microscope*. 9th Edition; Eastman Kodak Company; 1988. Chapter 3, p. 112-123.
77. Inoue S. *Video Microscopy*. 1st Edition; Plenum Press; 1986. p. 584-591.
78. Kirat K, Burton I, Dupres V, Duprene Y. Journal on Microscopy; 2005. 218: p. 199-207.
79. Lee H, Neville K. *Handbook of Epoxy Resins*. McGraw–Hill; 1981. p. 302-308.
80. Atae C A, Cabrerizo M V, Gomez L. *Measurement of surface tension and contact angle*. Journal of Measurement Science and Technology; 2001. 12: p. 288-298.
81. Cabrerizo M A, Wege H A, Holgado T. *Axisymmetric drop shape analysis*. Journal of Scientific Instrumentation; 1999. 70:5; p. 2438-2443.
82. Balkenende A R, van de Boogaard H J A P, Scholten M, Willard N P, Langmuir. *Evaluation of Different Approaches to Assess the Surface*

Tension of Low Energy Solids by Means of Contact Angle Measurements.
1998. Vol. 14: p. 5907-5912.

83. Li D, Neumann A W. *Contact Angles on Hydrophobic Solid Surfaces and Their Interpretation.* Journal of Colloid and Interface Science; 1992. Vol. 148:1.
84. Derrick O N, Esio O O, Rhoda G H. Article on Determination of Contact Angle from Contact Area of Liquid Droplet Spreading on Solid Substrate. retrieved on 11, 2007.
85. Shafrin E G, Zisman W A. *Constitutive Relations in the Wetting of Low Energy Surfaces and the Theory of the Retraction Method of Preparing Monolayers.* Journal of Physical Chemistry; 1960. Vol. 64:5; p. 519-524.
86. Petrie E M. *Theories of Adhesion, Handbook of Adhesives and Sealants.* 2nd edition; McGraw-Hill; New York; 2006. Chapter 2; p. 564-579.
87. Kinloch A J. *Adhesion and Adhesives.* Chapman and Hall; New York; 1987. p. 25.

Appendix

Appendix A

Paddy and Pitt's table for contact angle

TABLE I
The Coefficients c_1 – c_8 for Eq. [5] for every 2° from 90 to 180°

θ (degrees)	c_1	c_2	$c_3 \times 10$	$c_4 \times 100$	$c_5 \times 1000$	c_6	c_7	c_8
180	.37641	–.24842	.73720	–1.17744	.79189	6.09530	1.23744	.35179
178	.37617	–.24837	.73701	–1.17728	.79189	6.09640	1.23746	.35185
176	.37600	–.24812	.73624	–1.17570	.79066	6.09395	1.23745	.35199
174	.37583	–.24789	.73567	–1.17465	.78981	6.08980	1.23758	.35222
172	.37517	–.24761	.73493	–1.17409	.78990	6.08827	1.23789	.35255
170	.37487	–.24752	.73498	–1.17506	.79103	6.08272	1.23850	.35293
168	.37498	–.24742	.73502	–1.17558	.79150	6.07131	1.23932	.35336
166	.37501	–.24749	.73565	–1.17775	.79339	6.05980	1.24051	.35385
164	.37471	–.24759	.73626	–1.18071	.79640	6.04951	1.24201	.35440
162	.37546	–.24774	.73715	–1.18300	.79810	6.02758	1.24380	.35493
160	.37585	–.24804	.73853	–1.18730	.80176	6.00770	1.24600	.35552
158	.37660	–.24829	.73966	–1.19077	.80461	5.98187	1.24851	.35611
156	.37773	–.24845	.74032	–1.18270	.80580	5.94949	1.25129	.35669
154	.37895	–.24856	.74083	–1.19456	.80718	5.91339	1.25437	.35724
152	.38031	–.24851	.74058	–1.19448	.80670	5.87248	1.25773	.35779
150	.38198	–.24814	.73906	–1.19112	.80327	5.82363	1.26122	.35828
148	.38357	–.24758	.73680	–1.18640	.79889	5.77155	1.26498	.35874
146	.38514	–.24677	.73346	–1.17926	.79252	5.71518	1.26896	.35915
144	.38698	–.24560	.72879	–1.16885	.78335	5.65067	1.27306	.35949
142	.38893	–.24411	.72278	–1.15525	.77146	5.57997	1.27734	.35974
140	.39054	–.24223	.71529	–1.13890	.75761	5.50668	1.28173	.35993
138	.39209	–.24000	.70635	–1.11933	.74116	5.42819	1.28627	.36003
136	.39370	–.23731	.69571	–1.09606	.72181	5.34260	1.29086	.36001
134	.39480	–.23433	.68395	–1.07122	.70167	5.25651	1.29562	.35991
132	.39604	–.23097	.67061	–1.04255	.67815	5.16264	1.30048	.35970
130	.39695	–.22717	.65568	–1.01119	.65299	5.06535	1.30539	.35936
128	.39752	–.22318	.64002	–.97893	.62739	4.96639	1.31052	.35892
126	.39788	–.21883	.62304	–.94434	.60026	4.86310	1.31574	.35834
124	.39801	–.21406	.60444	–.90682	.57108	4.75518	1.32099	.35761
122	.39783	–.20914	.58534	–.86903	.54207	4.64511	1.32647	.35675
120	.39739	–.20394	.56520	–.82965	.51219	4.53175	1.33208	.35574
118	.39666	–.19850	.54418	–.78914	.48175	4.41545	1.33785	.35460
116	.39575	–.19293	.52273	–.74842	.45154	4.29571	1.34388	.35330
114	.39478	–.18726	.50094	–.70762	.42160	4.17145	1.35022	.35182
112	.39346	–.18135	.47824	–.66573	.39124	4.04462	1.35670	.35020
110	.39195	–.17542	.45552	–.62446	.36178	3.91526	1.36361	.34840
108	.39056	–.16958	.43307	–.58422	.33339	3.78028	1.37109	.34643
106	.38903	–.16371	.41047	–.54430	.30563	3.64184	1.37905	.34428
104	.38763	–.15797	.38822	–.50543	.27890	3.49764	1.38778	.34196
102	.38632	–.15243	.36663	–.46821	.25370	3.34896	1.39751	.33947
100	.38535	–.14714	.34564	–.43232	.22968	3.19278	1.40849	.33678
98	.38502	–.14240	.32627	–.39937	.20786	3.02740	1.42152	.33393
96	.38539	–.13825	.30847	–.36909	.18799	2.85215	1.43719	.33094
94	.38737	–.13532	.29407	–.34404	.17149	2.66011	1.45777	.32780
92	.39164	–.13418	.28459	–.32619	.15943	2.44648	1.48653	.32462
90	.39808	–.13528	.28158	–.31790	.15325	2.21553	1.52810	.32165